Traitement des eaux contenant de la tétracycline avec la laccase de Trametes Versicolor immobilisée sur des monolithes de silice macroporeux

Sher Ahmad

THÈSE POUR OBTENIR LE GRADE DE DOCTEUR
DE L'UNIVERSITÉ DE MONTPELLIER

En Génie des procédés

École doctorale GAIA

Unité de recherche : Institut Européen des Membranes (UMR 5635)

TRAITEMENT DES EAUX CONTENANT DE LA TETRACYLINE AVEC LA LACCASE DE *TRAMETES VERSICOLOR* IMMOBILISEE SUR DES MONOLITHES DE SILICE MACROPOREUX

Présentée par Sher AHMAD

Le 9 Décembre 2020

Sous la direction de : Jose Sanchez Marcano

Marie-Pierre Belleville

Devant le jury composé de

Mme. Estelle COUALLIER, Chargée de Recherche HDR, CNRS GEPEA UMR 6144	Rapporteur
M. Pedro LOZANO, Professeur, Doyen, Faculté de Chimie, Université de Murcia	Rapporteur
Prof. Eric DUBREUCQ, Professeur, Montpellier SupAgro	Président du jury
Dr. Jose SANCHEZ MARCANO, Directeur de Recherche, Institut Européen des Membranes	Directeur de thèse
Dr. Marie-Pierre BELLEVILLE, Maitre de Conférences, Polytech Montpellier	Invitée

UNIVERSITÉ DE MONTPELLIER

ABSTRACT

In this research work, silica monoliths with high porosity (83 %), double pore size distribution (20 μm and 20 nm macro- and mesopores diameters, respectively) and high surface area (370 m^2 g^{-1}) have been used as solid supports to immobilize a laccase from *Trametes versicolor* by covalent grafting with glutaraldehyde. Enzymatic monoliths were applied to degrade tetracycline (TC) in aqueous solutions in a tubular "Flow Through Reactor" configuration with recycling. During the first 5h of reaction at pH 7, 40–50% of TC was degraded, and then a threshold was reached. One of the hypotheses explaining this behaviour is a possible co-substrate lack (oxygen) near catalytic sites. Enzymatic monoliths were used during 75 h of sequential operation without losing activity. A mathematical model built coupling the Michaelis-Menten reaction kinetics with a dynamic mass balance allowed computing TC degradation efficiency. Simulation results revealed that the global process is controlled by the enzymatic kinetics but the monolith size could be adapted to degrade 100 % TC in a single pass.

Keywords: Silica monoliths, Laccase, Water treatment, Modelling and simulation.

RESUME

Dans ce travail de recherche, des monolithes en silice présentant une très grande porosité (83 %), une double distribution de taille de pores (des macropores de diamètre 20 μm et des méseopores de diamètre 20 nm) et une très grande surface spécifique (370 m^2 g^{-1}) ont été utilisés comme supports pour immobiliser une laccase de *Trametes versicolor* par greffage covalent avec du glutaraldéhyde. Les monolithes enzymatiques ont été utilisés pour dégrader la tétracycline (TC) en solution aqueuse dans un réacteur de configuration tubulaire type "Flow Through Reactor" avec recyclage. Au cours des 5 premières heures de réaction à pH 7 ; 40 à 50 % de la TC a été dégradée, puis un seuil a été atteint. Une des hypothèses pouvant expliquer ce comportement est un éventuel manque de co-substrat (oxygène) à proximité des sites catalytiques. Des monolithes enzymatiques ont été utilisés pendant 75 h de fonctionnement séquentiel sans perte d'activité. L'efficacité de la dégradation de la TC a pu être simulée à travers un modèle mathématique construit en couplant la cinétique de la réaction (Michaelis-Menten) avec un bilan matière en régime dynamique. Les résultats de la simulation ont révélé que le procédé global est contrôlé par la cinétique enzymatique mais que la taille des monolithes pouvait être adaptée pour dégrader 100 % de la CT en un seul passage à travers un monolithe.

Motts clés : Monolithes en silice, Laccase, Traitement de l'eau, Modélisation et simulation.

AKNOWLEDGEMENTS

First of all, I would like to thank my thesis director Dr. Jose Sanchez-Marcano for his support and advice throughout this journey. I appreciate the opportunity he gave me to join his research group. Similarly, my gratitude goes to my co-advisor Dr. Marie-Pierre Belleville, who was always available to discuss my work and gave me her valuable advice especially for experimental part.

I am very thankful to all those people who were involved in this project, this sincere contribution had high impact on my PhD thesis. Dr. Anne Galarneau, Mr. Wasim Sebai and Mr. Eddy Petit, thank you all for your contribution in this research work and scientific guidance. I would also thanks to my IEM colleagues Gabriella Vollet, Marine Harguindeguy, Wasim Sebai, Kyllian Goovaerts and Azariel Valencia for giving moral support and helping me to learn French culture and language. I am very thankful to my Pakistani friends in Montpellier who supported me in every situation.

I would like to thank jury members, Dr. Estelle Couallier, Prof. Eric Dubreucq and Prof. Pedro Lozano for accepting to be part of my thesis review and defense. Similarly, I am very thankful to Higher Education Pakistan (HEC) and Campus France, who funded and managed my stay in France.

Finally, I would like to thank my mother, my wife and my cute little baby Manha, my brother and sisters for their love, patience and unconditional support; without you this wouldn't have been possible.

Table of Content

List of Figures

List of Tables

List of Abbreviations

ABTS: 2,2'-azino-bis (3-ethylbenzothiazoline-6-sulphonic acid)

TEOS: Tetraethoxysilane

APTES: (3-aminopropyl) triethoxysilane

DO: Dissolved oxygen

ER: Enzymatic reactor

GLU: Glutaraldehyde

TC: Tetracycline

PPs: Pharmaceutical products

WWTP: Wastewater treatment plant

PBER: Pack bed enzymatic reactor

FBER: Fluidized bed enzymatic reactor

SEM: Scanning electron microscopy

TGA: Thermogravimetric analysis

EDCs: Endocrine-disrupting chemicals

EU WFD: European Union Water Framework Directive

AOP: Advance oxidation processes

PAC: Powdered activated carbon

GAC: Granular activated carbon

ASP: Activated sludge process

SMX: Sulfamethoxazole

SDM: Sulfadimethoxine

MBRs: Membrane bioreactors

AMBR: Aerobic membrane bioreactors

ANMBR: Anaerobic membrane bioreactors

SRT: Sludge Retention time

HRT: Hydraulic Retention time

TCS: triclosan

NP: Nonyl phenol

HRP: Horseradish peroxidase

MnP: Manganese peroxidase

NOR: Norfloxacin and

(CIP) Ciprofloxacin

List of Symbols and notations

$\frac{\Delta Abs.}{\Delta t}$= Change in absorbance of ABTS per unit time (minute)

V_T= Total volume of the ABTS solution used (L)

m= Mass of the crushed monolith used (wet basis) (g)

A_{sp}= Specific activity of the immobilized enzyme (Ug^{-1})

ε= Molar absorption coefficient of ABTS ($M^{-1}cm^{-1}$)

d= Path length of length (1 cm)

$A_{immobilized}$ = Theoritical immobilized activity (U).

$A_{observed}$ = Immobilized activity experimentally determined (U).

$A_{initial}$= Activity of the stock laccase solution used for immobilization step (U).

A_{left}= Activity of the unreacted laccase solution after immobilization step (U).

$A_{rinsing}$= Activity of the rinsing solution (U).

$\rho_{immobilization}$= Immobilization yield (%).

V = rate of substrate consumption (µmol min^{-1}).

V_{max} = Maximum rate of substrate consumption (µmol L^{-1} min^{-1}).

K_M = Michaelis-Menten constant (µmol L^{-1}).

S = Substrate concentration (µmol L^{-1}).

k = Permeability coefficient (m^2)

Q = Flow rate (m^3 s^{-1}),

A = Cross section of the monolith (m^2),

μ = Viscosity of the fluid (μ = 1.002 m Pa s at 20 °C for water),

l = Length of the monolith (m)

ΔP = Difference of pressure between the outlet and the inlet of the monolith (Pa).

u_{ave} = Average velocity (m s^{-1}) (Darcy velocity) (1-3 mm s^{-1}),

L_{bed} = Length of monolith (5 mm),

D_L = Dispersion coefficient ($1.5*10^{-9}$ m^2 s^{-1}).

V= Volume of the TC solution in the tank (mL).

Q = Flow rate (mL/min).

$\frac{dC_{TC}}{dt}$ = TC degradation rate.

$C_{in}{}^{n+1}$= Inlet TC concentration for a loop (n+1).

$C_{out}{}^{n+1}$= Outlet TC concentration for a loop (n+1).

n= Number of loops.

L= Half the thickness of the meso-porous skeleton.

D_e = Effective diffusion coefficient ($m^2\ s^{-1}$)

D = Diffusion coefficient

ε = Porosity

τ= Tortuosity inside the meso-pores.

Synthèse de travaux en français

Contexte

La présence dans l'environnement des produits pharmaceutiques (PPs) ou de leurs métabolites a considérablement augmenté ces cinquante dernières années, en raison de leur utilisation intensive. Ces molécules font partie, avec les produits phytosanitaires des micropolluants, car ils se trouvent à des concentrations relativement faibles dans les eaux usées (Halling-Sørensen et al., 1998), les eaux fluviales (Burns et al., 2018), les sédiments (Kerrigan et al., 2018) et le milieu marin (Björlenius et al., 2018). Les PPs qui appartiennent à la classe des contaminants émergents peuvent avoir un impact sur la santé des êtres vivants, y compris les humains, même si leurs effets toxicologiques précis restent mal connus. La pollution par les PPs se caractérise par le fait qu'elle est principalement générée par les humains eux-mêmes, et résulte de leur excrétion après consommation (Baker et al., 2014; Choi et al., 2018 ; Jones et al., 2014). L'excrétion d'une proportion importante des PPs sous forme non-métabolisée, conjuguée ou métabolisée est responsable de l'augmentation de cette pollution émergente dans les stations d'épuration des eaux usées (Coutu et al., 2013; Gerrity et al., 2011; Thiebault et al., 2017b). Cependant, certains de ces micropolluants sont très réfractaires à la dégradation et les installations actuelles de traitement sont inefficaces pour les éliminer complètement, quelle que soit la chaîne de traitement utilisée (Alvarino et al., 2018; Thiebault et al., 2017a).

La présence des PPs dans les effluents des usines de traitement d'eau, a permis leur transfert vers les milieux aquatiques. Et dans certains, cas ils se trouvent dans l'eau potable destinée à la consommation humaine (Bruce et al., 2010; de Jongh et al., 2012; Jones et al., 2005) ou polluent les sols agricoles suite à l'épandage de boues d'épuration (Hospido et al., 2010; Ivanová et al., 2018; Siemens et al., 2010). Plusieurs traitements tertiaires ont été proposés pour améliorer l'élimination des PPs des eaux usées, notamment les traitements par oxydation avancée (Almomani et al., 2016; Goi, 2005 ; Kanakaraju et al., 2018 ; Kıdak et Doğan, 2018), les techniques d'adsorption physique (charbon activé, graphène, etc.) (Rajapaksha et al., 2019; Rocha et al., 2020) et les traitements biologiques (bioréacteurs à boues activées/membranes) (Hörsing et al., 2011; Li et al., 2013). Toutefois, le besoin élevé en énergie et/ou les coûts de gestion élevés de ces procédés peuvent les rendre trop chers pour une application à grande échelle (Grandclément et al., 2017).

La dégradation enzymatique des PPs peut être une option parmi les autres traitements tertiaires évoqués précédemment, car les enzymes catalysent des réactions biochimiques dans des

conditions de fonctionnement modérées (pH, température, force ionique etc.). En raison de la capacité de certaines enzymes à oxyder une grande variété de PPs, les procédés enzymatiques sont étudiés comme une option intéressante pour la dégradation des micropolluants réfractaires et en particulier la dégradation des PPs (Naghdi et al., 2018a).

Parmi les enzymes qui ont été testées à ce propos, les oxydoréductases sont capables d'oxyder une grande variété de PPs comme les phénols, certains médicaments et hormones présents dans les eaux usées. Parmi les oxydoréductases, trois types d'enzymes : à savoir les laccases, les tyrosinases et les peroxydases ont été les plus étudiées ces dernières années (Singh Arora et Kumar Sharma, 2010; Demarche et al., 2012b; De Cazes et al., 2014).

Bien que la dégradation des PPs par des laccases libres ait démontré sa faisabilité à petite échelle, pour mettre en œuvre à grande échelle ce procédé, le biocatalyseur doit présenter une grande stabilité et être réutilisable. En effet, le procédé doit pourvoir fonctionner en mode continu (Gasser et al., 2014). L'immobilisation des enzymes sur des supports solides appropriés peut être une des solutions aux problèmes liés au procédés enzymatiques susmentionnés, car l'immobilisation augmente généralement la stabilité des biocatalyseurs pendant le stockage ainsi que dans les conditions de réaction (Sheldon, 2007; Iyer et Ananthanarayan, 2008; Cabana et al., 2009; Patel et al., 2014; Zhang et al., 2015; Zheng et al., 2016; Ji et al., 2017). Plusieurs techniques d'immobilisation comme l'adsorption, le piégeage ou l'encapsulation ont été appliquées pour l'immobilisation d'enzymes sur des supports solides. Cependant, l'immobilisation covalente sur supports solides améliore leur stabilité ainsi que la durabilité du procédé à long terme (Zdarta et al., 2018). Les supports inorganiques comme la silice, la zircone, les charbons actifs ont été étudiés pour l'immobilisation des enzymes en raison de leur résistance mécanique, thermique et au pH. Par ailleurs, ils présentent généralement une bonne stabilité opérationnelle, de bonnes propriétés de sorption, une inertie et une relative facilité de fonctionnalisation de surface (Arca-Ramos et al., 2016 ; Sadeghzadeh et al., 2020 ; Mohamadi et al., 2018 ; Bebić et al., 2020 ; Zdarta et al., 2020).

Différentes configurations deréacteurs enzymatiques (ER) ont été étudiées, tels que les réacteurs à lit fixe (PBER) (Nguyen et al., 2016 ; Bilal et Iqbal, 2019), les réacteurs à lit fluidisé (FBER) (Lloret et al, 2012 ; Piao et al., 2019) ainsi que les réacteurs à membrane enzymatique (EMR) (De Cazes et al., 2014 ; Barrios-Estrada et al., 2018 ; Gamallo et al., 2018). La dégradation des PPs dans des PBER ont montré de faibles taux de conversion en raison des limitations dues à la diffusion et/ou au manque d'oxygène co-substrat fondamental pour la réaction de dégradation (Tušek et al., 2017). Les FBER semblent être intéressants en raison de

leur grande efficacité de dégradation (Lloret et al., 2012). Cependant, ils présentent des coûts opérationnels élevés et des problèmes de pertes de charge peuvent avoir lieu. Les réacteurs à membrane enzymatique (EMR) ont été les plus étudiés pour la dégradation enzymatique des PP.

Les EMR présentent certaines propriétés intéressantes car ils peuvent être utilisés dans différentes configurations (enzyme immobilisée sur la surface de la membrane ou sur un solide formant un lit inséré à l'intérieur du compartiment interne d'une membrane tubulaire). De plus, les procédés membranaires étant modulaires ils permettent un changement d'échelle relativement simple. Néanmoins, les EMR peuvent également présenter certains inconvénients comme le colmatage des membranes ou une faible réactivité. Ji et al, (2016c) ont observé moins de 10 % de dégradation de la carbamazépine avec la laccase de *Trametes versicolor* dans un EMR. Barrios-Estrada et al, (2018b) ont trouvé que seulement 33 % de la concentration initiale de bis-phénol-A (BPA) se dégrade en 24h avec une laccase immobilisée sur les membranes céramiques. Par ailleurs, De Cazes et al. (2014) n'ont trouvé que 56 % de la dégradation de la TC en 24 h avec une laccase de *Trametes versicolor* immobilisée sur des membranes céramiques. Dans les deux derniers travaux, la conversion obtenue n'est pas très élevée ; ces résultats ont été en partie expliqués par la faible quantité d'enzymes immobilisées en raison de la surface spécifique limitée des membranes céramiques.

Afin de surmonter certains de ces inconvénients, comme les problèmes de diffusion rencontrés sur les PBER ou la surface spécifique limitée des EMR, des monolithes poreux hiérarchisés ont été récemment appliqués dans les ER avec un grand succès (Biggelaar et al., 2019). Les monolithes macro-méso poreux ont une structure extrêmement poreuse avec des macropores interconnectés et un réseau continu de squelette méso poreux. Les macropores ayant un diamètre de pore de l'ordre de (30-50 μm) contribuent à l'écoulement à travers les monolithes, en limitant les pertes de charge tandis que les mésopores ayant un diamètre de pore de l'ordre de (5-20 nm) fournissent une grande surface (500-700 m^2 g^{-1}) disponible pour l'immobilisation ; cela devant permettre d'immobiliser une très grande quantité d'enzyme et ainsi augmenter la réactivité en comparaison aux EMR.

Ce projet de recherche, avec une double approche expérimentale et de modélisation vise à étudier la dégradation enzymatique de PPs par une laccase immobilisée sur des monolithes en silice. Les monolithes en silice ont été sélectionnés comme matériau de support car ils présentent une grande surface disponible pour l'immobilisation des enzymes ainsi que de grands diamètres de macropores permettant des flux élevés avec une faible perte de charge. La

tétracycline (TC) a été choisie comme molécule modèle de PPs car elle a une cinétique de réaction relativement bien connue permettant ainsi d'établir un modèle mathématique et de pouvoir simuler le procédé a d'autres échelles que celle du laboratoire. Les monolithes de silice ont été préparés par le procédé sol-gel selon la méthode précédemment expliquée par Galarneau et al. (2016) et ont été préactivés avec un aminosilane, puis gainés avec des gaines transparentes en Teflon™ thermorétractables afin être utilisés comme réacteurs à flux continu. Dans ce travail de recherche, la laccase commerciale de *Trametes versicolor* a été sélectionnée comme biocatalyseur car cette enzyme n'a besoin que d'oxygène comme co-substrat et elle a de très bonnes propriétés oxydantes vis-à-vis de nombreux micropolluants comme les antibiotiques. En outre, cette enzyme est actuellement disponible auprès de fournisseurs commerciaux. Pour ce faire une laccase commerciale de *Trametes versicolor* a été immobilisé par liaisons covalente via du glutaraldéhyde (GLU), dans les monolithes en silice pré-activés et gainés.

Une installation à l'échelle du laboratoire a été mise au point en connectant en série trois monolithes enzymatiques et en faisant passer à travers ces derniers une solution de TC, préparée dans l'eau osmosée. La solution est mise en circulation et recyclée dans le réservoir d'alimentation grâce à une pompe HPLC. La caractérisation de la surface des monolithes (bruts et activés) a été réalisée par analyse MEB, par porosimétrie Hg et adsorption d'azote. La chromatographie liquide à haute performance (HPLC) couplée à l'analyse par spectrométrie de masse a été réalisée pour l'analyse de l'évolution de la concentration de la TC dans la solution de TC. Le travail de recherche expérimental a été effectué dans des conditions de laboratoire à très petite échelle (débit de 1 ml min^{-1}) et à une concentration de TC relativement élevée (20 mg L^{-1}), si on tient compte les débits (de l'ordre de milliers de M^3/jour, selon le nombre d'habitants) et le niveau de concentration réelle de la TC couramment trouvée dans les eaux usées des villes (~0,28 µg L^{-1}) (Danner et al. 2019). La modélisation et la simulation sont des outils fondamentaux pour reproduire des expériences dans les conditions qui sont coûteuses ou impossibles à réaliser, mais leur principal avantage est de pouvoir calculer le changement d'échelle du procédé en utilisant des paramètres à l'échelle du laboratoire. Les rares modèles de transport de fluides à travers les monolithes qui ont été rapportés dans la littérature, tiennent compte de la structure microscopique interne et ont développé des approches pour la simulation des champs de vitesse, de la diffusion et de la dispersion des espèces chimiques au sein de la structure poreuse (Jungreuthmayer et al., 2015; Tallarek et al. 2002; Meyers et Liapis., 1999). Ces modèles sont basés sur la morphologie et la structure réelle des monolithes poreux, ce qui a nécessité des techniques de calcul complexes couplés aux techniques de traitement d'images

ainsi que des temps de calcul et des coûts de simulation relativement importants. En outre, la littérature ne présente aucune étude de modélisation, qui permette de simuler le couplage entre une cinétique de réaction et le transport des espèces dans des monolithes macroporeux. Dans cette thèse il est développé un modèle de transport de masse CFD en régime permanent basé sur une géométrie monolithique homogénéisée. Ce modèle a été couplé à une modélisation du bilan de transport de masse transitoire dans réservoir d'alimentation de la solution de TC afin de calculer la variation de la concentration de TC en fonction du temps. Le modèle développé a aussi été appliqué pour étudier la dégradation de la TC aux concentrations réelles trouvées dans les eaux usées, puis pour proposer le changement de l'échelle du procédé pour le traitement des trois cas : des eaux usées d'origine municipale, hospitalière et industrielle.

Objectifs de la thèse

L'objectif principal de ce travail de recherche est d'étudier la possible utilisation des monolithiques enzymatiques pour la dégradation des PPs. Cet objectif a été divisé en deux parties: 1-l'étude expérimentale à l'échelle du laboratoire de la dégradation de la TC dans l'eau osmosée (réaction modèle de PPs) ; 2-proposer un modèle permettant d'étudier d'une part le transport des fluides et espèces au travers les monolithes enzymatiques en le couplant à la cinétique de dégradation enzymatique et d'autre part de faire la simulation de la mise à l'échelle du procédé pour la dégradation des PPs avec des exemples réels.

Pour l'objectif principal de ce travail de recherche, il a été nécessaire de:

- Immobiliser par liaison covalente de la laccase sur des monolithes de silice par GLU comme agent de réticulation.
- Mesurer l'activité de la laccase immobilisée et de la laccase libre.
- Estimer les paramètres cinétiques de la réaction (V_{max} et K_M) pour deux substrats : ABTS et TC.
- Etudier la stabilité au stockage de la laccase immobilisée
- Réaliser des tests de dégradation de la TC en batch pour étudier l'effet des paramètres du procédé ainsi comme la concentration en oxygène en produits de dégradation, possibles inhibiteurs de la réaction de dégradation de la TC.
- Mettre en place d'un pilote du laboratoire pour tester la dégradation de la TC avec de monolithes activés en mode de recyclage continu.
- Etudier la stabilité opérationnelle des monolithes activés pour la dégradation de la TC en mode de recyclage continu et effets du débit de recyclage.

- Développer un modèle CFD en utilisant une géométrie des monolithes considérée comme homogène, ce modèle étant couplé à la cinétique enzymatique et à un modèle de transport de masse transitoire sur le réservoir d'alimentation pour calculer l'évolution de la dégradation de la TC.
- Appliquer le modèle développé pour simuler la dégradation de la TC contenue dans des eaux résiduelles réelles tout en réalisant le changement d'échelle pour des procédés de taille industrielle.

Schéma de la thèse

Comme il a été expliqué ci-dessus cette thèse concerne l'étude de la dégradation de la TC, considérée comme un PPs récalcitrant modèle, par une laccase immobilisée sur des supports monolithiques, dans un réacteur tubulaire en flux continu avec recyclage, à travers d'une double approche expérimentale et théorique via la modélisation et la simulation. Cette thèse est structurée en 6 chapitres, comme suit;

Le **chapitre 1** présente le contexte et les objectifs de ce travail de recherche.

Le **chapitre 2** présente l'état de l'art concernant la présence et le devenir des PPs dans les eaux usées ainsi que leurs traitements potentiels afin d'éviter leur rejet dans l'environnement. Les différentes techniques utilisées pour éliminer/dégrader les PPs dans les eaux usées sont présentées et la dégradation enzymatique des PPs par les laccases est décrite en détail. Différentes techniques d'immobilisation et types de réacteurs enzymatiques sont présentés en bref avec leurs avantages et leurs inconvénients. Enfin, les supports monolithiques utilisés pour l'immobilisation des enzymes et les propriétés des différents modes de transport sont décrits.

Le **chapitre 3** présente les méthodes et le matériel expérimental utilisés dans ce travail de recherche pour caractériser les monolithes à laccase immobilisée et pour déterminer la cinétique enzymatique. Ainsi, sont décrits en détail, les méthodes expérimentales utilisées pour déterminer l'activité de la laccase libre et immobilisée, les paramètres de la cinétique de réaction, la stabilité de la laccase immobilisée lors du stockage et les effets d'autres paramètres tels que l'oxygène dissous (OD) ainsi que les effets possibles des produits inhibiteurs et enfin le pilote du laboratoire conçu et utilisé pour étudier la réaction de dégradation de la TC avec des monolithes enzymatiques en utilisant le concept de « Flow Through Reactor ».

Le **chapitre 4** présente en détail les résultats de la partie expérimentale. Le chapitre commence par les résultats de la caractérisation de la surface et structure des monolithes avant et après l'immobilisation. Ensuite, les résultats de l'activité des laccases immobilisées et du rendement

de l'immobilisation sont brièvement abordés. Les résultats des paramètres cinétiques de réaction (K_M et V_{max}) pour pour l'ABTS ainsi que la TC sont brièvement discutés. Les résultats des tests de dégradation de la TC effectués au niveau pilote avec des monolithes insérés dans un réacteur tubulaire fonctionnant en continu avec recirculation à sont également discutés en détail.

Le **chapitre 5** est divisé en deux parties ; la première partie est consacrée à l'élaboration d'un modèle mathématique pour la dégradation de la TC dans l'eau avec des monolithes enzymatiques en considérant une configuration de réacteur à flux continu avec recyclage. La construction du modèle a été réalisée en deux étapes: dans un premier temps, un modèle de type CFD en régime permanent ainsi qu'en fonction du temps a été développé dans COMSOL MULTIPHYSICS® 5.3. Certains paramètres du modèle, comme la cinétique de réaction et le coefficient de perméabilité, ont été obtenus à partir de résultats expérimentaux (chapitres 3 et 4). La modélisation a été réalisée en considérant une géométrie homogénéisée des monolithes et la cinétique utilisée correspond au modèle cinétique de Michaelis-Menten (V_{max} et K_M) obtenu avec des monolithes activés et broyés dans un réacteur parfaitement agité. Le pourcentage de dégradation de la TC lors d'un seul passage à travers le réacteur monolithique a été calculé. Dans un second temps, un modèle dynamique de bilan de matière a été développé dans MATLAB® 2017 pour calculer la variation de la concentration en TC en fonction du temps dans le réservoir d'alimentation. Les deux modèles ont ensuite été couplés via la fonction Live-link de COMSOL-MATLAB et exécutés simultanément. Ce couplage a permis de calculer de l'évolution de la concentration en TC dans le réservoir d'alimentation. Les limites de transfert de masse externe et interne ont également été étudiées. La seconde partie de ce chapitre est consacrée à l'étude des simulations en ne considérant que les temps de réaction initiaux, et en ne considérant qu'un seul passage dans les réacteurs monolithiques. En effet, la simulation de la distribution des concentrations de TC à travers les monolithes est présentée pour un état stationnaire et en régime transitoire. L'influence des limitations de diffusion interne et externe au sein de la structure des monolithes est également prise en compte. Enfin, les résultats de la simulation de réacteurs monolithiques enzymatiques à grande échelle pour la dégradation complète de la TC ainsi que leur mise en œuvre pour le traitement des eaux usées dans des exemples réels sont présentés.

Le **chapitre 6** présente la conclusion générale des travaux de recherche effectués lors de cette thèse pour la dégradation des PPs ainsi que les perspectives pour les travaux futurs.

Résultats, conclusions et perspectives

Des monolithes de silice présentant des structures macro-/mésoporeuses uniformes (diamètres des macro- et mésopores de 20 μm et 20 nm, respectivement), une porosité élevée (83 %) et une surface élevée (370 m^2 g^{-1}) ont été préparés à l'ICGM. Les monolithes ont été greffés avec des groupes amine- (0,9 mmol NH_2 g^{-1}) et utilisés pour immobiliser la laccase de *Trametes versicolor* par liaison covalente via du glutaraldéhyde (GLU) (1,0 mmol GLU g^{-1}). Les monolithes activés ainsi obtenus présentent une activité enzymatique vis-à-vis de l'ABTS de 20 U $g^{-1}_{monolithe}$. Le rendement d'immobilisation basé sur la différence entre l'activité initiale et finale de la solution enzymatique utilisée pour l'immobilisation est égal à 80%. L'efficacité d'immobilisation (E) et de l'activité exprimée ($A_{exprimé}$) étaient respectivement égales à 310 % et 250 %. La valeur de la constante d'affinité K_M pour les enzymes libres et immobilisées (monolithes broyés) avec les deux substrats étudiés (ABTS et TC) ont révélé qu'après immobilisation, la valeur K_M apparente diminue de 1,6 et 4 fois pour ABTS et TC, respectivement. Ces résultats montrent qu'après l'immobilisation, l'affinité de la laccase pour le substrat augmente. Les monolithes activés par la laccase stockés à 4°C ont conservé plus de 90% de leur activité après 30 jours de stockage, ce qui montre que les monolithes activés peuvent être stockés relativement très longtemps sans perdre leur activité.

Les résultats des tests de perméabilité à l'eau montrent que les monolithes sont très perméables (coefficient de perméabilité, k= 5,95 10^{-12} m^2) en raison de leur structure macroporeuse interconnectée. Les monolithes activés ont été ensuite utilisés pour la dégradation de la tétracycline (TC) en solutions aqueuses (20 mg L^{-1}) dans un réacteur tubulaire en flux continu (1 ml min^{-1}) mais avec recyclage de la solution de TC. Pendant les premières 5 heures de réaction à pH de 7 la concentration de TC diminue d'un 40 à 50 %, mais ensuite cette concentration reste constante. Afin d'étudier la stabilité opérationnelle de la laccase immobilisée les monolithes enzymatiques ont été utilisés en fonctionnement séquentiel pour une durée totale de 75 heures sans perte d'activité. Par ailleurs, 85% de l'activité initiale des monolithes est obtenue après 30 jours de stockage à 4°C et pH 7 ce qui confirme une très bonne stabilité des enzymes immobilisées. Les effets de différents facteurs tels que l'oxygène dissous (OD), la concentration des produits de dégradation et le flux de recirculation sur l'efficacité de la dégradation des TC ont été étudiés. Il a été observé que l'OD et les produits de dégradation augmentent le taux de dégradation de la TC alors que le flux de recirculation n'a aucun effet sur la dégradation du TC dans la gamme de variation des paramètres étudiés dans ce travail.

Un modèle mathématique a été développé et été réalisé en deux parties : dans la première partie, un modèle de CFD en régimes permanent et transitoire a été développé dans COMSOL MULTIPHYSICS® 5.3. Certains paramètres du modèle, comme la cinétique de réaction et le coefficient de perméabilité, ont été obtenus à partir de résultats expérimentaux (chapitre 3). La modélisation a été basée sur le modèle de cinétique de réaction de Michaelis-Menten (V_{max} et K_M) et considère une géométrie homogénéisée des monolithes. La dégradation de la TC lors d'un unique passage à travers les monolithes a été calculée. Dans la seconde partie, un modèle dynamique de bilan de transport de masse a été développé dans MATLAB® 2017 pour calculer la variation de la concentration en TC en fonction du temps dans le réservoir d'alimentation. Les deux modèles ont été couplés via la fonction Live-link de COMSOL-MATLAB et ont été exécutés simultanément. Ce couplage de modélisation a permis de calculer l'évolution dans le temps de la concentration en TC dans la cuve d'alimentation. Cependant, le modèle développé a été validé avec les résultats expérimentaux, mais seulement pendant les 2 premières heures de réaction, c'est-à-dire pendant les temps de réaction initiaux lorsque la concentration de TC et d'oxygène ne sont pas limitantes. Après 5 heures de réaction, la concentration expérimentale en TC atteint un plateau, indiquant qu'il y a certainement des limitations cinétiques ou de transfert de masse qui ne sont pas prises en compte dans les équations du modèle. Néanmoins, si le temps de séjour est faible et que le système monolithique fonctionne en mode d'écoulement unique, ce modèle peut être applicable.

Par la suite, toutes les simulations ont été effectuées en considérant un seul monolithe (avec une longueur équivalente à la somme de trois monolithes en série utilisés expérimentalement) et un seul passage de la solution de TC dans le monolithe (pas de recyclage de la solution) afin d'avoir une con concentration d'entrée constante avec une conversion faible et ainsi éviter les limitations observées auparavant. La simulation CFD en régime permanent ont montré qu'en un seul passage, seul 0,2 % de la CT est oxydé. Cette très faible conversion de CT est due à deux facteurs : une cinétique de réaction très lente ($4{,}4 \times 10^{-5}$ µmol L^{-1} min^{-1}) et un flux convectif relativement élevé ($5{,}9 \times 10^{-4}$ m s^{-1}) (Figure 1-1).

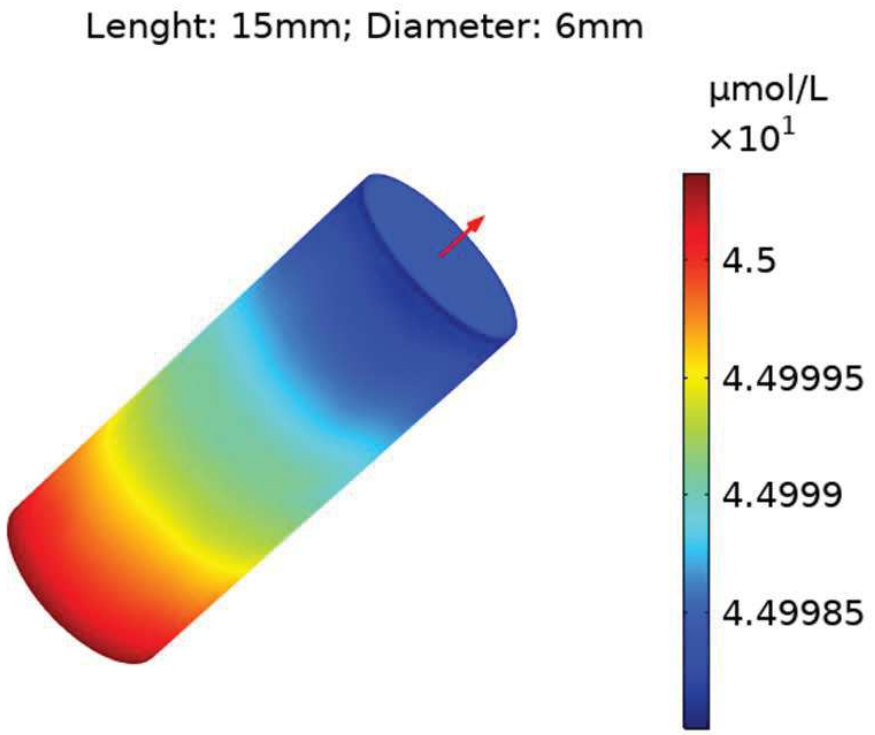

Figure 1-1. Distribution de la concentration en TC en état stationnaire sur toute la longueur du réacteur. Débit : 1 ml min^{-1} ; concentration de TC à l'entrée de 45 µmol L^{-1} (20ppm) ; vitesse linéaire de la solution : 5,9x10^{-4} m s^{-1} ; taux de réaction : 4,4x10^{-5} µmol L^{-1} min^{-1}.

Ce résultat suggère que pour dégrader complètement la TC en un seul passage, soit la cinétique de la réaction doit être très élevée (ce qui dépend de la nature des enzymes, de leur concentration dans les monolithes ainsi que des protocoles d'immobilisation) soit en augmentant les dimensions du monolithe. La taille optimale des monolithes a ainsi été calculée et il a pu être déterminé que des monolithes de 50 cm de long et de 20 cm de diamètre permettaient de dégrader complètement la TC lors d'un passage unique au débit de 1 ml min^{-1} mais pour une eau contenant seulement 0,28 µg L^{-1}, concentration courante que l'on trouve actuellement dans les eaux usées d'origine domestique, comme le suggèrent Danner et al. (2019) et (Abejón et al., 2015).

La dernière partie du travail concerne des calculs de simulation en vue d'une possible mise en œuvre à grande échelle de monolithes enzymatiques dans les stations d'épuration municipales. Pour ce faire, la configuration en parallèle des monolithes a été suggérée pour augmenter la capacité de traitement, car la capacité d'un monolithe unique est basée sur un débit de 1-5 mL min^{-1}. Le nombre calculé de monolithes et la surface nécessaire pour traiter les débits des eaux usées municipales (70 000 m3/jour pour une ville de 200.000 habitants) étaient de 24 305 000.

Ce nombre de monolithes est extrêmement élevé et certainement pas réalisable. En effet, le procédé monolithique enzymatique n'est ni pratique ni économique pour être mis en œuvre à grande échelle.

Pour conclure, la laccase a été immobilisée avec succès sur des monolithes en silice avec un rendement et efficacité d'immobilisation élevés. Les monolithes activés par la laccase ont été capables de dégrader entre 40 à 50 % d'une solution de 20 ppm de TC à l'échelle du laboratoire. Cependant, certains paramètres semblent limiter la vitesse de dégradation : concentration en OD, les limitations de la vitesse de réaction ou de transfert de matière. Les résultats de la simulation ont montré un bon accord avec les résultats expérimentaux dans les 5 premières heures de réaction, ce qui a montré que le modèle ne tient pas compte de certaines limitations cités ci-dessus, cependant il peut être utilisé sans raisonnablement pendant les temps initiaux de la réaction.

La mise en œuvre à grande échelle des monolithes enzymatiques pour les eaux usées municipales, hospitalières et industrielles proposée par la modélisation et la simulation, ne semble pas être possible en raison du très grand nombre de monolithes enzymatiques nécessaires pour traiter les eaux usées. La raison de ce grand nombre de monolithes est en premier lieu la très faible cinétique de réaction enzymatique. C'est pourquoi des améliorations du procédé enzymatique sont nécessaires, elles comprennent l'immobilisation d'une laccase beaucoup plus active sur la surface des monolithes. Dans ce cas, la vitesse de réaction peut être augmentée, et par conséquent, le nombre de monolithes requis pour traiter les eaux usées peut être considérablement réduit. Une autre solution possible serait l'application du procédé au traitement des concentrés obtenus par nanofiltration des eaux contenant des antibiotiques. Dans ce cas, les volumes à traiter seraient beaucoup plus faibles et nécessiteraient de capacités de traitement moins importantes. En contrepartie, du fait d'une concentration en antibiotiques relativement plus élevée et il faudrait alors résoudre le problème des limitations en oxygène.

Chapter 1

Introduction

1. INTRODUCTION

1.1 Background

Due to high consumption of pharmaceutical products (PPs) since 1960s, their occurrence is significantly increased within various environmental compartments such as wastewaters (Halling-Sørensen et al., 1998), river waters (Burns et al., 2018), sediments (Kerrigan et al., 2018) and sea waters (Björlenius et al., 2018). PPs are considered as emerging micropollutants as they may impact the health of living beings, including humans, even if their precise toxicological effect remains poorly recognized (Arnold et al., 2014; Carlsson et al., 2006). However, several disorders have already been observed among fauna such as fish or bacteria at field relevant concentrations or in real solutions (Arnold et al., 2014; Brodin et al., 2013; Saaristo et al., 2018). Contamination by PPs is distinctive in that it is mostly generated by people themselves, via the consumption/excretion of PPs (Baker et al., 2014; Choi et al., 2018; Jones et al., 2014). After being consumed, a significant proportion of PPs is excreted in maternal, conjugated or degraded forms which causes the transfer of this contamination toward wastewater treatment plants (WWTP) (Coutu et al., 2013; Gerrity et al., 2011; Thiebault et al., 2017b). However, the current facilities installed in WWTP are inefficient to completely remove PPs, regardless of the treatment techniques used (Alvarino et al., 2018; Thiebault et al., 2017a). Due to their recalcitrant nature, PPs remain in wastewater effluents and their transfer within aquatic environments can lead them to enter drinking water (Bruce et al., 2010; de Jongh et al., 2012; Jones et al., 2005) or to contaminate agricultural soils following spreading of sewage sludge (Hospido et al., 2010; Ivanová et al., 2018; Siemens et al., 2010). Several tertiary treatments have been proposed to improve the removal of PPs from wastewater including chemical treatment (advance oxidation treatment) (Almomani et al., 2016; Goi, 2005; Kanakaraju et al., 2018a; Kıdak and Doğan, 2018), physical adsorption techniques (carbon, graphene etc.) (Rajapaksha et al., 2019 ; Rocha et al., 2020) and biological treatment (activated sludge/membrane bioreactors) (Hörsing et al., 2011; Li et al., 2013). However, the high energy requirement and/or high management costs of these processes can make them too expensive for a field application (Grandclément et al., 2017).

Enzymatic degradation of PPs can be an alternate option among the other tertiary treatments discussed previously, since enzymes mediate biochemical reactions at a rapid rate under mild operating conditions (pH, temperature, solvents and ionic strength). Due to the ability of certain enzymes to oxidize a wide variety of PPs, enzymatic processes are being explored as an

interesting option for the degradation of micropollutants and in particular the degradation of PPs (Naghdi et al., 2018a).

Oxidoreductases enzymes are able to oxidize large variety of PPs like phenols, drugs and hormons in wastewater. Among oxidoreductases, three enzymes: Laccases, Tyrosinase and peroxidases are the most studied in recent past (Singh Arora and Kumar Sharma, 2010; Demarche et al., 2012b).

In this research work, Laccase from *Trametes versicolor* has been selected as biocatalyst because among different oxidative enzymes as it only requires oxygen as co-substrate; it has very good oxidative properties towards many micropollutants such as antibiotics. Moreover, this enzyme is currently available from commercial providers.

Although the degradation of PPs by free laccase has demonstrated its feasibility on small batch scale, in order to implement it on a large scale, the process must be operated in continuous mode and the biocatalyst must show high stability and be reusable (Gasser et al., 2014). Immobilizing enzymes on suitable solid supports can be one of the solutions to above mentioned problems related to enzymatic process, because immobilization generally increases the stability of enzymes during storage as well as under reaction conditions (Sheldon, 2007; Iyer and Ananthanarayan, 2008; Cabana et al., 2009; Patel et al., 2014; Zhang et al., 2015; Zheng et al., 2016; Ji et al., 2017). Several immobilization techniques like adsorption, entrapment, encapsulation has been applied for enzyme immobilization on solid supports. However, covalent immobilization of enzyme on solid supports enhanced the enzyme stability on solid support and long-term process sustainability (Zdarta et al., 2018). Inorganic support materials like silica, zirconia, active carbons are explored for immobilization of enzymes due to their mechanical strength, resistance to temperature and pH, operational stability, good sorption properties, inertness and easy surface functionalization (Arca-Ramos et al., 2016); (Sadeghzadeh et al., 2020); (Mohamadi et al., 2018); (Bebić et al., 2020); (Zdarta et al., 2020).

Enzymatic reactors (ER) have been explored in different reactor configuration like packed bed reactors (Nguyen et al., 2016a); (Bilal and Iqbal, 2019), fluidized enzymatic bed reactors (FEBR) (Lloret et al., 2012); (Piao et al., 2019) as well as enzymatic membrane reactors (EMR) (de Cazes et al., 2014); (Barrios-Estrada et al., 2018b); (Gamallo et al., 2018). The packed-bed enzymatic reactors (PBER) for the degradation of PPs suffered from low degradation rates due to oxygen limitations (Tušek et al. 2017). Even if FEBRs seems to be interesting due to high degradation efficiency (Lloret et al., 2012), they present high operational

costs and pressure drops problems can occur. Enzymatic membrane reactors (EMR) are the most investigated reactors for enzymatic degradation of PPs. These reactors present some interest properties because they can be used in different configurations (enzyme immobilized on membrane surface or on a solid bed inserted inside the membrane lumen). Moreover, membrane systems are modular and scale up is easily designed. Nevertheless, some drawbacks can also be present like membrane clogging, low reactivity etc. Ji et al., (2016c) observed less than 10 % of carbamazepine degradation with laccase from *Trametes versicolor* without using mediators. Barrios-Estrada et al., (2018b) found only 33% of initial concentration of BPA degraded in 24h with immobilized laccase on ceramic membranes. Similarly, de Cazes et al., (2014a) found only 56 % of TC degradation in 24 h with laccase from *Trametes versicolor* immobilized on ceramic membranes. In the last two works the limited conversion achieved can be explained by the low amount of enzymes immobilized due to the limited specific surface of ceramic membranes. In order to overcome some of these disadvantages like diffusional problems encountered for example on PBER or limited specific surface of EMR, hierarchal porous monoliths have been recently applied in catalysis with great success (Biggelaar et al., 2019). Macro-meso porous monoliths have highly porous structure having interconnected macropores and a continuous meso-porous skeleton network. Macropores having pore diameter in the range of (30-50 μm) contribute to flow through the monoliths, while mesopores having pore diameter in the range of (5-20 nm) provide a large surface area (500-700 m^2 g^{-1}) available for immobilization.

This research project aims at experimental as well as modelling investigation of enzymatic degradation of PPs by laccase immobilized on silica monoliths. Monoliths were selected as a support material due to their large surface area available for enzyme grafting and large flow-through pores which ensures high flow with low pressure drop. Another advantage of silica monolith is the easy-scale up and ready to use after immobilization step. Tetracycline (TC) was selected as a model PP to determine the reaction kinetics. Silica monoliths were prepared by sol-gel process according to the method previously explained by Galarneau et al. (2016) and were preactivated with amino groups and then cladded with heat shrinkable transparent gains to be used as continuous flow reactors. Laccase from *Trametes versicolor* was immobilized in preactivated silica monoliths cladded inside Teflon™ gains via crosslinking with glutaraldehyde (GLU). A lab scale set up was developed by connecting three laccase-activated monoliths in series with HPLC pump for TC degradation in osmosed water. Monoliths (raw as well as immobilized) surface characterization was carried out by SEM

analysis as well as Hg porosimetery. High performance liquid chromatography coupled with mass spectrometric analysis were carried out for TC concentration analysis.

This research work was carried out at experimental lab conditions at very small scale (1 mL min^{-1}) and relatively high TC concentrations (20 mg L^{-1}) compared to actual TC concentrations found in municipal wastewater (0.28 µg L^{-1}) (Danner et al. 2019). Therefore, modelling and simulation becomes potential tools as it replicates the experiments at the conditions that are costly or not possible by experiments. Another advantage of modelling is to propose scale up of the process by using lab-scale parameters. The few reported models of mass transport through monoliths considers the microscopic structure and developed approaches for simulation of velocity fields, diffusion and dispersion of chemical species within the porous structure (Jungreuthmayer et al., 2015); (Tallarek et al. 2002); (Meyers and Liapis., 1999). These models are based on morphology and real structure of the porous monoliths, which required high computational techniques like image processing techniques as well as relatively large computing times and simulation costs especially for large scale geometries required for practical engineering problems. Moreover, in literature, there is no specific modelling study, which simulates the reaction kinetics coupled with transport of species within macroporous silica monoliths.

In the modelling part, a steady-state CFD mass transport model based on homogenized monolith geometry was coupled to transient mass transport balance modelling of feed tank to compute TC concentration change with time. The developed model was applied to study the TC degradation at actual wastewater concentrations and then to propose the scale up of the enzymatic monolithic process for municipal wastewater treatment.

1.2 Research objectives

The main objective of this research work is to study the feasibility of enzymatic monolithic supports for PPs degradation in osmosed water at lab-scale through experimentation and then to propose the scale up of the enzymatic monolithic process for PPs degradation through modelling and simulation based on lab-scale parameters.

In order to achieve the main objective, following objectives were accomplished during this research work.

- Synthesis of silica monoliths with uniform macro/meso porosity.
- Covalent immobilization of laccase on silica monoliths via GLU as a cross linking agent.

- Activity measurement of immobilized and free laccase.
- Estimation of reaction kinetic parameters (V_{max} and K_M) for two substrates: (2,2′-Azino-bis(3-ethylbenzothiazoline-6-sulfonic acid)) (ABTS) and Tetracycline (TC)**.**
- Storage stability of immobilized laccase
- TC degradation tests in batch to study the effect of process parameters like DO concentration and TC inhibiting degradation products.
- Lab-scale set up for laccase-immobilized monoliths and TC degradation tests in continuous recycle-mode.
- Operational stability of immobilized monoliths for TC degradation in continuous recycled mode and effects of recycled flow rate.
- Development of CFD model for homogenized monolith geometry coupled with transient mass transport model on feed tank to compute TC degradation.
- Application of the developed model for actual TC concentration found in wastewater.
- Scale up of the enzymatic monolithic process for the degradation of TC at municipal wastewater treatment plant scale.

1.3 Thesis Outline

This thesis describes the ability of enzymatic monolithic supports for the bio-degradation of TC (a recalcitrant antibiotic) through experimentation, modelling and simulation. This thesis is structured in 6 chapters, as follows;

Chapter 1 introduces the background and the research objectives of this research work.

Chapter 2 presents the state of the art regarding the occurrence and fate of the PPs in wastewater and their potential treats to the environment. Different techniques used to remove/degrade PPs in wastewater are described in detail. The enzymatic degradation of PPs by laccases is described in detail. Different immobilization techniques and enzymatic reactors configuration are discussed in brief with their advantages and disadvantages. Finally, the monolithic supports used for enzyme immobilization and the transport properties of the monoliths are described in brief.

Chapter 3 presents the experimental methods and materials used in this research work to characterize the monoliths with immobilized laccase and to determine the enzymatic kinetics. Batch experimental approach to determine activity of free and immobilized laccase, reaction kinetics parameters, storage stability of immobilized laccase and effects of parameters like dissolved oxygen (DO) as well as possible inhibiting products effects is described in detail.

Finally, a lab-scale set up is described in detail to study the applicability of monoliths in flow through mode for TC degradation, and operational stability tests are described in detail.

Chapter 4 presents the results of the experimental part in detail. The chapter starts with monoliths surface characterization results before and after immobilization. Then, immobilized laccase activity and immobilization yield results are discussed in brief. The results of reaction kinetic parameters (K_M and V_{max}) for TC as well as for ABTS are discussed briefly. Results TC degradation tests carried out with laccase-activated flow through monoliths are discussed in detail.

Chapter 5 This chapter is divided into two parts; first part is devoted to the model development for the TC degradation in water by enzymatic monolithic reactors considering the flow-through reactor configuration with recycling. Simulation results of the developed model are presented in second part of the chapter. The building of the model was carried out in two parts: in the first part, steady-state as well as time-dependent CFD model was developed in COMSOL MULTIPHYSICS® 5.3. Some model's parameters, like reaction kinetics and permeability coefficient were obtained from experimental results (chapter 3). The modelling was based on the reaction kinetic model of Michaelis-Menten (V_{max} and K_M) and considers a homogenized geometry of monoliths. Indeed, the TC degradation in a single pass was computed. In the second part, a dynamic mass transport balance model was developed in MATLAB® 2017 to compute TC concentration change with time in the feed tank. Both models were coupled via COMSOL-MATLAB Live-link feature and run simultaneously. This modelling coupling allowed determining the computation of TC concentration evolution in the feed tank. External and internal mass transfer limitations were also studied. The model developed was validated with the experimental results, but only during first 5 hours of reaction, it means during initial reaction times when TC and oxygen concentration are not limiting, After 5 hours of reaction, experimental TC concentration reaches a plateau, indicating there are certainly kinetic or mass transfer limitations that are not considered in model equations.

The second part of this chapter is devoted to study the simulations considering only the initial reaction times, like a single pass through monolithic reactors, it means under conditions where the model has been validated. Indeed, the simulation of TC concentration distribution through monoliths is presented for steady-state as well as time-dependent conditions. The influence of internal and external diffusion limitations within the monoliths structure is also considered. Finally, results of simulated large-scale enzymatic monoliths for complete TC degradation as well as their implementation for wastewater treatment are presented.

Chapter 6 presents the general conclusion of the research work carried out for the investigation of enzymatic monolithic supports for the degradation of PPs and outlook for future work**.**

Chapter 2

Literature review

2. LITERATURE REVIEW

Summary

This chapter is devoted to the state of the art concerning the most recent research works carried out in the field of degradation/removal of pharmaceutical products (PPs) which are currently encountered in wastewaters in concentrations ranged from ng L^{-1} to µg L^{-1}. Several pharmaceutical products are recalcitrant in nature and are not removed completely by the classical wastewater treatment plants. Indeed, many research efforts are underway to develop advanced and efficient techniques to completely remove PPs from wastewater; they include biological, physical and chemical processes and each one presents particular advantages and disadvantages.

Enzymatic processes have been recently explored for PPs degradation. However, enzymes tend to loose activity and hence long-term stability is a challenge for such processes. Indeed, enzymes immobilization on suitable supports is an alternative to increase their stability and to facilitate their separation from liquid substrates. Most of the research on wastewater treatment by immobilized enzymes has been carried out at a very small scale. Indeed, the scale up of such processes by the implementation of immobilized support materials at industrial scale is an important challenge for these processes. Non-conventional supports, which include highly porous monoliths, provide large surface area to enzymes immobilization and allow very large permeability. Moreover, monolithic reactors which are modular and then can be easily scaled-up have been recently applied with success in some enzymatic reactions.

2.1 Occurrence of micropollutants in water

Micropollutants are refractory chemical compounds that are found in surface and/or underground waters at concentrations ranged in between µg L^{-1} to below ng L^{-1} (Kim et al., 2016). Micropollutants includes chemicals like pharmaceuticals, flame retardants, perfumes, plasticides, waterproofing agents, plasticizers and insulating foams (Verliefde et al., 2007). These chemical products can have long-term ecotoxicological effects on marine microbial life as well as on human health (Martin-Laurent et al., 2019). Among the micropollutants, Pharmaceutical Products (PPs) could be particularly dangerous and harmful for living organisms and environment because they could have a biological activity even at concentrations as low as ng L^{-1}.

With the emergence of new diseases, new PPs are being manufactured. Currently, PPs represent more than 3000 different molecules with several thousand tons consumed each year in animal husbandry, aquaculture and human treatment (de Cazes et al., 2014a). PPs are not completely metabolized in human/animal body and hence after being consumed, they enters the environment through different sources, mainly due to wastewater from animal husbandry, household and hospital wastewater (Charuaud et al., 2019; Wang and Wang, 2016). After being introduced into wastewater by the sources mentioned above, PPs reach wastewater treatment plants (WWTP) (Bu et al., 2013; Ebele et al., 2017). Nevertheless, WWTP which are mostly based on activated Sludge processes are not capable to completely remove these emerging micropollutants (Phonsiri et al., 2019). Therefore, some of the PPs are captured by WWTP (biodegradation, adsorption etc), but non-negligible amounts of PPs remain in the treated water and are therefore disposed of in the environment. Moreover, after saturation activated sludges are disposed directly or used as a fertilizer and then it is possible that PPs can reach the soil if sludges are discharged without any treatment. Similarly, the treated water from WWTP carries the PPs to soil when it is used for irrigation purposes. Animal manure which is used as a fertilizer can also be a direct source of veterinary drugs released into the environment (Song and Guo, 2014). Once the PPs reached the soil through the sources mentioned above, they can reach surface and ground waters through soil leaching (J. Carter et al., 2019) and ultimately ends up in food chain through agriculture (Klatte et al., 2017; Rivera-Utrilla et al., 2013). The scheme of possible sources and pathways of PPs is shown in more details in Figure 2-1.

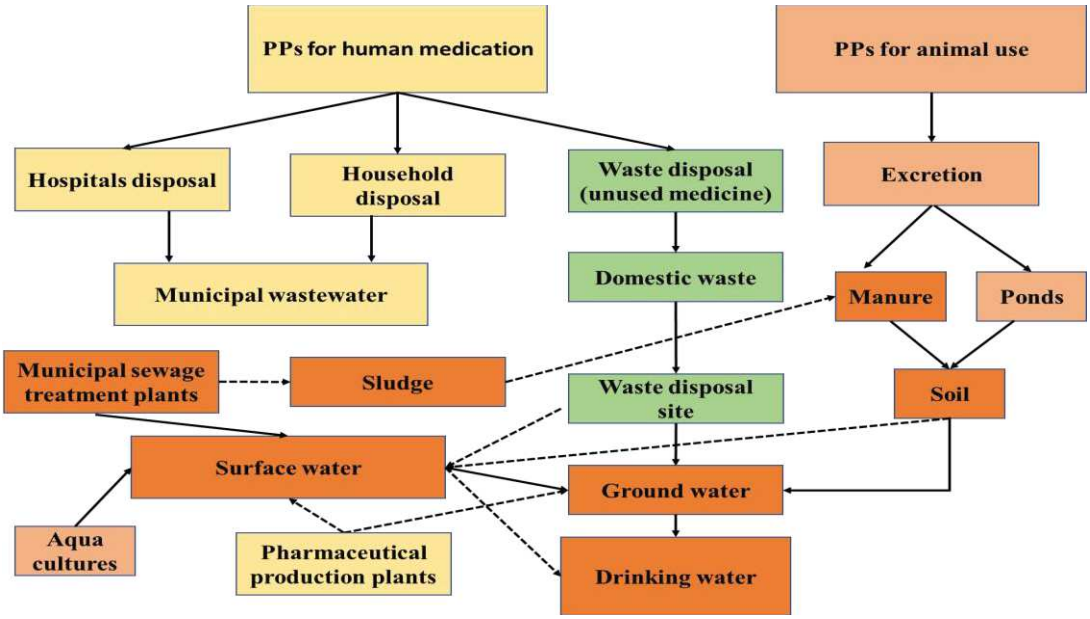

Figure 2-1. Possible sources and pathway of pharmaceutical products into water environment.

PPs have been present in the waters for decades, however their detection has not been possible due to unavailability of sophisticated analytical techniques and instruments to detect concentrations in the range of ng L^{-1}. With the advancement in analytical techniques and development of advance analytical instruments during the last years of seventies the first PPs have been detected in waters. Since then about 275 different PPs are being detected in a large concentration range from ng L^{-1} to µg L^{-1} (Zenker et al., 2014). Recently, commonly used PPs like antibiotics, analgesics, steroids anti-inflammatories etc. have been found in many water reservoirs (surface as well as ground) and rivers of different countries like Canada and Brazil (Ternes et al., 1999), China (Luo et al., 2014), France (Vystavna et al., 2012,Charuaud et al., 2019), Germany (Meyer et al., 2016, Boulard et al., 2020), India (Sharma et al., 2019), Italy (Castiglioni et al., 2020), Spain (Gómez-Canela et al., 2019; Pico et al., 2019; Szymańska et al., 2019), South Africa (Archer et al., 2017), Unit States (Phonsiri et al., 2019).

Increasing concentration of PPs in surface water is a real global concern, because PPs are recalcitrant in nature and their effect on aquatic, terrestrial and human life is widely unknown (Nilsen et al., 2019). Some of the studies reported on toxicological effects of PPs on aquatic life suggested that continuous exposure to Endocrine-disrupting chemicals (EDCs) may impair reproductive function in aquatic life (Tyler et al., 1998), (Palace et al., 2009), (Kidd et al., 2014). These studies concluded that exposure to low concentrations of PPs may not cause apparent toxicity but subtle changes in the physiological behaviour of the organisms. These subtle behaviour change can potentially cause adverse ecological effects in terms of population levels (Blasco et al., 2016). Moreover, more recent studies have over lighted that exposure to endocrine disruptor compounds (EDCs) has been suggested as a contributing factor to not only to endocrine disorders but even as factor of cancer in humans (Mallozzi et al., 2017; Soto and Sonnenschein, 2010).

In view with the long-term effects of PPs and to preserve the water quality, regular monitoring programme for the commonly used PPs have been established in Europe and United States. European Union Water Framework Directive (EU WFD) was set with the aim to achieve and sustain the good ecological and chemical status of surface water. First directive 2000/60/EC was published to set strategies to identify the risky substances and prioritize their regular monitoring (Directive, 2000). In 2008, second directive 2008/105/EC was published, 33 chemicals were selected as priority substances, and the monitoring programme was defined to control the emissions of these compounds. In 2013, the directive 2013/39/EU, 45 more priority substance including two commonly used pharmaceutical (diclofenac and EE2) and a

natural hormone estradiol (E2) were included in the list of priority substances, which required regular monitoring. In 2015, the monitoring substance list was revised list for European Union with the inclusion of three antibiotics and the natural hormone estrone (E1) (Barbosa et al., 2016).

2.2 Removal efficiencies of conventional wastewater treatment plants (WWTP)

WWTPs are the main route for removal/ degradation of PPs, once they are released from the source point. Conventional WWTP uses activated sludge system which has the capacity to remove PPs mainly by sorption. Removal efficiency of PPs in WWTP depends on different factors like physiochemical properties of the PPs and operating conditions such as pH, sludge retention time (SRT) and hydraulic retention time (HRT) (Roberts et al., 2016). Therefore, variations in removal efficiency of WWTP for different PPs have been observed. Removal efficiencies of WWTP for different PPs reported in the literature are summarized in Table 2-1.

From literature, it can be noticed that WWTPs are not able to completely remove all the PPs present in wastewater. WWTPs shows very poor removal efficiencies to antibiotics like tetracyclines and sulfamethazine as reported by some authors (Ghosh et al., 2009; Lin and Tsai, 2009; Miao et al., 2004; Li and Zhang, 2011; Gulkowska et al., 2008; Blair et al., 2015 ; Karthikeyan and Meyer, 2006; Jelic et al., 2011; Yang et al., 2014).

From Table 2-1, it can be seen that negative removal efficiencies were observed for WWTP in some of the cited literature. Reasons for the negative efficiencies of WWTP found can include improperly addressing the fluid dynamics of a WWTP, conjugate compounds that are not detected at the influent could be retransformed into the original compound due to biological processes, desorption from the return activated sludge may occur during the secondary treatment process, and PPCPs may be released from fecal particles as the feces are being broken down by microbes.

Table 2-1. Removal efficiency of conventional WWTP for commonly prescribed antibiotics and their concentration reported in the literature (Burch et al., 2019)

Antibiotics	Eff. Concen. (ngL^{-1})	Removal efficiency (%)	References of data collection	Country/region of research
Sulfamethoxazol	13-7400	-36 to 50%	(Blair et al., 2015);(Göbel et al., 2007);(Miao et al., 2004);(Lin and Tsai, 2009);(Karthikeyan and Meyer, 2006);(Prabhasankar et al., 2016);(Xu et al., 2007).	Canada; China; India; Switzerland; Taiwan; USA
Sulfamethazine	30-363	-5 to 20%	(Blair et al., 2015); (Miao et al., 2004); (Karthikeyan and Meyer, 2006);(Jelic et al., 2011);(Yang et al., 2014).	Canada; Spain; USA
Tetracycline	16-620	-88 to 22 %	(Ghosh et al., 2009); ;(Lin and Tsai, 2009); (Miao et al., 2004);(Li and Zhang, 2011);(Gulkowska et al., 2008)	Canada; China; Japan; Taiwan
Trimethoprim	1-1066	-53-90 %	(Batt et al., 2007);(Watkinson et al., 2007) ;(Jelic et al., 2011); (Lin and Tsai, 2009); (Göbel et al., 2007); (Prabhasankar et al., 2016);	Australia; India; Spain; Switzerland; Taiwan; USA
Ciprofloxacin	7-2200	-89 to 30%	(Batt et al., 2007); (Göbel et al., 2007); (Lin and Tsai, 2009); (Lin and Tsai, 2009) ;(Jelic et al., 2011)	Australia; India; Spain; Switzerland; Taiwan; USA
Norfloxacin	27-140	-165 to 20%	(Karthikeyan and Meyer, 2006); (Blair et al., 2015);(Golet et al., 2003); (Lindberg et al., 2006)	Switzerland; China; Canada
Clarithromycin	57-8100	-73%	(Blair et al., 2015); (Giger et al., 2003)	USA; Switzerland

2.3 Techniques used for Pharmaceutical products removal from water

Keeping in view, the long-term ecological effects of PPs in water and inability of conventional WWT to efficiently remove all the compounds, it is therefore important to explore new efficient and economical techniques to either completely remove the PPs from wastewater or degrade PPs into less toxic compounds. The different techniques used to treat PPs in water are broadly classified as physical adsorption, advance oxidation processes (AOP), membrane base techniques and biodegradation.

2.3.1 Physical adsorption

Physical adsorption technique is the simplest and commonly used technique in WWTPs to capture PPs from wastewater. In order to improve the adsorption capacity for PPs, different adsorbents have be explored and developed (Wang and Wang, 2016). Most commonly adsorbents used are carbon-based adsorptive materials which includes activated carbon (Rajapaksha et al., 2019 ; Rocha et al., 2020) graphene (Al-Khateeb et al., 2014); carbon nanotubes and magnetic activated carbon (Rocha et al., 2020). Recently, some low cost non-conventional sorbents have been also explored like agriculture solid waste, industrial solid waste and natural clay minerals. For example, Bamboo waste activated carbon have been used for the adsorption of Ibuprofen with adsorption capacity 278.5 (mg/g) (Rajapaksha et al., 2019).

2.3.1.1 Activated carbon

Activated carbon is a conventional adsorbent which exits in two different forms i-e: powdered activated carbon (PAC) and granular activated carbon (GAC).The activated carbon has shown good capability to remove endocrine disruption compounds (Liu et al., 2009) and PPs from wastewater (Altmann et al., 2014 ; Rodriguez et al., 2016). The capacity of activated carbon to absorb PPs depends of different factors like hydrophobicity, PPs physicochemical properties, PPs charge (Rodriguez et al., 2016), molecular weight of the PPs as well as water matrix (Mailler et al., 2015). In literature, PAC showed higher removal efficiency than GAC during a pilot scale study (Meinel et al., 2014). Different studies carried out to remove PPs by using PAC or GAC are summarized in Table 2-2.

2.3.1.2 Graphene

Graphene is an allotropic form of carbon. Due to their large surface area graphene and graphene oxide have been recently applied to remove pharmaceutical products (Al-Khateeb et al., 2014). Table 2-2 summarizes the PPs removal capacity of graphene and graphene oxide. Like PAC and GAC the removal efficiency of graphene and its oxide depends on various

factors like physiochemical properties of PPs, pH and contact time. The effect of these factors on graphene performance has been studied by different authors (Kyzas et al., 2015; Yang and Tang, 2016). Graphene and its oxide exhibit higher surface area than activated carbon therefore, it is obvious that removal capacity is higher for graphene and its oxide. Graphene has shown promising removal capacity in batch experiments conducted in a laboratory-scale setup with synthetic PPs solution (Wang and Wang, 2016). However, possibility of large-scale implementation needs to be investigated through experiments with real wastewater (the effect of water matrix).

Table 2-2. Removal efficiency of activated carbon and graphene reported in the literature (Wang and Wang, 2016).

Compounds	Adsorbent	Initial concentration	Source water	Removal efficiency (%)	Ref.
Hormones					
Estriol	PAC (5 mg/l)	100 ng L^{-1}	Surface water	~60	(Snyder et al., 2007)
Estrone				~72	
Antibiotics					
Sulfamethoxazole	PAC (5 mg L^{-1})	100 ng L^{-1}	Surface water	~35	(Snyder et al., 2007)
	PAC (50 mg L^{-1})	600 ng L^{-1}	WWTPs effluents	~60	(Altmann et al., 2014)
	Graphene (0.1 g L^{-1})	100 µg L^{-1}	Synthetic water	~34	(Yang and Tang, 2016)
Tetracycline	PAC (0.6 g L^{-1})	0.19 mmol L^{-1}	Synthetic water	n.a	(Ji et al., 2010)
Nonsteroidal anti-inflammatory drugs					
Ibuprofen	PAC (5 mg L^{-1})	100 ng L^{-1}	Surface water	~15	(Snyder et al., 2007)
	Graphene	10 mg L^{-1}	Synthetic water	~95	(Rizzo et al., 2015)
Diclofenac	PAC (5 mg L^{-1})	100 ng L^{-1}	Surface water	~40	(Snyder et al., 2007)
	Graphene	10 mg L^{-1}	Synthetic water	~95	(Rizzo et al., 2015)
Paracetamol	PAC (5mg L^{-1})	100 ng L^{-1}	Surface water	~70	(Snyder et al., 2007)
	Graphene (0.1 g L^{-1})	1 mg L^{-1}	Synthetic water	~46	(Yang and Tang, 2016)

2.3.1.3 Carbon nanotubes

Carbon nanotubes are cylindrical tubes fabricated of rolled up graphene sheet. Carbon nanotubes applications on the removal of PPs and endocrine disrupting compounds have been reviewed by Jung et al., (2015). Carbon nanotubes in PPs removal applications have been explored for different PPs such as ketoprofen (Liu et al., 2014), carbamazepine (Liu et al., 2014), sulfamethoxazole (Ji et al., 2009), ibuprofen and triclosan (Cho et al., 2011). All these studies confirmed that carbon nanotubes have high adsorption capacity of PPs however adsorption capacity depends on the surface chemistry, physiochemical properties of the PPs and properties of the carbon nano tubes (Jung et al., 2015).

2.3.1.4 Advantages and disadvantages of physical adsorption technique

Adsorption of PPs onto the activated carbon, graphene, graphene oxide and carbon nanotubes have shown promising results in terms of removal of variety of PPs when applied to real wastewater (in case of activated carbon) as well as synthetic water (graphene). However, several problems are associated with this technique are, low adsorption capacity to the macromolecular substances, high cost of graphene, complex preparation methods of carbon nanotubes and interaction with PPs. Along with these application restricted issues, recycling and regeneration of activated carbon, graphene and carbon nanotube after saturation is an another challenge (Wang and Wang, 2016).

2.3.2 Advanced oxidation processes (AOP)

In Advanced oxidation processes (AOPs), oxidative radicals ($OH^{\bullet}$, $O_2^{\bullet-}$., $HO_2^{\bullet}$) are generated (Kanakaraju et al., 2018b). These radicals are highly reactive that can degrade a large variety of organic and inorganic micropollutants in water (Kanakaraju et al., 2018a). $OH^{\bullet}$ radical have attracted the most attention because of its non-selective nature, strong reactivity and strong oxidizing capabilities (E^o = +2.80 V) (Goi, 2005). $OH^{\bullet}$ radicals are produced with the help of oxidizing agents like ozone (O_3) or hydrogen peroxide (H_2O_2). The semiconductor catalysts or UV radiations are used as a catalysts to produce $OH^{\bullet}$ radicals (Homem and Santos, 2011; Rivera-Utrilla et al., 2013).

Advanced oxidation-based techniques applied for the degradation of PPs are broadly categorized into three subcategories: photochemical processes; non-photochemical processes and hybrid processes.

2.3.2.1 Ozonation

Ozonation (O_3) technique involves the production of reactive radicals either by simple (O_3) or mixture of O_3 and H_2O_2 (O_3/H_2O_2), or O_3 and UV (O_3/UV). The reactive radicals produced then degrade PPs in water by a single oxidation reaction (Almomani et al., 2016; Goi, 2005; Kanakaraju et al., 2018a; Kıdak and Doğan, 2018). From research studies on ozonation, it can be concluded that due to the high reactivity of the free radicals, ozonation technique is very efficient to degrade PPs (Zhao et al., 2017). Nevertheless, full scale implementation of this technique is limited by short life time of ozone and high energy consumption (Ikehata et al., 2006). Zhao et al. (2017) observed complete degradation of indomethacin (anti-inflammatory drug) within 7 min. Similarly, Dantas. et al. (2011) and Wang et al. (2011) found high degradation for propranolol and tetracycline with this advanced oxidation technique. Moreover, some research studies have reported that despite high removal efficiencies of PPs sometimes low mineralization (total oxidation) is reached. Therefore, despite fast degradation rates, the challenge associated with this technique is the formation of non-toxic degradation by-products (Almomani et al., 2016). Indeed, it is very important to study the nature of degradation products.

2.3.2.2 Fenton oxidation

During Fenton oxidation, reactive radicals ($OH^{\bullet}$) ions are produced by a mixture of iron salts (Fe^{2+}) and H_2O_2 under mild acidic conditions.

Research studies carried out with Fenton and Photo-Fenton processes for the oxidation of PPs suggest that both processes are effective for the degradation of PPs. The Fenton reactions are enhanced by UV-Vis radiation in order to produce additional $OH^{\bullet}$ radicals (Goi, 2005; Legrini et al., 1993). Various PPs like antibiotics, analgesic and antineoplastic drugs have successfully been degraded by photo-Fenton process. (Alalm et al., 2015; Sirtori et al., 2011; Trovó et al., 2011). For example, a complete disappearance of amoxicillin was observed by using ferrixalate complex within 5 min, whereas and 15 min were necessary using $FeSO_4$ (Trovó et al., 2011). Though, the use of ferroioxalate complex leads to a toxicity increase in the final solution (degradation products). In another study, Michael et al., (2012) found a complete degradation of 100 µg L^{-1} of loxacin and trimethoprim with Fe^{2+} (5 mg L^{-1}) and H_2O_2 (75 mgL^{-1}) under solar photo-Fenton conditions. Davididou et al. (2017) applied ferrioxalate-based photo-Fenton reaction using UVA-light emitting diodes (LEDs) to degrade and mineralize

antipyrine. They found complete degradation of antipyrine in 3 min and 93 % of total organic carbon (TOC) in 60 min.

Relative to other AOPs like UV and O_3, Fenton process is not an energy intensive process. However, it is observed that the reaction is significantly influenced by pH (Perini et al., 2018) with optimum operating conditions at low acidic conditions (pH 3–5) (Malato et al., 2002). At a pH higher than 3, Fe^{3+} precipitates as $Fe(OH)_3$, decreasing the performance of the process. Recently, few studies have been carried out at a neutral pH in order to deal with large-scale operations (Perini et al., 2018). Giraldo-Aguirre et al. (2018) studied the removal of oxacillin at pH~6 and found a complete degradation of 203 μmol L^{-1} solution of oxacillin in the first 50 min in the presence of 90 μmol L^{-1} of Fe^{2+}, 10 mmol L^{-1} of H_2O_2 and irradiation with a 30 W light source (365 nm).

Therefore, more research is required at a wide pH range using natural and wastewater matrices. Indeed, research is underway to investigate different approaches to overcome the low acidic condition requirements of Fenton and photo-Fenton reactions.

2.3.3 Biological treatment processes (De Cazes et al., 2014).

2.3.3.1 Sorption in activated sludge process (ASP)

As explained above, ASP which is the conventional and mostly adopted system for biological wastewater treatment is not specifically designed for the removal of antibiotics (Cheng et al., 2018). In literature, research studies carried out on lab-scale as well as full-scale concluded that PPs are only partially removed in conventional WWTPs with the removal efficiencies varying between negative to 99% (Hu et al., 2018). In ASP, the removal of PPs takes place either by biosorption or by biodegradation (Yang et al., 2011; Hörsing et al., 2011; Li et al., 2013). The adsorption process is a complicated process which is highly affected by the physio-chemical properties of the sludge, pollutants and the operating conditions (Kim et al., 2005). The value of solid-liquid partitioning coefficient or sorption coefficient (K_d), determines the extent of sorption of PPs onto the biological sludge. If the K_d value is high, the sorption capacity will be also great (Riaz et al., 2018). The effect of K_d values on the overall absorption capacity of sulfamethoxazole (SMX) and sulfadimethoxine (SDM) on sludge has been highlighted by Yang et al. (Yang et al., 2011) who reported adsorption of 31% and 19% for SMX and SDM respectively.

2.3.3.2 Membrane Bioreactors

Membrane bioreactors (MBRs) consist of two units: a bioreactor tank and a membrane module to retain sludge (suspended solid). MBRs can be named and classified according to the operating conditions used: Aerobic membrane bioreactors (AMBR) and Anaerobic membrane bioreactors (ANMBR). Both types of MBRs have been recently explored for PPs removal from wastewater.

Several studies carried out on the removal of PPs with MBRs have demonstrated that AMBRs present higher removal efficiency in in comparison to ASP (Radjenović et al., 2009). Higher removal (sorption) efficiency in AMBR was due to higher biomass concentration and smaller-sized sludge flocs coupled with a larger surface area (Sipma et al., 2010). Similarly, the higher biodegradation efficiency of AMBR was also related to a high SRT which enhances sludge enrichment with slow-growing bacteria and more diverse microbial population (Park et al., 2017). In AMBR processes, the majority of PPs are removed by both sorption and biodegradation process while biodegradation is found to be the major removal pathway for sulphonamides (Wen et al., 2018).

Shi et al. (2018) studied the effect of various operating parameters in AMBR processes, their results concluded that the removal efficiency in AMBRs depends also on PPs physiochemical properties and initial concentrations of PPs. Other studies carried out with AMBR suggested that PPs removal is highly affected by the type of membrane (García Galán et al., 2012), and operating conditions like temperature, HRT (Prasertkulsak et al., 2016), SRT (Tambosi et al., 2010), pH (Tadkaew et al., 2010), and dissolved oxygen (Hai et al., 2011). Among the different parameters studied, SRT is one of the most influential. Research studies demonstrated that an average SRT of 30 days enhanced removal of PPs (Hu et al., 2018; Shi et al., 2018; Wen et al., 2018). Furthermore, membrane configuration can also play an important role, flat sheet membrane module is able to retain higher biomass concentration in comparison to hollow fiber membrane module, hence the degradation rate is higher when flatsheet membrane module is used (Nguyen et al., 2017).

Meng et al. (2017) observed that AMBR showed variable removal efficiencies for different PPs due to the nature of PPs. They also observed that membrane fouling is one of the major drawbacks of continuous wastewater treatment in a MBRs. Sheng et al. (2018) observed that presence of PPs in wastewater could enhance membrane biofouling by influencing microbial communities and fouling factors such as sludge particle size, and soluble microbial

products (SMPs). However, data related to the effects of different PPs on membrane biofouling are limited and further studies are required to explore the effect of PPs on biofilms.

2.4 Enzymatic degradation of PPs (De Cazes et al., 2014)

Enzymes are biocatalysts that mediate biochemical reactions at a rapid rate under mild operating conditions (pH, temperature, solvents and ionic strength). Due to the ability of certain enzymes to oxidize a wide variety of compounds, enzymatic processes are being explored as an interesting option for the degradation of micropollutants and in particular the degradation of PPs (Naghdi et al., 2018a).

Another advantage of enzymatic process is that, enzyme as biocatalyst can degrade environmental pollutants at low concentration with a lower risk of being inhibited by the effect of these compounds. Hence enzymatic degradation of micropollutants can be a promising technique for the degradation of PPs from wastewater (Karam and Nicell, 1997).

Currently, the enzymatic degradation of micropollutants from various effluents into less toxic compounds is being studied at the laboratory scale. Among the enzymes, oxidoreductases enzymes are able to oxidize large variety of PPs like phenols, drugs and hormons in wastewater. Among oxidoreductases, three enzymes: Laccases, Tyrosinase and peroxidases are the most studied in recent past (Singh Arora and Kumar Sharma, 2010; (De Cazes et al., 2014).

The characteristics and structural properties of these three oxidoreductases are discussed in detail in the following paragraphs.

2.4.1 Laccases (EC 1.10.3.2.)

Laccases (EC 1.10.3.2.) which are multi-copper oxidoreductases have the ability to oxidise a wide range of aromatic and nonaromatic compounds in the presence of oxygen as a co-substrate (Hautphenne et al., 2016). Three different copper sites are found in laccase structure which are named as: blue copper (T1), normal copper (T2), and coupled binuclear copper (T3) as shown in Figure 2-2. T1 site accepts electrons from reducing substrates while T2 and T3 copper centres form a trinuclear copper cluster that is responsible of the binding and the reduction of oxygen (Morozova et al., 2007). The oxidation efficiency of laccases depends on the redox potential difference between the T1 copper of the enzyme and the substrate. Indeed, compounds which present a low ionization potential are not directly oxidized. In such cases mediators are required to start the oxidation process (Ji et al., 2016c).

The proposed catalytic reaction mechanism is illustrated in Figure 2-3. In the first step, the T1 copper site accepts electrons from reducing substrates, the electrons are then transferred

onto the T2/T3 copper cluster where reduction of molecular oxygen to water takes place (Senthivelan et al., 2016), (Solomon et al., 1996).

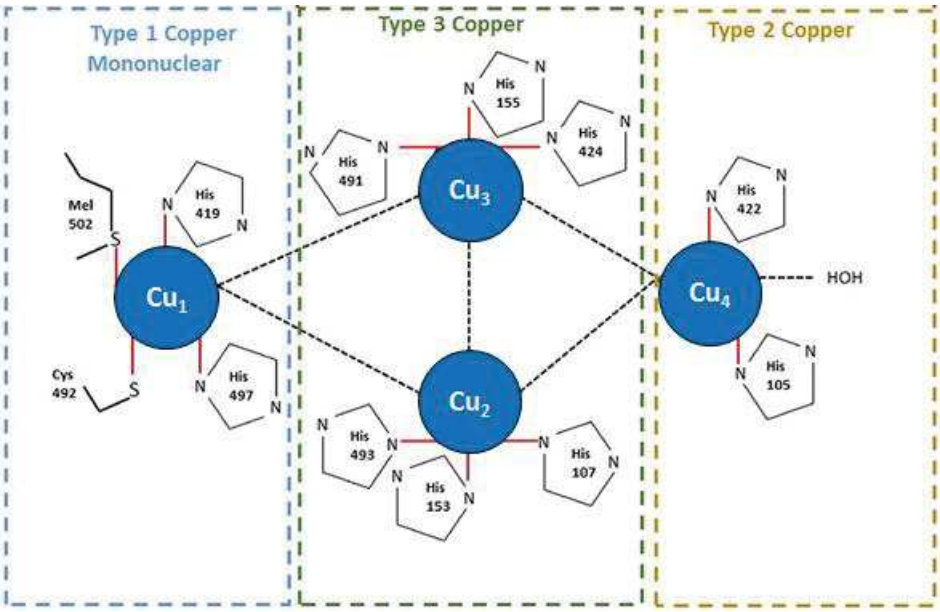

Figure 2-2. Schematic diagram of the four copper sites of the laccase catalytic center (Barrios-Estrada et al., 2018a).

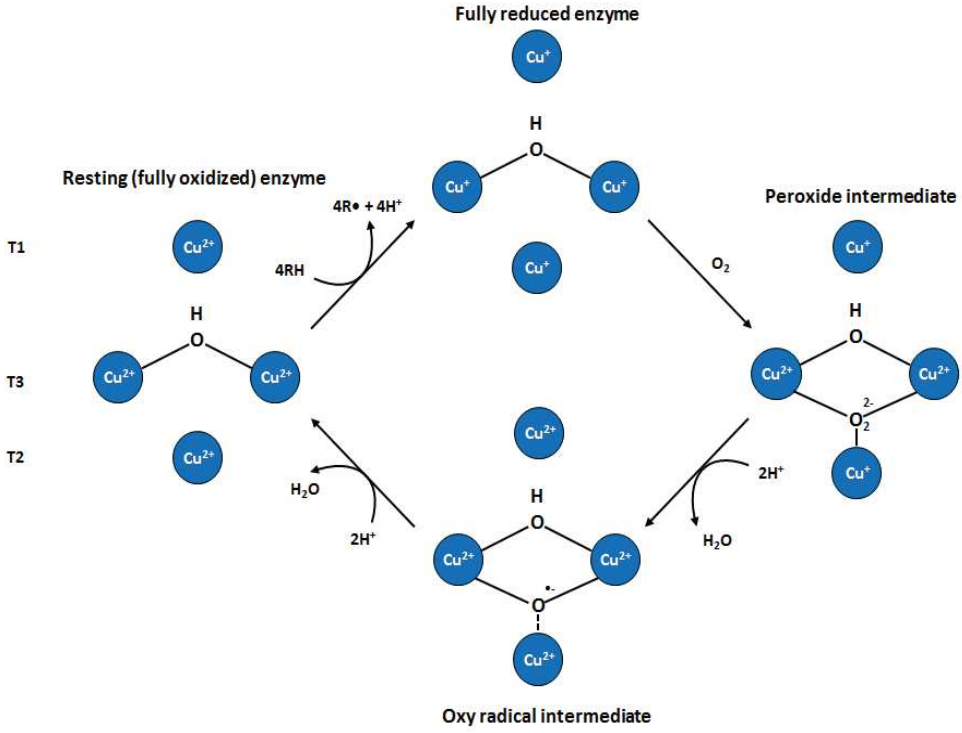

Figure 2-3. Reactions at the copper centers during catalytic cycle (Wong, 2009)).

Laccases can be categorized on the basis of the source of extraction. Laccase from *Trametes versicolor* is the most widely used probably due to the relatively high potential of its T1 site compared to other laccase sources and its commercial availability (Morozova et al., 2007). Nevertheless, laccases from other sources like *Pycnoporus sanguineus* CS43 have also successfully been applied for the degradation of endocrine disrupting compounds (EDC), nonyl phenol (NP) and triclosan (TCS) in lab-scale experiments (Ramírez-Cavazos et al., 2014). Similarly, other laccases produced by growing fungal strains on poultry litter, have been successfully applied for the removal of estradiol (Liu et al., 2016).

2.4.2 Tyrosinase (EC 1.10.3.1)

Tyrosinase (EC 1.10.3.1) is an oxidoreductase that like laccase contains copper and can oxidize a variety of pharmaceutical products. Tyrosinase contains one T3 copper centre and utilizes oxygen as a cofactor; however, its catalytic mechanism is different from that of laccases (Shuster Ben-Yosef et al., 2010). Tyrosinases have a broad specificity and have the ability to oxidize a wide range of phenolic compounds (Faccio et al., 2012). Fairhead and Thöny-Meyer, (2012) observed that, as in the case of laccase-catalyzed reactions, the degradation of phenolic compounds by tyrosinases leads to the formation of polymers which can then be removed from the wastewater by physical removal methods.

2.4.3 Peroxidases (EC 1.11.1.X)

Peroxidases (EC 1.11.1.X) are another type of oxidoreductases enzymes that require hydrogen peroxide as a co-substrate to catalyse oxidative reactions (Medina et al., 2017). Peroxidases from different sources have been studied to degrade pharmaceutical products. For example, horseradish peroxidase (HRP) from *Armoracia rusticana* (Melo and Dezotti, 2013), chloroperoxidase from *Caldariomyces fumago* (Li et al., 2017), lignin peroxidases (Mao et al., 2010), manganese peroxidase (MnP) from *Phanerochaete chrysosporium* (Inoue et al., 2010), soybean peroxidase (Al-Ansari et al., 2009), black radish peroxidase (Altinkaynak et al., 2017) have been applied to transform and/or detoxify organic pollutants (Torres et al., 2003). Among all the mentioned type of peroxidases, the most applied peroxidase is HRP. This peroxidase can use not only H_2O_2 but also other peroxides in order to oxidize a wide range of micropollutants. During the catalytic cycle, the peroxide oxidizes the enzyme (which has a Fe^{3+}) and as a result water molecule is formed as a by-product. Then the positive charge peroxidase (Fe^{4+}-$R^{+\cdot}$) oxidises the substrate molecule, this forms a substrate radical and an intermediate (Fe^{4+}). In a second step the intermediate is further reduced by a

second substrate molecule, regenerating the peroxidase and producing another free radical (Martínez, 2002). The catalytic cycle is further illustrated in the Figure 2-4. During the catalytic process, several products are formed as reported in the case of phenolic compounds, those products are dimers, trimers, and oligomers of the oxidized monomer molecule which is the initial phenolic compound (Margot et al., 2015).

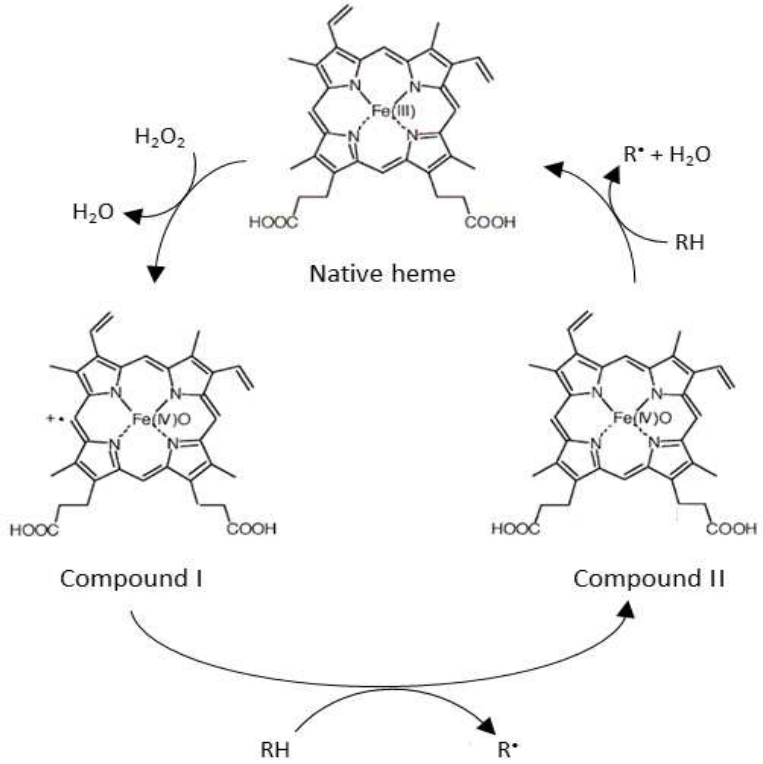

Figure 2-4. Catalytic cycle of peroxidases (Adapted from (Torres et al., 2003)).

In this present work, a laccase from *Trametes versicolor* has been selected as biocatalyst because among different oxidative enzymes it only needs oxygen as co-substrate; it has very good oxidative properties towards many micropollutants as antibiotics. Moreover, this enzyme is currently available from commercial providers.

2.5 Degradation of pharmaceutical products by laccases

As explained above, laccases have been widely applied for the removal of pharmaceutical products from wastewaters. Laccases can be applied either in free form or immobilized on a suitable solid support.

2.5.1 Free laccases for the degradation of PPs

In free form, laccases can be categorized as crude laccases or purified laccases.

2.5.1.1 Crude laccases

Crude laccases mean the utilization of enzymes extracted directly from microbial cultures without prior purification. Crude laccases have been investigated by several research groups to explore their oxidizing capability for the degradation of PPs (see Table 2-3). For example, Guo et al. (2014) investigated the degradation of sulfamethoxazole (SMX) by crude laccase from *Phanerochaete chrysosporium*, they observed the degradation yields up to 50% with crude laccase activity of 6076 U L^{-1}. Furthermore, the study at different enzyme concentrations did not show any change in degradation yield indicating that reaction was limited when substrate concentration became too low. Similarly, Gao et al. (2018) applied the laccase extracted from *Pycnoporus sanguineus* culture for the degradation of commonly used antibiotics like SMX, norfloxacin (NOR) and ciprofloxacin (CIP). They observed that after 72 hours of reaction in the presence of crude laccase, SMX was degraded only 29%, while CIP and NOR were resistant to degradation (3% and 2% respectively). The degradation of four tetracyclines (tetracycline, chlortetracycline, doxycycline and oxytetracycline) in the presence of a cell-free extract from *Trametes versicolor* was carried out by Suda et al. (2012), these authors observed that in the first 4h of reaction, the degradation of tetracyclines ranged from 5-14%. Tran et al. (2010) investigated the degradation of 10 PPs at the concentrations of real wastewater (10 µg L^{-1}) with a crude laccase solution having activity of 1500 U L^{-1}. They observed that 3 compounds, diclofenac, naproxen and indomethacin were completely degraded in the first 12 h of reaction, while the other compounds were only partially degraded. Cabana et al. (2009) studied the laccase from *coriolopsis polyzona* for the degradation of triclosan (TCS) and two other endocrine disrupting chemicals and observed that 65% of initial TCS (5 mg L^{-1}) was degraded during the first 4h of reaction at pH 5 and 50°C.

Table 2-3. Degradation of pharmaceutical micropollutants by crude laccases

Laccase source	Pharmaceutical	Concentration (mg L^{-1})	Reaction conditions	Efficiency (%)	Reference
Trametes versicolor	Carbamazepine	1	60 U mL^{-1}, 10 mL, pH 6, 150 rpm, 24 h	30	(Naghdi et al., 2018b)
	Chlortetracycline	5	10 nkat mL^{-1}, 0.5 mL, pH 4.5, 30°C, 150 rpm, 4 h	48	(Suda et al., 2012)
	Diclofenac	0.5	500 U L^{-1}, 100 mL, pH 4.5, 50°C, 150 rpm, 5h	99	(Lonappan et al., 2017)
	Diclofenac	0.01	1500 U L^{-1}, 10 mL, pH 4.5, 30°C, 125 rpm, 12 h	100	(Tran et al., 2010)
	Ibuprofen			15	
	Naproxen			100	
	Tetracycline	5	10 nkat mL^{-1}, 0.5 mL, pH 4.5, 30°C, 150 rpm, 4h	16	(Suda et al., 2012)
Pycnoporus sanguineus	Diclofenac	10	100 U L^{-1}, pH 5, 25°C, 8 h	50	(Rodríguez-Delgado et al., 2016)
	Sulfamethoxazole, Norfloxacin, Ciprofloxacin	10	170 U L^{-1}, 25 mL, 72 h	29,3,2	(Gao et al., 2018)
Phanerochaete chrysosporium	Sulfamethoxazole	10	96-6076 U L^{-1}, 5 mL, pH 4.5, 30°C, 48 h	≤ 50	(Guo et al., 2014)
Coriolopsis polyzona	Triclosan	5	100 U L^{-1}, pH 5, 50°C, 8h	65	(Cabana et al., 2007)

2.5.1.2 Purified laccases

Purified laccases are obtained after their separation from crude extracts by some processes like membrane techniques or size exclusion chromatography (Lloret et al., 2010).

Purified laccases obtained from white rot fungi (WRF) are certainly the most widely applied to remove the PPs from wastewater as shown in Table 2-4. Different literature investigation concluded that laccase in purified form was able to degrade variety of PPs. For example, Tran et al. (2010) applied commercially available purified laccase from *Trametes versicolor* for the oxidation of different PPs and observed complete oxidation of diclofenac, naproxen and indomethacin in the first few hours. Similarly, laccases purified from *Pleurotus ostreatus*, *Paraconiothyrium*, *Trametes versicolor* and *Pycnoporus sanquines* have successfully been applied to the removal of different PPs like acetaminophen, ketoconazole and TCS (Stadlmair et al., 2017; Tahmasbi et al., 2016; Yousefi-Ahmadipour et al., 2016).

Margot et al. (2013) studied the effect of process parameters in case of degradation of diclofenac, mefenamic acid and TCS by commercial *Trametes versicolor* laccase. The results of their study suggested that pH values as well as nature of compound had significant effects on degradation with optimum pH value between 4-6 and temperature 25 °C. It was also observed that the presence of other PPs in the reaction mixture could enhance the degradation. For example, in case of diclofenac, the degradation yield increased from 25 to 95% when mefenamic acid was also present in the reaction medium.

However, some PPs are very recalcitrant to enzymatic oxidation and in this case the observed degradation yields are very low. For example, De Cazes et al., (2014a) observed that after 24 h of reaction, only 30% tetracycline was degraded with commercial *Trametes versicolor*. Prieto et al. (2011) studied the same commercial purified laccase and observed only 16% of degradation of CIP (5 mg L^{-1}). Nguyen et al. (2014) and Tran et al. (2010) reported low degradation of CBZ (<38%) irrespective of the type of laccase used. The inability of laccase to degrade some compounds such as CBZ has been related to the presence of functional groups (amide) in the structure of these substrates (Yang et al., 2013).

It can be concluded from literature studies, that laccases either in crude or purified forms have shown the ability to degrade a wide range of PPs at different range of operational conditions. However, the experiments were mostly carried out at laboratory scale, in model solutions with only a one or a mixture of PPs. Therefore, to implement enzymatic degradation techniques for practical applications, more investigations with real wastewaters and at large

scale need to be carried out. One of the main challenges to implement enzymatic process on large scale is the reusability of the biocatalyst. It is only possible by immobilizing enzymes on suitable supports. Many research works have been carried out to explore the immobilization techniques and the enzyme activity behaviour after immobilization. In next section, the different enzyme immobilization techniques and their advantages/disadvantages are briefly discussed.

Table 2-4. Degradation of Pharmaceutical products by purified Laccases.

Laccase source	Pharmaceutical	Concentration (mg L^{-1})	Reaction conditions	Efficiency (%)	Reference
Trametes Versicolor	Ciprofloxacin	10	16.7 nKat mL^{-1}, 30°C, 150 rpm, 20 h	16	(Prieto et al., 2011)
	Tetracycline	20	0.01 g L^{-1}, 100 mL, pH 6, 25°C, 24 h	30	(De Cazes et al., 2014a)
	Carbamazepine	0.01	6000 U L^{-1}, 10 mL, pH 4.5, 30°C, 125 rpm, 3 h	38	(Tran et al., 2010)
	Diclofenac			100	
	Ibuprofen			38	
	Ketoconazole	300	1 U mL^{-1}, pH 4.5, 45°C, 6h	98	(Yousefi-Ahmadipour et al., 2016)
Myceliophthora thermophila	Diclofenac	5	2000 U L^{-1}, 20 mL, pH 4, 25°C, 8h	65	(Lloret et al., 2010)
Pleurotus ostreatus	Diclofenac	0001	1.5 µM, 1.5, pH 7.4, 25°C, 20 min	40	(Stadlmair et al., 2017)
	Acetaminophen			100	
Asperguillus oryzae	Diclofenac	5	90 µM min^{-1} , 200 mL reaction	21	(Nguyen et al., 2014)
	Carbamazepine			10	
	Sulfamethoxazole			9	
Paraconiothyrium variable	Imipramine	0.12	1.63 U, 5 mL, pH 4.9, 37°C, 5.7 h	99	(Tahmasbi et al., 2016)
G lucidum	Triclosan	0.05	5 U, 1 mL, pH 4, 30°C, 24 h	57	(Murugesan et al., 2010)

2.5.2 Immobilized laccase for the degradation of PPs

Although the degradation of PPs by free laccase has demonstrated its feasibility on small batch scale, in order to implement it on a large scale, the process must be operated in continuous mode and the biocatalyst must show high stability and be reusable (Gasser et al., 2014). Immobilizing enzymes on suitable solid supports can be one of the solutions to above mentioned problems related to enzymatic process, because immobilization generally increases the stability of enzymes during storage as well as under reaction conditions. Different authors studied the stability of immobilized enzymes and observed that after immobilization the stability of biocatalysts was enhanced against harsh conditions of temperature, pH and pressure (Sheldon, 2007; Iyer and Ananthanarayan, 2008; Cabana et al., 2009; Patel et al., 2014; Zhang et al., 2015 ; Zheng et al., 2016; Ji et al., 2017). Moreover, immobilization on solid supports allows an easily separation from liquid solutions and then the reusability of enzymes is enhanced.

Enzyme immobilization can be carried out by different ways, but most commonly, enzyme molecules are attached to a solid support which is insoluble in the reaction environment. This results in immobilized biocatalyst and ultimately, change in the state of enzyme from homogenous (free enzyme) to heterogeneous (immobilized enzyme).

Different immobilization techniques are used in literature however, the five main immobilization techniques can be classified as:

1. Covalent attachment
2. Adsorption
3. Encapsulation
4. Entrapment
5. Cross-linking

Enzymes immobilization methods can be broadly classified as physical and chemical methods. Physical methods involve the creation of relatively weak interactions such as hydrogen bonds, ionic and hydrophobic interactions while chemical methods involve surface modification via covalent bonding. The physical methods can be further categorized into entrapment and adsorption. These methods are easy and prior functionalization of the support is not required. Adsorption immobilization involves hydrophobic interactions, van der Waals forces or ionic interactions between enzyme and solid supports. These bonds are relatively

weak however the native structure of the enzyme is not fundamentally changed and thus activity of the enzymes can be preserved. Entrapment immobilization is carried out by entrapping enzyme in a polymer organic or inorganic matrix. In literature, different techniques of entrapments have been reported, they include gel/fiber, metal-organic frameworks embedding (MOF) and encapsulation (Liang et al., 2020; Hong et al., 2017).

Chemical immobilization methods involve enzyme attachment to the support by covalent bonds via a cross-linking agent. The chemical bonds created as a result of this immobilization between the enzyme and solid support significantly decrease the leakage of the enzyme and increases its reusability (Zdarta et al., 2018). Chemical bonds can also be created by cross-linking enzymes to each other, resulting a cross-linked enzyme aggregate (CLEA) (Zdarta et al., 2018).

The selection of immobilization method depends on the type of specific functional group available on the support surface. Entrapment methods works relatively better with polymers having surface functional groups like –OH, C=O, and $–NH_2$; because they are able to form a polymeric network around the enzyme molecule. However, if support surface contains functional groups like –OH, COOH, C=O, –SH, $–NH_2$, both adsorption and covalent immobilization can be carried out.

For immobilization of enzyme on any support material, three necessary steps should be followed:

- The support material should be chosen to provide surface compatibility for enzyme binding.
- Once the suitable support is selected, the operating conditions such as pH and temperature should be favourable in order to operate at an optimal level of performance.
- The characterization of the catalytic behaviour of the resulting biocatalyst should be studied under operational conditions.

Although there are few prerequisites for enzyme immobilization, but there is no specific technique for specific enzyme in order to accomplish the immobilization process. The selection of the most suitable support material and type of immobilization method is mainly dependent on the nature of the enzyme and the biocatalytic process. Selection of support material for enzymes such as laccases for wastewater treatment has to result not only in efficient bio degradation of toxic compounds but also to preserve the immobilized enzymes from

denaturation (Bilal et al., 2019). Different support materials can potentially be applied for enzyme immobilization, however for their effective utilization there are few pre-requisites:

- Chemical moieties between material surface and enzymes, large surface area, chemical stability and good sorption properties (Hoarau et al., 2017).
- Biocompatibility, non-toxic, eco-friendly and inert to degradation products.
- Hydrophilic nature of the carrier, structural and mechanical or operational stability (Barbosa et al., 2013).

Table 2-5 summarizes the characteristics, main advantages and drawbacks of different immobilization methods. Covalent immobilization methods involve the formation of chemical bonds which provide stable attachment and hence reduce enzyme inactivation. However, in some cases due to conformational changes induced by covalent bonds, the decrease in the activity of the immobilized enzymes is observed (Sheldon, 2007). In contrast, adsorption and entrapment methods are simple and have less effects on the enzyme structure but the immobilized enzymes are less stable during the process (Durán et al., 2002). The immobilization method plays a key role in determining the process specification like process economy, process efficiency and reaction kinetics (Naghdi et al., 2018c). Since the characteristics of all the enzymes are different from each other, one of the key steps in implementing a bio-catalytic process for practical applications is to correctly select the immobilization protocol.

Table 2-5. Different immobilization techniques, their characteristic, advantages and drawbacks.

Immobilization Methods	Main functional groups of the support	Interactions	Strength of interactions	Advantages	Disadvantages
Adsorption	$–NH_2$, –SH, –OH, C=O, COOH, epoxy groups	hydrogen bonds, ionic interactions, hydrophobic interactions	weak	no enzyme modification, simple and inexpensive reusability of the support	enzyme leaching, poor process stability, low efficiency
Covalent binding	$–NH_2$, –SH, –OH, C=O	covalent bonds	strong	strong and stable interactions, multipoint attachment, reducing of enzyme leakage	complicated process, expensive enzyme chemical modification loss of functional conformation of enzyme
Encapsulation	$–NH_2$, –OH,	ionic interactions, hydrophobic interactions	weak	cheap and simple, no enzyme modification, protection of the enzyme	loss of catalytic properties, pore size limitations.
Entrapment	$–NH_2$, –OH, C=O	ionic interactions, hydrophobic interactions, covalent bonds	weak/strong	fast immobilization technique, cheap, less chances of conformational changes, no enzyme modification	generation of unwanted products, pore diffusion limitations, limited industrial application.
Cross-linking	C=O, $–NH_2$	covalent bonds	strong	no support needed, high strength of interactions	enzyme leaking

2.6 Support materials for enzyme immobilization

The supports used for immobilization can be classified based on their origin, from organic to inorganic and hydride as well as composite supports. Some important characteristics of the support materials used and their advantages and disadvantages are summarized in Table 2-6.

Inorganic support materials recently applied for enzyme immobilization and degradation of PPs are summarized in Table 2-7. There are two main conclusions from this data: Immobilized enzymes are able to degrade large variety of PPs at different degradation efficiency (20-100%), laccase from *Trametes versicolor* is commonly used enzyme for the degradation of PPs. From this data, it is difficult to conclude about the selection of the specific material for immobilization and type of enzyme compatible for the degradation of all PPs. Therefore, it is important to know about the nature of the PPs present in wastewater and the enzyme affinity for those PPs in order to efficiently degrade them. Similarly, it is also important to know the compatibility of solid support with respect to the enzyme in order to carry out an effective immobilization.

Table 2-6. Characteristics of support materials used for enzyme immobilization.

Classification	Materials	Advantages	Disadvantages
Organic materials	biopolymers: cellulose, collagen, agar, alginates synthetic polymers: ion exchange resins, polystyrene, polyamide, polyacrylonitrile.	presence of reactive functional groups, high affinity of peptides, biocompatibility, limited negative effect on enzyme structure, abundant in nature.	usually needs functionalization, may present diffusional barriers. Synthetic polymer: Difficult preparation procedures, usually not eco-friendly
Inorganic materials	Silica, zirconia, active carbons, porous glass, multi-walled carbon nanotubes, titania, magnetite.	temperature and pH stability, mechanical resistance, operational stability, good sorption properties, inertness, easy surface functionalization, relatively cheap.	possibility of unspecific interactions, without surface modification, have weak laccase-support interactions, may present diffusional barriers
Hybrid and composite materials	silica-magnetite, silica-zinc oxide, chitosan-silica, chitosan-clay, polyamide-chitosan, Polyvinyl alcohol-4-hydroxybenzaldehyde.	reusability of the matrix, strong binding of the enzyme, high stability, properties of the support material designed for selected enzyme and catalytic process	expensive

Table 2-7. Solid Support materials used for laccase immobilization and their application in micropollutants degradation.

Support material	Pharmaceutical	Enzyme source	Immobilization technique	Reaction conditions	Removal (%)	References
Magnetic CLEAs	Acetaminophen	*Trametes versicolor*	Cross-linking	pollutant concentration (50 µg L^{-1}) , laccase activity (1000 U L^{-1}), total reaction volume (10 mL) reaction, operating conditions (pH 7, 30°C), reaction time (6 h); mode of operation (batch)	27	(Arca-Ramos et al., 2016)
	Diclofenac			pollutant concentration (100 µg L^{-1}); laccase activity (1000 U L^{-1}), reaction volume (10 mL); reaction operating conditions (pH 7, 20˚C), reaction time (12 h), mode of operating (batch)	95	(Kumar and Cabana, 2016)
	Mefenamic acid				99	
	Sulfamethoxazole	*Cerrena unicolor*		pollutant concentration (100 mg L^{-1}), laccase activity (20 U ml^{-1}), operating conditions (pH 7, 25°C), reaction time (48 h); Mode of in operation (batch)	29	(Yang et al., 2017a)
	Diclofenac				65	
	Bisphenol A	*Trametes hirsuta*		pollutant concentration (60 ppm), total volume of reaction (10 mL), reaction conditions (pH 7, 35°C), total reaction time (11h), mode of operation (batch)	87	(Sadeghzadeh et al., 2020)

Epoxy-functionalized silica (gel)	Phenol P-chlorophenol Catechol	*Myceliophtora thermophile*	Covalent immobilization	pollutant concentration (10 mL), amount of laccase (3 mg of immobilized laccase), reaction time (24 h), operating conditions (pH 4.5, 25 °C)	24 40 95	(Mohamadi et al., 2018)
Mesostructured cellular foam (MCF) silica	Tetracycline	*Trametes versicolor*	Adsorption + Covalent immobilization	total reaction volume (10 mL), pollutant concentration (1 mg L^{-1}), operating conditions (pH 4.5,25 °C), reaction time (1.5 h), surface area (500m^2 g^{-1})	100	(Zdarta et al., 2020)
Amino modified fumed nano-silica (AFNS)	Lindane	*Myceliophthora thermophila*	Adsorption	laccase concentration (2 mg of immobilized laccase), total reaction volume (2mL), pollutant concentration (30µmol L^{-1})	44	(Bebić et al., 2020)
Hierarchical zeolite Y	Bisphenol A (BPA)	*Trametes versicolor*	Adsorption	reaction volume (5 mL), pollutant concentration (2mM), laccase activity (8 U mL^{-1}), mode of reaction (batch reactor), operating conditions (40°C, 120 rpm) reaction time (1h).	40	(Taghizadeh et al., 2020)
Cross-linked carbon nanotube membranes	Carbamazepine Ibuprofen	*Trametes versicolor*	Adsorption	pollutant concentration (20 µM), 0.45 U cm^{-2} of laccase, operating condition (pH 5.5), reaction time (48 h), mode of operating (membrane cell)	48 60	(Ji et al., 2016a)

Cross-linked carbon nanotube membranes	Clofibric acid				45	(Ji et al., 2016a)
Biochar	Carbamazepine	*Trametes versicolor*	Adsorption	pollutant concentration (20 ng L^{-1}), total reaction volume (20 mL), reaction conditions (25°C), reaction time (24 h), mode of operation (batch reactor)	66	(Naghdi et al., 2017)
Activated carbon	Sulfamethoxazole	*Asperguillus oryzae*	Adsorption	pollutant concentration (2.5 mg L^{-1}), total reaction volume (100 mL), reaction conditions (25°C), reaction time (2 h), mode of operation (batch reactor)	92	(Nguyen et al., 2016b)
Activated carbon	Diclofenac	*Asperguillus oryzae*	Adsorption	pollutant concentration (2.5 mg L^{-1}), total reaction volume (100 mL), operating conditions (25°C), reaction time (2 h), mode of reaction (batch reactor)	90	(Nguyen et al., 2016b)
TiO_2 multichannel membrane	Ciprofloxacin	*Trametes versicolor*	Covalent immobilization	pollutant concentration (11 µg L^{-1}), mediator concentration (1mM), total reaction volume (5 L), reaction conditions (pH 6, 25°C), total reaction time (24 h), operating mode (EMR)	93	(Becker et al., 2016)
Poly (lactic-co-glycolic acid) nanofiber	Diclofenac	*Pleurotus florida*	Covalent immobilization	pollutant concentration (50 mg L^{-1}), total laccase activity (4 U), mediator concentration (25 mM SYR), reaction conditions (pH 4, 30°C), reaction time (5h)	100	(Sathishkumar et al., 2012)

CPC silica beads	Sulfamethoxazole	*Trametes versicolor*	Covalent immobilization	pollutant concentration (50 mg L^{-1}), laccase activity (1 U mL^{-1}), mediator concentration (1mM HBT), total reaction volume (5 mL), reaction conditions (pH 5, 40°C) , reaction time (1 h), mode of operation (batch reactor)	76	(Rahmani et al., 2015)
	Sulfathiazole				85	
Mono-channel ceramic membrane	Tetracycline	*Trametes versicolor*	Covalent immobilization	pollutant concentration (20 mg L^{-1}), amount of laccase (0,01 g L^{-1}), operating conditions (pH 6, 25°C), reaction time (24 h) mode of operation (continuous recycled mode)	56	(De Cazes et al., 2014a)
TiO_2 multichannel membrane	Amoxicillin	*Trametes versicolor*	Covalent immobilization	pollutant concentration (10 µg L^{-1}), Mediator concentration (1mM SYR), total reaction volume (5 L reaction), operating conditions (pH 6, 25°C), total reaction time (24 h in EMR)	95	(Becker et al., 2016)
TiO_2 nanoparticles	Carbamazepine	*Trametes versicolor*	Covalent immobilization	pollutant concentration (20 µM), mediator concentration (1mM PCA), laccase activity (0.5 U mL^{-1}), operating conditions (pH 7, 25 °C), mode of operation (batch reactor)	60	(Ji et al., 2016c)

TiO_2 nanoparticles	Diclofenac	*Pycnoporus sanguineus*	Covalent immobilization	particle size: 21 nm, 50 mg total reaction volume (10 mL), pollutant concentration (10 mg L^{-1}), operating conditions (pH 4, 25 °C, 500 rpm), total reaction time (8h), total activity (100 U L^{-1}), mode of operation (batch reactor)	68	(García-Morales et al., 2018)
	Acetaminophen				90	
Carbon nanotube modified electrospun fibrous membranes	Ibuprofen	*Trametes versicolor*	Encapsulation	pollutant concentration (10 mg L^{-1}), amount of laccase (2 mg), total reaction volume (30 mL), operating conditions (pH 7, 25°C), reaction time (5 h), mode of operation (batch reactor)	100	(Dai et al., 2016)

2.7 Enzymatic reactors (ER) for the degradation of PPs

Even if the use of immobilized laccases gives promising results in terms of activity, stability and reusability it is also important to choose the right type and configuration of reactor for easy scale up of the enzymatic process up to industrial scale. Different type of reactors such as packed-bed reactors, fluidized-bed reactors or membrane reactors have been used to carry out the degradation of PPs, they are presented in Table 2-8.

The packed-bed enzymatic reactors (PBER) for the degradation of PPs reported in the literature suffer from low degradation rates. Tušek et al. (2017) observed only 6% degradation of catechol in 90 minutes, according to the authors this very low degradation was due to oxygen limitation within the reactors.

There are only few studies on enzymatic fluidized-bed reactors (FEBR) for the degradation of PPs. Lloret et al. (2012) found 90-100% of oestrogens degradation in a FEBR using laccase immobilized on Eupergit®C. Similiarly, Piao et al. (2019) found 50-80% degradation of bisphenol A in a FEBR with a laccase immobilized on mesoporous silica. They explained their results by the uniform distribution of the biocatalyst and the availability of oxygen. Even if FEBRs seem to be interesting they present high operational costs and pressure drops problems can occur. Along with these challenges, deactivation of biocatalysts can occur due to stress force.

Enzymatic membrane reactors (EMR) are the most investigated reactors for enzymatic degradation of PPs. These reactors present some interest properties because they can be used in different configurations (enzyme immobilized on membrane surface or on a solid bed inserted inside the membrane lumen). Moreover, membrane systems are modular and scale up is easily designed. Nevertheless, some drawbacks can also be present like membrane clogging, low reactivity etc. Ji et al., (2016c) observed less than 10 % of carbamazepine degradation with Laccase from *Trametes versicolor* without using mediators. Barrios-Estrada et al., (2018b) found only 33% of initial concentration of BPA degraded in 24h with immobilized laccase on ceramic membranes. Similarly, De Cazes et al., (2014a) found only 56 % of TC degradation in 24 h with laccase from *Trametes versicolor* immobilized on ceramic membranes. In the last two works the limited conversion achieved can be explained by the low amount of enzymes immobilized due to the limited specific surface of ceramic membranes.

Table 2-8. Enzymatic reactors types used for PPs degradation in literature .

Reactor type	Micropollutant	Enzyme type	Immobilization technique	Process conditions	Efficiency	Reference.
Membrane hybrid reactor	Carbamazepine (CBZ)	*Laccase (T. versicolor)* immobilized on Tio_2 particles	Covalent attachment	PVDF membrane (0.1 µm); SiO_2 immobilized particles suspended; 20µM, 50 mL CBZ solution; 96h operation; 0.5 U mL^{-1}	less than 10% without mediator, 70 % with mediator p-coumaric acid (PCA)	(Ji et al., 2016b)
Packed-bed reactor	sulfamethoxazole, carbamazepine, diclofenac and bisphenol A	Laccase from *Aspergillus oryzae* immobilized on Granular activated carbon (GAC)	Physical Adsorption immobilization	7.5 g of GAC in 1 cm*22cm (d*L) reactor;	Sulfamethoxazole (60%), carbamazepine (60%), diclofenac (60%) and bisphenol A (90%)	(Nguyen et al., 2016a)
Packed-bed reactors	Textile dyes	Legnine peroxide immobilized on Ca-alignate bead	Covalent attachment	5 g of immobilized Ca-alignate; flow rate: 2.5 mL min^{-1}	80 % dye removal	(Bilal and Iqbal, 2019)
Packed-bed reactors	Catechol	Laccase from *Trametes versicolor* immobilized on microchannel glass beads	Covalent attachment	volume: 43 mL; concentration of pollutant (4 mmol L^{-1}); pH 5.5; Flow rate: 10.7 mL min^{-1};	6% degradation in 90 minutes,	(Tušek et al., 2017)
Horizontal rotating reactor (HRR)	Textile dyes	Laccase from Coriolus versicolor immobilized on bacterial	Adsorption	dimensions of HRR diameter of 9.0 cm and a length of 15 cm. 250 mL of dye with 50 mg	88 % decolorization efficiency in 5h with mediators.	(Yuan et al., 2020)

		nanocellulose strips (BNC)		L^{-1} initial concentration		
Enzymatic Membrane reactor;	bisphenol A (BPA); Estrogen 17b-estradiol (E2)	laccase from *Myceliophthora thermophila* immobilized on fumed silica microparticles (fsMP)	Covalent attachment	10 mL stirred tank, ultrafiltration polyethersulfone membrane, activity (1000 U L^{-1}), (2.5 mg L^{-1} E2 and 10 mg L^{-1} BPA); reaction time: 24 h	complete removal of BPA, 80 % E2 (Including 30-45 adsorption in membrane)	(Gamallo et al., 2018)
Magnetic separator reactor	bisphenol A (BPA); Estrogen 17b-estradiol (E2)	laccase from *Myceliophthora thermophila* immobilized on fumed silica microparticles (fsMP)	Covalent attachment	20 mL stirred tank, membrane, activity (1000 U L^{-1}), (2.5 mg L^{-1} E2 and 10 mg L^{-1} BPA); reaction time: 24 h	degradation of 80 % BPA, 60-80 % E2 after 24h of operation	(Gamallo et al., 2018)
Enzymatic membrane reactors	Bisphenol A (BPA)	Laccase from *Trametes versicolor & P. sanguineus* immobilized on ceramic membranes	Covalent immobilization via Gultaraldehyde cross linking	20 mg L^{-1} BPA, Activity (620 U L^{-1}); Multichannel ceramic membrane (TiO_2); 24 h, 25°C, Volume: 2 L	33% degradation in 24h of reaction.	(Barrios-Estrada et al., 2018b)
Melamine sponge porous Monolithic reactor	Sulfamethoxazole (SMX); 2,4,6-trichlorophenol (TCP)	Laccase from *Trametes versicolor* immobilized on Melamine sponge (MeS)	Immobilization via Fe^{3+} linking to amines of MeS	10 mL of 100 µM SMX & 2,4,6-TCP	100% decolourisation of dyes	(Zou et al., 2019)
Membrane reactors	Tetracycline	Laccase from *Trametes versicolor* immobilized on	Covalent immobilization via GA crosslinking	2 L of 20 mg L^{-1} tetracycline solution. reaction time: 24h,	56 % degradation in 24 h.	(De Cazes et al., 2014a)

		ceramic membranes		operating conditions: 25°C, pH 6		
Fluidized-bed reactor	Estrogens E1, E2, EE2	Laccase immobilized on Eupergit C	Covalent immobilization	4 g of biocatalyst (25U g^{-1}), reaction conditions (25°C, pH 7), flow rate: 2.5 L min^{-1}	92-100 % degradation in 03 h.	(Lloret et al., 2012)
Fluidized-bed reactor	Bisphenol A	Laccase immobilized on silica mesoporous structure	Adsorption + crosslinking via GA	laccase activity (0.068 U mL^{-1}), pollutant concentration (25 mg L^{-1}), optimum flow rate: 7 mL min^{-1}	50-80 % in 08 h.	(Piao et al., 2019)

2.8 Porous monoliths for enzyme immobilization

Even if some reported results are promising, all the reactors presented in the previous sections have been investigated in batch at very small scale. In addition, these systems present some drawbacks such as pressure drop, attrition of biocatalyst, low amount of immobilized enzyme due to a limited specific surface, diffusional limitations etc. In order to overcome some of these disadvantages like diffusional problems encountered for example on PBER, hierarchal porous monoliths have been recently applied in catalysis with great success (Biggelaar et al., 2019).

Monolith is a single homogenous porous structure having hierarchical macro-meso channels/pores interconnected through thin wall skeleton. Porous Monolith prepared from inorganic or polymer materials, containing interconnected macro-meso pore networks, can be prepared in various desired shapes and provide unique advantages such as a very high specific surface area for immobilization and then a fast kinetics. Moreover, monoliths can have a high porous volume up to 80%, and then can be crossed by a relatively high flux with very low pressure drop (Sachse et al. 2011).

As explained above, macro-meso porous monoliths have highly porous structure having interconnected macropores and a continuous meso-porous skeleton network. Macropores having pore diameter in the range of (30-50 μm) contribute to flow through the monoliths, while mesopores having pore diameter in the range of (5-20 nm) provide a large surface area (500-700 m^2 g^{-1}) available for immobilization. Due to the interconnected macropores, monoliths are highly permeable which allows the fluid to pass through the monoliths in the form of macro channels, while the meso-porous skeleton network having thickness in the range of (3-15μm) helps reducing the diffusion length which enhance the mass transfer within the mesopores as explained by Haas et al. (2017). Due to these exceptional properties, monoliths have been applied as a flow-through porous reactors as explained by Sachse et al. (2011) and Fletcher et al. (2011).

Another interesting feature of the monoliths is their preparation method, which allows the size of macropores as well as mesopores to be controlled independently, allowing the monoliths to be prepared according to the process requirement. According to Galarneau et al. (2016) the diameter of the macropores can be adjusted between 1 to 30 μm while the diameter of the mesopores can be adjusted between 8 to 20 nm, leading to high specific surface area ranged from 300 to 700 m^2 g^{-1} with a total porosity of about 85%.

Monoliths can be prepared on various materials (polymers, silica, carbon etc.). Among the reported inorganic monoliths, silica macro-porous monoliths have been extensively investigated because they can be obtained with tailored texture, structure and surface functionalities, using bottom up sol-gel chemistry methods (Biggelaar et al., 2019; Brun et al., 2011; Debecker, 2018; P. Haas et al., 2017). Recently, enzyme immobilized silica monoliths have been used as ER with continuous flow in variety of applications. For example, Biggelaar et al., (2019) immobilized transaminases via covalent bounds with glutaraldehyde used as a cross-linking agent, onto macrocellular silica monoliths to perform transamination reaction in a continuous flow mode. Hou et al. (2019) immobilized Horseradish peroxidase isoenzyme C (HRP) and Engyodontium album proteinase K (proK) via non covalent adsorption of conjugates on porous silica monoliths and found high operational stability. Calza et al., (2016) immobilized soybean peroxidase (SBP) on silica monoliths and used them in combination with photo-catalytic treatment for the degradation of commonly used dyes and carbamazepine, a very refractory pharmaceutical. The combined process yielded 100% degradation of dyes in first 2 h while carbamazepine was degraded within first 60 minute. Alotaibi et al., (2018) immobilized lipase from *Candida Antarctica* on silica monoliths and applied them in a continuous flow reactor for a transesterification. They reported a continuous ester production for more than 100 h without deactivation of enzymes and concluded that highly porous structure enhanced immobilized enzyme loading and hence productivity. Similarly, Szymańska et al., (2013) studied, the covalent immobilization of invertase on silica monoliths which were used as a continuous flow reactor for the reaction of sucrose hydrolysis. It was observed that the rate of sucrose hydrolysis was 1000 times higher in the monolithic bioreactor compared to MCF-based slurry system.

2.8.1 Transport modelling in monoliths

There are very few modelling and simulation studies available in literature describing the flow patterns within the macroporous structure of monoliths. Those studies are mainly aimed to compute the average permeability, porosity and to rebuilt, by image processing techniques the 2D or 3D structure, as well as the flow pattern within the macroporous structure. For example, Jungreuthmayer et al. (2015) aimed to compute the permeability and to model the pressure drop and flow behaviour in macroporous channels of a polymethacrylate monolith. For this purpose, the monoliths were cut into 50 nm slices and those slices were analysed by SEM. Then, by image processing a 3D monolithic structure was constructed. According to them, simulated permeability was in good agreement with experimental values.

In a more classical approach, Tallarek et al. (2002**)** applied Kozeny–Carman equation to calculate the permeability of porous monoliths. Equivalent particle diameter (characteristic length) for monoliths was derived based on the equivalence in the permeability.

Meyers and Liapis. (1999) constructed a cubic lattice network of interconnected pores to propose the structure of a monolith. Inter porous velocity and diffusion coefficient of the molecules was studied within the built porous structure. The results indicated that transport phenomena in the porous medium are strongly affected by porous structure like pore size distribution and pore interconnectivity.

Hlushkou et al. (2010) simulated the fluid flow within the macroporous structure of a silica monolith. Confocal laser scanning microscopy (CLSM) was used to rebuilt by calculation the structure of the monolith. A segment of 60 μm × 60 μm × 12 μm from a 100 μm i.d. capillary silica monolith was reconstructed. Simulations were carried out on obtained 3D structure in order to analyse the flow velocity field and to calculate the hydraulic permeability of the silica monolith.

All the above-mentioned approaches applied for simulation of velocity field, diffusion and dispersion of chemical species (mostly applied for chromatography) within the porous structure. These models are based on morphology and real structure of the porous monoliths, which required sophisticated computational techniques coupled with image processing as well as relatively high computing time and cost especially for large scale geometries required for practical engineering problems. To our knowledge in literature, there is no specific modelling study, which simulates the reaction kinetics coupled with transport of species within the macroporous silica monoliths.

To conclude, in the literature, most of the supports used for enzyme immobilized were applied in batch process at low scale. Membranes were widely used as a flow through support for immobilized enzymes, however they suffered from low degradation rates because of limited surface area and flux limitation. As silica monoliths have highly porous structure with large surface area available for enzyme grafting. Therefore, in this research work, silica monoliths will be applied to immobilize laccase from *trametes versicolor* via covalent grafting and then laccase-loaded monoliths will be used for PPs degradation in water at laboratory scale. According to our knowledge, enzyme loaded-silica monoliths are never tested for PPs degradation in water.

Chapter 3

Materials and methods

3. MATERIALS AND METHODS

Summary

The aim of this chapter is to show the experimental methods and materials used in this research work to characterize the monoliths with immobilized laccase and to determine the enzymatic kinetics. Moreover, the methods for the determination of the enzymatic monoliths stability for the degradation of tetracycline (TC) in osmosed water are also described. This chapter is divided into four parts: i-e; materials, analytical techniques applied, continuous stirred tank batch reactor mode studies (CSTR) and flow-through reactor studies (FTR) in continuous recycled mode. CSTR studies were carried out with free and immobilized laccase to determine activity, reaction kinetics parameters (K_M and V_{max}), storage stability of immobilized laccase and effects of parameters like dissolved oxygen (DO) as well as possible inhibiting products effects. FTR studies were carried out with laccase activated monoliths for TC degradation in continuous recycled-mode. Operational stability tests were carried out for TC degradation, to observe the activity loss during continuous operation.

3.1 Materials

The synthesis and structural characterization of monoliths were carried out by M. Wassim Sebai. Synthesis and pre-activation of monoliths with (3-Aminopropyl) triethoxysilane **(**APTES) at Institute Charles Gerhardt Montpellier (ICGM) whereas surface and structural characterizations were performed at Institute Européen des Membranes (IEM).

Commercial Laccase from *Trametes versicolor* (1.10.3.2)

Brown powdered commercial laccase (Activity ≥ 0.5 U mg^{-1}) was purchased from Sigma-Aldrich and stored at -4°C. One unit (U) corresponds to the amount of laccase which converts 1 µmol of catechol per minute at pH 5.0 and 25 °C.

Tetracycline (TC) (≥98.0%)

Dark yellow tetracycline powder (≥98.0%) was purchased from Sigma-Aldrich and was stored at 4°C. TC solution was prepared in osmosed water. The chemical structure of TC is shown in Figure 3-1.

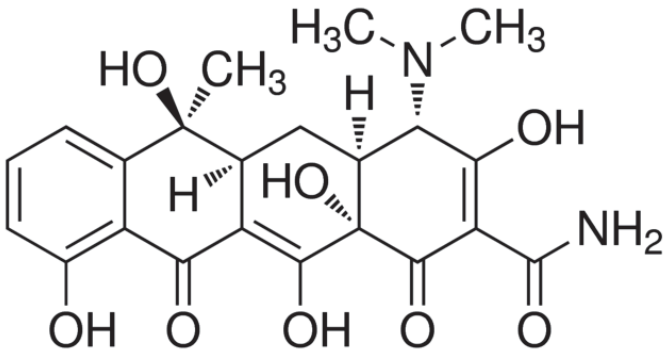

Figure 3-1. Chemical structure of TC

Glutaraldehyde (25% v/v)

Grade II glutaraldehyde solution (25% v/v) solution in water was purchased from Sigma Aldrich and stored at room temperature.

2,2'-azino-bis (3-ethylbenzothiazoline-6-sulphonic acid) (ABTS)

ABTS is a peroxidase substrate suitable for enzyme activity measurement. This substrate produces a soluble product that is green in colour and can be read by spectrophotometer at 405-420 nm. ABTS in powdered form (≥98.0%) was purchased from Sigma Aldrich, and stored at 2-4 °C.

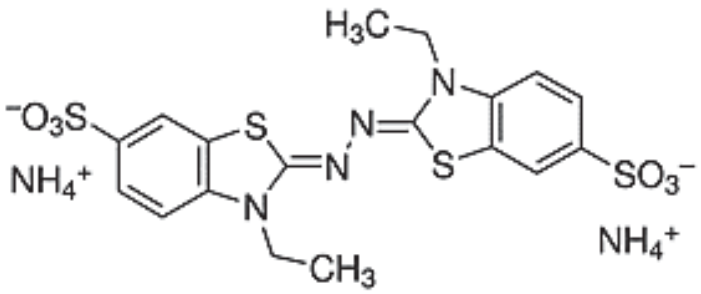

Figure 3-2. Chemical Structure of ABTS

Nitric acid (HNO_3)

HNO_3 was purchase solution (68%) was purchased from Sigma Aldrich and stored at room temperature.

Polyethylene glycol (PEG) (100 kDa, 98%)

PEG was purchased from Sigma Aldrich and stored at room temperature.

Tetraethoxysilane (TEOS) (99 %), (3-aminopropyl) triethoxysilane (APTES) (99 %)

TEOS and APTES were purchased from Sigma Alrich and stored at room temperature**.**

3.2 Analytical techniques

3.2.1 Scanning electron microscopic (SEM) analysis of monoliths

SEM analysis of monoliths were carried out with a scanning electron microscope Hitachi (MODEL S-4800). Specimens were prepared by cutting monoliths in thin slices (1-2 mm), then double-sided adhesive tape was used to fix the specimens to the stub. Applied voltage: 0.1 kV-30 kV. Scanning Resolution: 6-100 µm.

3.2.2 Porosity determination of monoliths

Porosity of monoliths was determined by mercury porosimetry (Micrometrics Autopore 9220) and nitrogen adsorption at 77 K (Micromeritics Tristar 3020). Before nitrogen adsorption measurements, monoliths were outgazed for 12h at 250°C and 80°C for raw and grafted silica monoliths respectively.

3.2.3 TGA analysis

The quantitative determination of the number of amine functions on the surface of the silica monolith was determined by thermogravimetric (TGA) analysis (PerkinElmer STA 6000) using a high-resolution program (from 40 to 900 °C) under air with a ramp of 10°C per minute. The number of grafted functions was determined by the loss of weight of the material from 200°C to 900°C and considering the dehydroxylation of the surface of the monolith.

As explained previously, structural analyses for surface characterization of the monoliths were carried out at IEM by Mr. Wasim Sebai (current PhD student working at Institute Charles Gerhardt Montpellier (ICGM) and Institute Européen des Membranes (IEM).

3.2.4 HPLC-MS quantitative analysis

HPLC-MS quantitative analyses were performed to observe the evolution of the TC concentration during enzymatic degradation.

HPLC–MS was carried out with a Waters 2695 pump, autosampler with 20µl loop, a Waters 2695 separation module (HPLC), and a Waters Micromass (Wythenshawe, Manchester,UK) Quattro Micro mass spectrometer was equipped with ESI. HPLC was carried out on a Waters - XSelect HSST3 100 mm*2.1 mm - 2.5 µm particles size; the column temperature was 25 °C. The mobile phase was Buffer A (HPLC grade water + 0.1% formic acid) and Buffer B (HPLC grade acetonitrile + 0.05% formic acid). The flowrate was constant at 0.25mL min^{-1}.

The triple quadrupole MS was operated in selected-ion-monitoring (SIR) mode with compounds being ionized in the positive electrospray ionization mode. To achieve the best sensitivity, the MS was adjusted to facilitate the ionization process. The detection conditions were as follows: capillary potential 3.5 kV, cone potential 30 V, source temperature 120 °C, desolvation temperature 450°C, cone gas flow 50 L h^{-1}, and desolvation gas flow 50 L h^{-1}. Nitrogen was used as nebulizer gas.

3.2.5 Spectrophotometric analysis

Spectrophotometric analysis was carried out to observe colour change during enzymatic oxidation of ABTS with Shimadzu UV-2401PC spectrophotometer, Japan. All the analyses were carried out at 25°C.

3.2.6 Dissolved oxygen (DO) measurement analysis

Online measurement of DO concentration in reaction solution was carried out with the help of optical DO meter VisiFerm RS-485 Himlton (Switzerland). The DO meter was inserted inside the reaction media and change in DO concentration was recorded every 5 minutes.

3.3 Experimental methods

3.3.1 Synthesis of monoliths and surface activation.

Silica monoliths functionalized with APTES were provided by Institute Charles Gerhardt Montpellier (ICGM) as part of the project (MUSE ANR-16-IDEX-0006 project DEMEMO). Mr. Wasim Sebai (current PhD student working in ICGM/IEM) synthesized the monoliths and functionalized with amino-groups by the method explained previously reported by Galarneau et al., (2016b).

3.3.2 Synthesis of silica monoliths

Silica monoliths with hierarchical porosity (macro-/mesoporosity) were synthesised by a controlled sol-gel process with TEOS and PEG. 24.561 g of H_2O and 2.419 g of HNO_3 (68%) were mixed for 10 min at ambient temperature and 2.577 g of polyethylene glycol (PEG 100 kDa) were added and stirred until homogenization. Then this solution was transferred to the freezer at -19 °C for 10 min. In parallel, 20 g of tetraethoxysilane (TEOS) were also put at -19 °C for 1 h. The acidic solution containing polyethylene oxide (PEG) was then placed in an ice bath at 0 °C. The TEOS was added and the mixture was stirred for 1 h. The resulting solution was poured into 8 PVC tubes of 10 cm length and 8 mm internal diameter and the tubes were kept at 40 °C for 3 days, washed and then poured in 150 mL of NH_4OH solution (0.1 M) in

autoclave at 100 °C for 24 h. The monoliths were then washed in water until neutral pH and then, poured in an ethanol bath (96 %) for 24 h for solvent-exchange. The monoliths were then dried at 40 °C for 24 h and calcined at 550 °C for 8 h (rate 2 °C/min).

3.3.3 Functionalization of silica monoliths with amino groups

The silica monoliths were functionalized by silanization with aminopropyltriethoxysilane (APTES) in ethanol in batch under reflux. 1.0276 mL APTES was added in 50 mL ethanol (99 %) and silica monoliths (0.7 g) were poured in this solution. This corresponds to an excess of 10 APTES molecules per nm^2 of silica surface. The mixture was then heated at 80 °C for 17 h under reflux. Then, the resulting monoliths were washed 3 times with ethanol (99 %) at ambient temperature and dried at 80°C for 20 h.

3.3.4 Cladding of monoliths

To be used in continuous flow, the monoliths were cladded with heat shrinkable transparent gains in Tetra-fluoroethylene-propylene of 6.4 mm diameter in accordance with the diameter of the monoliths and heated at 180° C for 2 h to form the reactors.

3.3.5 Activation of silica monoliths with laccase

Laccase from *Trametes versicolor* was immobilized in preactivated silica monoliths cladded inside Teflon™ gains (Provided by ICGM) via crosslinking with glutaraldehyde (GLU). GLU was chosen as a cross-linking agent, because it is highly reactive with amine groups under neutral pH at 25°C and the bonds produced are chemically and thermally more stable than those obtained from other aldehydes (Nimni et al., 1987), (Migneault et al. (2004). Three steps were necessary to immobilize the laccase:

Silica monoliths were first wetted with citrate phosphate buffer solution (pH 7, 0.1 M) 0.5 mL by passing the solution through the monolith. The purpose of the wetting was to provide the reaction condition for glutaraldehyde and then for laccase.

Silica monoliths were filled manually with 0.5 mL of glutaraldehyde solution (4% v/v) prepared in citrate phosphate buffer (pH 7, 0.1 M) and allowed to react for 30 minutes. The concentration of glutaraldehyde was chosen according to the amount of amino groups attached to monoliths (0.8 mmol NH_2 $g_{monolith}^{-1}$). The cross-linking reaction time was selected as suggested by P. Monsan, (1978). After the reaction, monoliths were rinsed three times with 0.5 mL of the same buffer solution to remove unreacted glutaraldehyde. During the reaction between glutaraldehyde and APTES the white or pale-yellow monoliths turn deep orange

within minutes. As explained by George et al. (1984) this change in colour is an indicator of the reaction leading to the formation of an aldimine (Schiff linkage (=CHN=), between the free amino groups of APTES and glutaraldehyde.

Finally, monoliths were filled with 0.5 mL of laccase solution (5±1 U mL_{sol}^{-1}) prepared by solubilizing the necessary amount of commercial powder of enzyme in the same citrate phosphate buffer (pH 7, 0.1 M). For this purpose, the enzymatic solution was introduced with the help of micropipette at the entrance of the cladded monolith, allowing the penetration into the monolith porosity by capillarity. Once the monolith is filled with the solution without any air bubbles entrapment, both sides of monolith were closed, and laccase could react for 1 hour. Afterward, the unreacted enzymatic solution was removed, and monoliths were rinsed three times with 0.5 mL of the same buffer solution. After immobilization, enzymatic monoliths were stored in the same buffer solution at 4°C. The schematics of covalent bonding steps are illustrated in Figure 3-3.

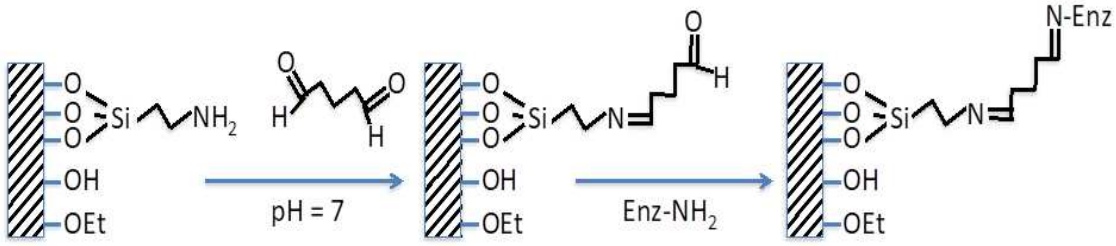

Figure 3-3. Reaction steps for enzyme covalent bonding through APTES loaded monoliths.

3.3.6 Batch experiments in continuous stirred tank reactor (CSTR)

3.3.6.1 Determination of specific activity, immobilization yield and theoretical activity recovery of immobilized monoliths

Activity (U m L^{-1}) of free laccase was measured using ABTS as substrate. 100 µL of diluted enzyme solution was added to 900 µL of 1 mM ABTS solution prepared in a citrate phosphate buffer solution (pH 4, 0.1 M), absorbance change was followed for 1 minute by spectrophotometry at 420 nm (ε = 36000 $M^{-1}cm^{-1}$), activity (U mL^{-1}) was then estimated by slope of absorbance vs time. 1U corresponds to the quantity of enzyme able to oxidize 1 µmol of substrate per minute.

Immobilization of enzymes on a support can be quantified in terms of specific activity (U g^{-1}), enzyme loading (mg of enzyme per gram of support), percent immobilization yield, expressed activity and immobilization efficiency. Activity of immobilized laccase was also

measured using ABTS as substrate and with known mass of activated monoliths previously crushed. Reaction was started by adding 5 mg of the active powder (wet basis) to 25 mL of ABTS solution (1 mM) prepared in a citrate phosphate buffer (0.1 M, pH 4) in a 50 mL flask at 25°C, under agitation of 250 rpm. The evolution of the absorbance at 420 nm during first 10 minutes was recorded with the help of a spectrophotometer as explained above. Samples of 1 mL were taken after each minute with the help of a syringe and a 0.2 µm syringe filter was used to avoid monolith particles in the sample. The specific activity (U $mg_{monolith}^{-1}$) was then calculated by equation (3.1).

$$A_{sp}\ (U.g^{-1}) = \frac{\Delta Abs.}{\Delta t}\frac{V_T}{d.\varepsilon.m} * 10^3 \qquad (3\text{-}1)$$

Where,

$\frac{\Delta Abs.}{\Delta t}$= Change in absorbance of ABTS per unit time (minute)

V_T= Total volume of the ABTS solution used (L)

m= mass of the crushed monolith used (wet basis) (g)

A_{sp}= Specific activity of the immobilized enzyme (Ug^{-1})

ε= Molar absorption coefficient of ABTS ($M^{-1}cm^{-1}$)

d= path length of length (1 cm)

The enzyme immobilization yield was calculated by the difference of activity between the stock laccase solution used for immobilization and the supernatant solution after immobilization. Stock laccase solution (10g L^{-1}) was prepared and kept under stirring at 100 rpm at 25 °C for 20 h before immobilization in order to get the stable activity of the enzyme solution as suggested by Boudrant et al. (2020). After immobilization step, unreacted laccase solution was separated and collected into a flask and then monoliths were rinsed with the citrate phosphate buffer (pH 7, 0.1 M). The rinsing solution was also collected in the flask together with unreacted laccase solution. Finally, the activity of the solutions (unreacted laccase + rinsing) was measured as explained above.

Immobilization yield (%) was calculated by using equation (3.2) and (3.3) using the same protocol as followed by (De Cazes et al., 2014). Similarly, Immobilization efficiency (%) and expressed activity was determined using equation (3.4) and (3.5):

$$A_{immobilized} = A_{initial} - (A_{left} + \sum A_{rinsing}) \quad (3\text{-}2)$$

$$\rho_{immobilization} = \frac{A_{immobilized}}{A_{initial}} \times 100 \quad (3\text{-}3)$$

$$Efficiency\ (\%) = \frac{A_{observed}}{A_{immobilized}} \times 100 \quad (3\text{-}4)$$

$$A_{expressed}\ (\%) = \frac{A_{observed}}{A_{inital}} \times 100 \quad (3\text{-}5)$$

$A_{immobilized}$ = Theoritical immobilized activity (U).

$A_{observed}$ = Immobilized activity experimentally determined (U).

$A_{initial}$= Activity of the stock laccase solution used for immobilization step (U).

A_{left}= Activity of the unreacted laccase solution after immobilization step (U).

$A_{rinsing}$= Activity of the rinsing solution (U).

$\rho_{immobilization}$= Immobilization yield (%).

3.3.6.2 Estimation of apparent reaction kinetic parameters (K_M, V_{max})

V_{max} is defined as the maximum reaction rate of the enzyme-catalysed reaction, and its value is dependent on the quantity of the enzymes used, i-e; higher the quantity of the enzymes used faster will be the reaction to reach the equilibrium position. While K_M, also called Michaelis-Menten constant is the concentration of substrate at which the reaction rate becomes half of V_{max}. It shows the affinity of the enzymes towards a substrate; higher the K_M value, lower is the enzyme affinity towards substrate and vice versa.

It has been reported that enzymes can partially loss their activity as well as affinity after immobilization due to conformation changes or steric hindrance (Secundo et. al 2013) and hence the immobilized enzyme process can be unfeasible for practical applications. However, different research studies have found exceptional operational stability with covalent immobilization of enzymes in comparison to other immobilization techniques, such as adsorption (Kashefi et al., 2019; Mahmoodi et al., 2020). Indeed, the determination of apparent reaction kinetic parameters (K_M, V_{max}) is fundamental to understand the behaviour and reactivity of laccase immobilized in monoliths.

Apparent reaction kinetic parameters for free and immobilized laccase (crushed laccase-activated monoliths) were determined using ABTS and TC as substrates in batch at 25 °C under continuous stirring (250 rpm). For this purpose, an equivalent amount of 0.01 U of enzyme (liquid solution of free enzyme or crushed laccase-activated monolith) was added to 25 mL of ABTS solution (20-100 µM in citrate phosphate buffer solution, pH 4). In the case of experiments with TC the amount of free (5.0 U) and immobilized enzyme (3.0 U) were added to 10 mL of TC solution (2-20 ppm in osmosed water, pH 6). Runs for both substrates were carried out in flasks under stirring and open to air. Linear regression was applied on the obtained data and then apparent reaction kinetic parameters (V_{max} and K_M) were determined by Lineweaver-Burke plot according to equation (3.6):

$$\frac{1}{V} = \frac{K_M}{V_{max}} \frac{1}{[S]} + \frac{1}{V_{max}} \tag{3-6}$$

Here V is the rate of substrate consumption (µmol min^{-1}); V_{max} is the maximum rate of substrate consumption (µmol L^{-1} min^{-1}) and K_M is the Michaelis-Menten constant (µmol L^{-1}) and S the substrate concentration (µmol L^{-1}).

3.3.6.3 Determination of storage stability of activated silica monoliths

Storage stability of immobilized enzymes is important for the process economy. To study this stability, about 15 monoliths were immobilized with the same protocol discussed previously, filled with buffer solution pH 7 and stored at 4°C. The activity of the activated monoliths was measured with the same protocol discussed earlier for the period of one month.

In order to make comparison of stability with free enzyme, a solution of free enzyme (10 g L^{-1}) was prepared in buffer pH 7 and kept at 4°C, the activity of the free enzyme was also measured over a one-month period using the same protocol discussed earlier for free enzyme activity.

3.3.7 Experiments with monoliths in continuous recycled mode

3.3.7.1 Development of monolith system for TC degradation

To determine the capacity of laccase-activated monoliths for TC degradation, a laboratory unit (Figure 3-4) was built connecting in series three monoliths. A TC solution (20 ppm in osmosed water) was flowed through the monoliths and recycled to a reservoir with a HPLC pump (Gibson model: 321, France). A pressure transducer was placed before the inlet of the monoliths to monitor the pressure changes during the process, temperature of the feed

tank was controlled placing the reservoir in a thermostatically controlled water bath. Air bubbling was done by a central air line of IEM only for those experiments where DO effects were studied. All the TC degradation tests were carried out in a close loop (complete recycling of the TC solution).

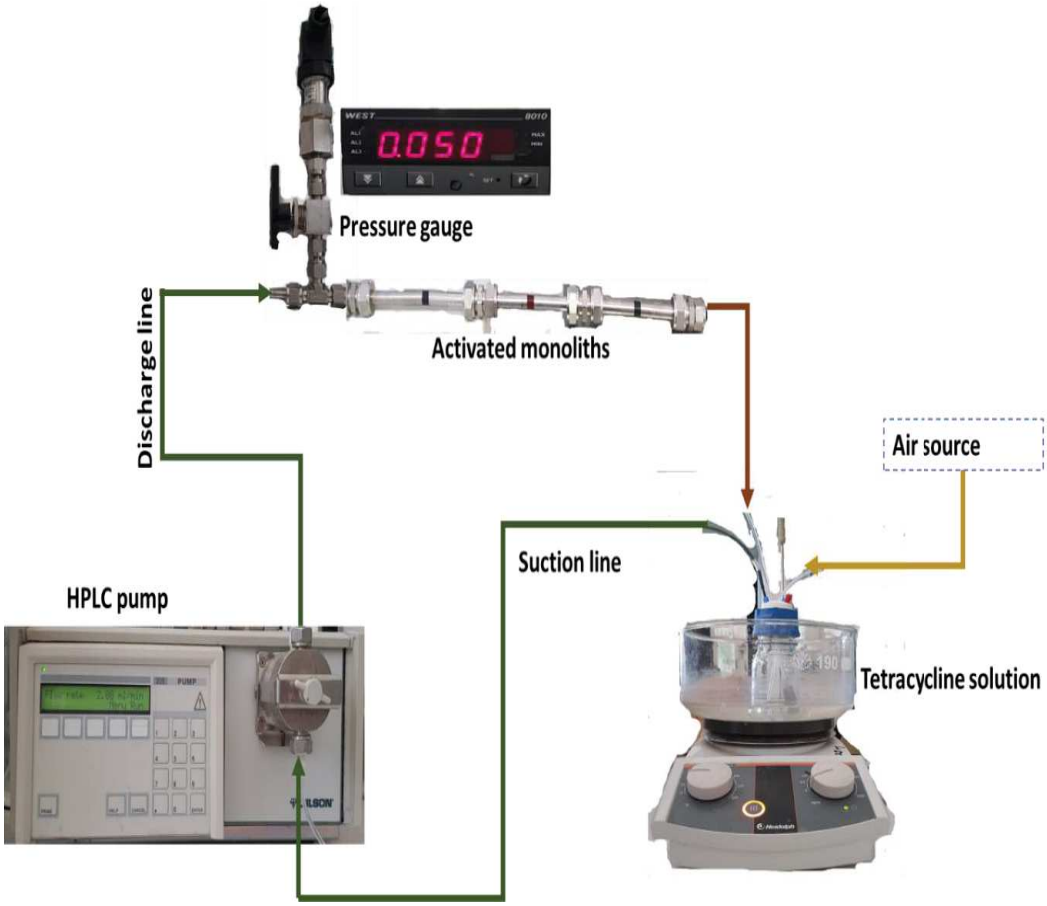

Figure 3-4. Laboratory set-up to study the TC degradation with enzymatic monoliths.

3.3.7.2 Permeability tests

Permeability is the property of porous materials that allows the fluid to pass through the pores of the materials. For the materials to be used as a flow-through reactor, it is very important to have high permeability. Permeability has direct relationship with the pore size, tortuosity and pore shape of the porous materials (Hubbert, 1956). Permeability of the porous material can be calculated from the slope of the flow rate-pressure drop relationship.

To measure the permeability coefficient, tests were carried out both before and after immobilization of enzymes by filtrating osmosed water through the monoliths. Monoliths of 0.6 cm diameter and 0.5 cm length were connected to a flow system consisting of a HPLC pump and a pressure gauge as shown in Figure 3-4. The flow rates were varied from 1 mL min^{-}

[1] to 5 mL min^{-1}. The back pressure exerted by monoliths was measured thanks to a pressure gauge and then permeability coefficient (k) was calculated by Darcy equation (3.7) as follows:

$$k = \frac{Q}{A}\frac{l}{\Delta P}\mu \qquad (3\text{-}7)$$

With k Permeability coefficient (m^2), Q the flow rate (m^3 s^{-1}), A the cross section of the monolith (m^2), μ the viscosity of the fluid (μ = 1.002 m Pa s at 20 °C for water), l the length of the monolith (m) and ΔP the difference of pressure between the outlet and the inlet of the monolith (Pa).

3.3.7.3 TC degradation tests

TC degradation tests were carried out with the system shown in Figure 3-4. TC solution (20 ppm) prepared in osmosed water pH 6, at 25°C was flowed through the enzymatic monoliths in continuous recycle-mode for 24h. The flow rate was kept at 1 mL min^{-1}. TC samples (0.1 mL) were taken from the TC feed tank and analysed by high-performance liquid chromatography coupled to triple-quadrupole mass spectrometry (HPLC–MS). Samples were injected through a Macherey-Nagel C18 column (50 mm x 2 mm) with a Waters e2695 Separations Module, and the 410 m/z fragment was detected with a Micromass Quattro micro API device.

3.3.7.4 Operational stability tests

As explained previously, one of the main advantages of covalent immobilization technique is due to the strong binding established with the support, which guarantees the operational stability of the biocatalyst and offers the possibility to reuse it.

The operational stability of laccase-activated monoliths under continuous operation was studied for TC degradation. For this purpose, TC (20 ppm) degradation tests were carried out following a sequential procedure: after 8 hours of reaction the pilot was emptied, rinsed with osmosed water and kept at room temperature overnight, then a new fresh TC solution was introduced and the run start again. The cycles were repeated for a total duration of 75 hours. The stability tests were carried out at two different flow rates, i-e 1 mL min^{-1} and 5 mL min^{-1}.

3.3.7.5 Effect of recirculation flow on TC degradation rate

In recirculation system, two residence times are involved: i-e, reaction time inside the reactor and residence time inside the feed tank. These both residence times are dependent on the recirculation flow rate. Therefore, in order to get the optimum recirculation flow, TC

degradation tests were carried out at different flow rates from 0.5 mL min^{-1} to 5 mL min^{-1} and their effect on TC degradation rate was observed. Each run was initiated with new activated monoliths ((0.5 ±0.1 U mL^{-1}) as well as freshly prepared TC solution (20 ppm). All the degradation runs were carried out for 24 h.

To study possible structural changes of the monoliths due to continuous operation, SEM observations of activated monoliths before and after the TC degradation tests were carried out. For this purpose, the degradation tests were done continuously for one week varying the flow rates from 0.5 mL min^{-1} to 5 mL min^{-1}.

3.3.8 Effect of parameters on TC degradation rate

3.3.8.1 Dissolved oxygen (DO)

Laccases require oxygen to degrade pharmaceuticals; therefore the presence of oxygen in excess is imperative. To study the effect of DO, experiments of TC degradation were carried out in batch with crushed activated monoliths. For this purpose, air at the flow rate of 30-40 mL min^{-1} was bubbled inside the stirred reaction media. For the degradation reaction with activated monoliths, in continuous recycled mode operation, the air was bubbled inside the feed tank (Figure 3-4). In both cases the DO concentration was continuously measured with a DO meter VisiFerm RS-485 from Himlton (Switzerland). This bubbling flow rate was sufficient to keep the solution at the oxygen saturation level. DO concentration was continuously recorded after each 5 minutes.

3.3.8.2 Effect of enzyme concentration on tetracycline degradation

Enzyme concentration is one of the important factors for tetracycline degradation. In order to study the effect of enzyme concentration, a set of batch experiments were carried out with crushed activated monoliths by varying the concentration of the enzyme from 0.05 to 0.6 U mL^{-1} while the initial TC was set at 20 ppm. The evolution of TC concentration was observed for 24h. Samples of 0.1 mL were collected into vials with the help of syringe filters and analysed in HPLC for tetracycline degradation.

3.3.8.3 Inhibition effect of TC degradation products

According to Jing et al. (2009) and Barth et al. (2015), enzymes can be inhibited due to formation of degradation products during the reaction. Experiments were thus realised to find out whether the TC degradation products have an effect on the efficiency of the degradation process.

For this purpose, runs were carried out in batch with crushed activated monoliths. An initial TC degradation test was carried out for 24 h with 50 mL of fresh TC solution (20 ppm), with an enzymatic concentration equivalent to 0.2 U mL^{-1}. Afterward, the reaction mixture (unconverted TC+ degradation products) was separated from immobilized enzymes (crushed activated monoliths) by filtration in a Büchner flask under vacuum. Then, further TC degradation experiments were carried with a reaction medium prepared by mixing a fresh concentrated TC solution with a volumetric fraction (50-90%) of the reaction mixture obtained from the initial experiment. The concentration of the fresh TC solution was adjusted to obtain the same initial TC concentration (20 ppm) for all experiments. the enzyme concentration was equal to 0.2 U mL^{-1}.

Chapter 4

Results and discussions

4. RESULTS AND DISCUSSIONS

SUMMARY

Silica monoliths with uniform macro-/mesoporous structures (20 µm and 20 nm macro- and mesopores diameters, respectively), high porosity (83%) and high surface area (370 m^2 g^{-1}) were prepared by ICGM. The monoliths were grafted with amino groups (0.9 mmol NH_2 g^{-1}) and used to immobilize laccase from Trametes versicolor by covalent grafting through glutaraldehyde (GLU) coupling (1.0 mmol GLU g^{-1}) leading to a laccase activity of 20 U g^{-1}. Immobilization yield based on difference between initial and final activity of the enzymatic solution used for immobilization was equal to 80%. The results of permeability tests suggested that monoliths are highly permeable (Permeability coefficient, k= 5.95 10^{-12} m^2) due to their interconnected macroporous structure. Laccase activated monoliths were used for the degradation of tetracycline (TC) in aqueous solutions (20 mg L^{-1}) in flow-through reactors under a configuration of continuous flow (1 mL min^{-1}) with recycling. TC degradation efficiency was found to be 40-50 % after 5 h of reaction at pH 7. Laccase activated monoliths were used during 75 hours of sequential operation without losing activity. After 30 days of storage at 4°C, 85% of the initial activity remained confirming a very good stability of enzymes immobilized on monoliths. The effect of different factors such as dissolved oxygen (DO), degradation products and recirculation flow on TC degradation efficiency were studied. It was observed that DO enhanced the TC degradation rate while degradation products and recirculation flow had no effect on TC degradation in the range of parameters variation studied in this work.

4.1 Structural characterization of monoliths (thesis W. Sebai, ICGM)

Nitrogen adsorption/desorption isotherms at 77 K and mercury porosimetry measurements showed that monoliths present a very high porous structure with a total porosity of $\varepsilon = 0.83$ ($V_{macro} = 3.0$ mL g^{-1}, $V_{meso} = 0.8$ mL g^{-1}), a low density of 0.20 g cm^{-3} and mesopores with a mean diameter of 18 nm developing a large specific surface area of 336 m^2 g^{-1}. The macroporous surface determined by mercury porosimetry is around 1 m^2 g^{-1}. After the activation, the quantitative determination of the number of amine functions on the surface of the silica monolith by TGA analysis showed that amino-functionalized monoliths contain 0.8 mmol NH_2 $g_{monolith}^{-1}$ corresponding to a grafting of 1.5 NH_2 per nm^2 with 72% of tridentate silanes (28% of bidentate). After laccase immobilization by covalent grafting through

glutaraldehyde bounds, important textural changes occur with a decrease of the specific surface area (164 $m^2 g^{-1}$), V_{meso} (0.5 mL g^{-1}) and mesopores diameter (15 nm). Figure 4-1 shows a SEM picture of the structure of a raw silica monolith 4.1 (a) and laccase-grafted monolith 4.1 (b). From Figure 4-1 (a) it can be noticed the interconnected macropores network of approximately 20 µm of average diameter and a skeleton thickness of around 6 µm. The aspect of grafted monolith presents a slight difference respect to the raw one, only the softness of the surface seems to be enhanced indicating the possible formation of a thin film of immobilized enzyme on the surface. This effect is more marked in Figures 4-1(c) and 4-1 (d) which show corresponding magnifications of Figure 4-1 (a) and 4-1 (b) respectively. Many hypotheses can be done to explain this behaviour; on one hand laccase grafting was occurring more extensively in the mesoporosity, on the other hand a very thin layer of the immobilized enzyme was perhaps covering the internal surface of the solid (as it is observed in Figures 4-1(b) and 4-1 (d)). The very thin coating does not significantly affect the macroporosity but it can partially cover mesopores' mouth. Moreover, the decrease of the specific surface, mesopores volume and diameter discussed above are also indications that both hypotheses are possible.

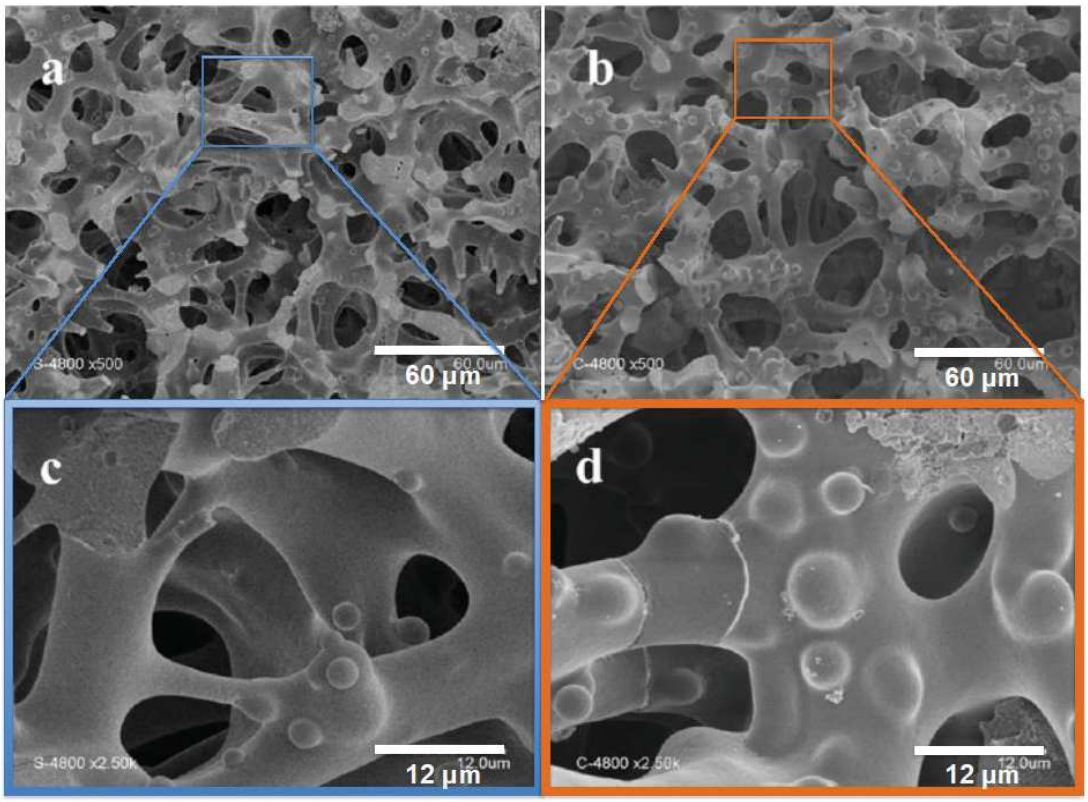

Figure 4-1. SEM of monoliths showing the macroporous structure. a) Raw monolith, b) Laccase-grafted monolith, c) and d) are respectively magnification figures a) and b).

4.2 Batch experiments in continuous stirrer tank reactor

4.2.1 Specific Activity and immobilization yield

The final activity of the biocatalyst and the immobilization yield are important factors for process efficiency and cost, but the immobilization efficiency and the expressed activity are also relevant parameters which permit to define and improve an immobilized enzyme preparation (Boudrant et al., 2020b). The activity of a single monolith (6 mm diameter and 5 mm length, mass of 50 mg) was determined using crushed activated monoliths as explained in section 3.3.6.1. Indeed, the mean activity of one activated monolith was of 5.0 ± 0.5 U and the immobilization yield was found equal to 80 ± 5%. This value, lower than 100 % may be the result of various phenomena such as diffusional limitations (the contact time was relatively low (1 h) and as stirring was not possible during immobilization, the enzyme solution was not renewed inside the monolith) or steric hindrance problem (some of the activated sites were not accessible).

Although the immobilization yield was not maximal, a significant increase in enzyme activity was observed after immobilization. Immobilization efficiency (E) and expressed activity ($A_{expressed}$) were respectively equal to 310 % and 250 %. Such enhancement of enzyme activity after immobilization is not surprising and has already been reported especially in the case of oxidoreductase enzymes (Boudrant et al., 2020b). The good catalytic properties of the enzymatic monoliths could be partly due to the choice of glutaraldehyde as cross-linker.

It is important to notice that the silica support preactivated with APTES presented a high density of amino groups (i.e. 1.5 NH_2 per nm^2); then it is possible that after activation with glutaraldehyde, the silica support acts as a hetero-functional support. Indeed, the properties of the surface of such support offer the possibility to immobilize enzyme through covalent bonds with glutaraldehyde but also via ionic exchange or hydrophobic interactions (Barbosa et al., 2014). According to Barbosa et al. (Barbosa et al., 2014), ionic exchange with amino groups occurs more rapidly than the reaction resulting on covalent bonds. Then there is thus no guarantee that the totality of enzymes which remained on the support were covalently grafted. Nevertheless, according to George et al. (George et al., 1984b), the colour change (from white or pale yellow to deep orange) confirmed the formation of an aldimine (Schiff linkage (=CHN=), between the free amino groups of APTES and glutaraldehyde. Furthermore, immobilization was probably also favoured by the structure of monoliths of extremely

interconnected macroporous and mesoporous network and the thin skeleton (6 μm), which facilitates the access to the numerous reactive sites.

4.2.2 Determination of apparent reaction kinetic parameters

Apparent kinetic parameters K_M and V_{max} for both free and immobilized enzymes (crushed monoliths) were determined with two different substrates ABTS and TC by the method discussed above in section 3.3.6.2. It should be noted that all the experiments were carried out under stirring conditions which permitted to keep the oxygen concentration constant (i.e. about 0.26 mM). The plots of 1/[S] vs 1/V for the experiments with ABTS and TC can be seen in Figure 4-2 and Figure 4-3. From these Figures, the values of V_{max} and K_M were calculated by the method discussed in section 3.3.6.2. Measured values are shown in Table 4-1. It can be observed that after immobilization the apparent K_M value decreased by 1.6 and 4 times for ABTS and TC, respectively. This result is surprising because generally structural conformation and diffusion limitations occur after immobilization. However, a similar trend has already been reported for laccase immobilized on membranes (De Cazes et al., 2015, 2014). V_{max} value depends on the concentration of the enzymatic solution (for free enzymes) or the amount of immobilized enzyme on a support. In this work the kinetic experiments with ABTS were carried out in order to have in both cases, the same amount of enzyme in terms of activity towards ABTS (i.e. 0.25 U). It was observed that V_{max} value was higher for immobilized enzymes indicating a better reactivity of immobilized biocatalyst. As in the case of K_M, this result is in good agreement with previous results reported by (De Cazes et al., 2015, 2014). On the contrary, the immobilized biocatalyst showed less reactivity towards TC than the free form. After immobilization V_{max} was more than 3-fold lower whereas the enzyme concentration was only 2-fold lower (activities used for free and immobilized form were respectively equal to 0.3 U mL^{-1} and 0.15 U mL^{-1}).

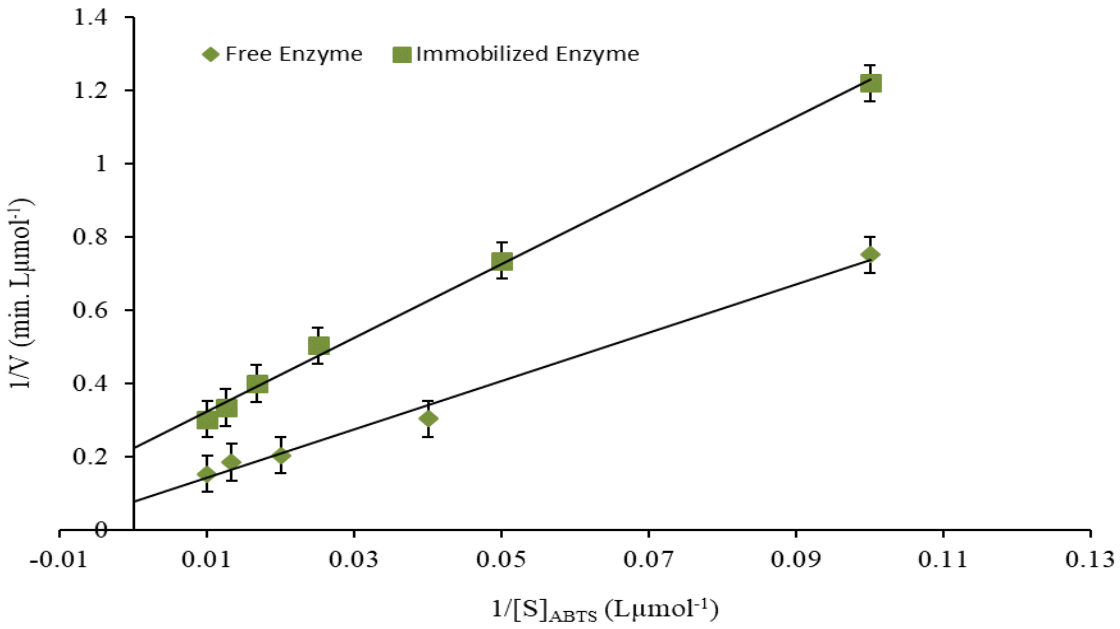

Figure 4-2. Reaction Kinetic parameter estimation in case of ABTS, Plot of inverse of substrate concentration vs inverse of reaction rate. Temperature (25°C); Enzyme concentration (0.01 U mL^{-1}). ABTS solution volume (Free enzymes: 1mL; Immobilized enzymes: 25mL).

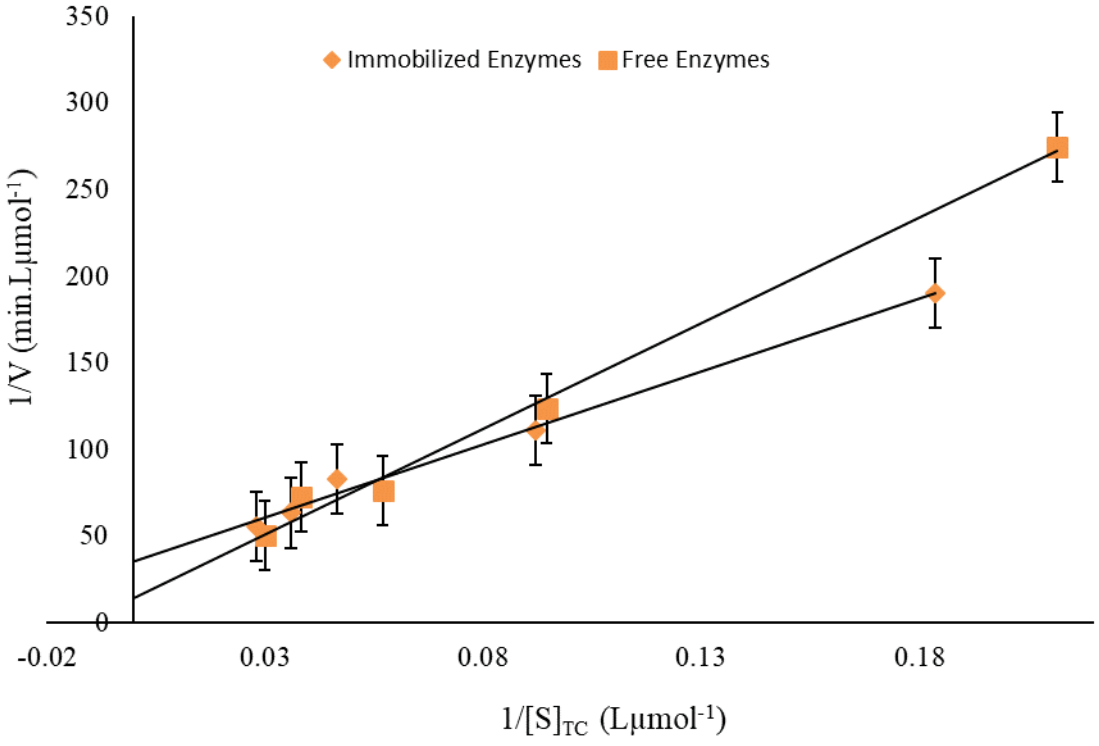

Figure 4-3. Reaction Kinetic parameter estimation in case of TC for free and Immobilized Laccase, Plot of inverse of substrate concentration vs inverse of reaction rate. Temperature (25°C); TC solution volume (10 mL). Enzyme concentration (Free 0.3 U mL^{-1}; Immobilize (0.2 U mL^{-1}).

Table 4-1. Apparent reaction kinetic parameters for the oxidation of ABTS and tetracycline (TC) with free and immobilized laccase.

Substrate	State of Enzymes	V_{max} (µmol min^{-1}) ±10%	K_M (µmol L^{-1}) ±10%
ABTS	Free	$1.3\ 10^{-2}$	85
	Immobilized	$6.4\ 10^{-2}$	50
TC	Free	$7.0\ 10^{-4}$	80
	Immobilized	$2.0\ 10^{-4}$	20

4.2.3 Storage stability of laccase-activated monoliths and free laccase

Storage stability of immobilized laccase is a key parameter for its practical application because of its impact on the cost of the process. Storage stability was studied for 30 days as explained in section 3.3.2.3. The results obtained demonstrated that there was no noticeable loss of enzymatic activity during the first 5 days of storage at 4 °C (Figure 4-4). Then during the other 25 days of storage the activity decreased slowly reaching approximately 85 % of the initial one. During the same period and storage conditions, free enzymes did not show any noticeable change in their activity. It can be concluded that immobilization didn't improve the stability of enzymes. However, activity lost remained low. It is possible that this small loss of enzymatic activity would be due to the release of non-covalently immobilized enzymes. As explained above, the highly activated silicate monolith acts as a hetero-functional support where non-covalent interactions can also take place between enzymes and functional groups of the solid support.

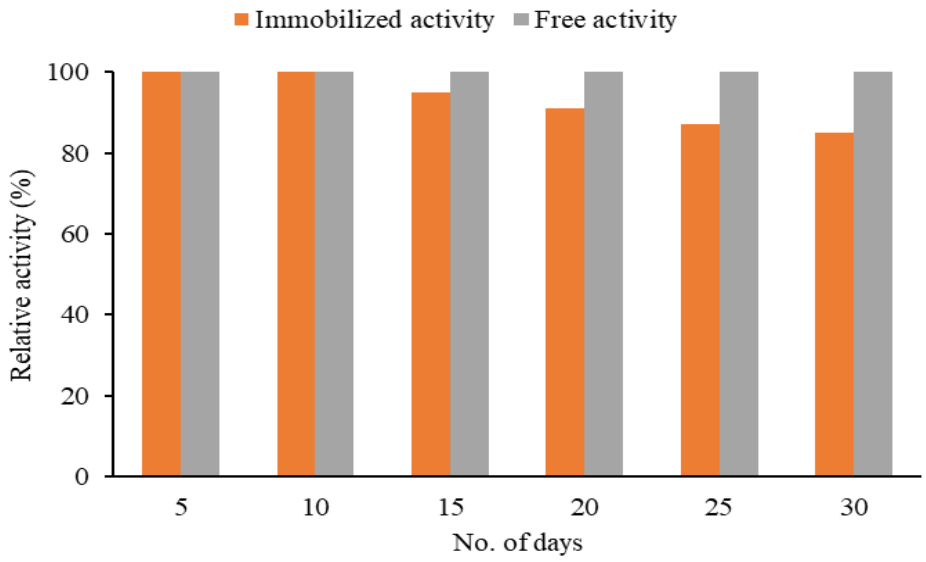

Figure 4-4. Comparison of Relative activity of immobilized and free enzymes stored at 4°C.

4.3 Continuous flow-through reactor

4.3.1 Permeability coefficient

When osmosed water flow rate varied from 1 to 4.5 mL min^{-1} through a cladded monolith, the upstream pressure increased linearly from 10 to 55 mbar as can be seen in Table 4-2. These measured values of upstream pressure are very low and confirmed that monoliths present interesting structure with very high porosity and communicating macropores.

Table 4-2. Effect of flow rate on back pressure before and after immobilization in case of 03 monoliths connected in series

Before Immobilization		After Immobilization	
Flow rate (mL/min)	**Back pressure (mbar)**	**Flow rate (mL/min)**	**Back pressure (mbar)**
0	0	0	0
1	6	1	7
1.5	8	1.5	9
2	12	2	14
2.5	20	2.5	22
3	26	3	27
3.5	34	3.5	36
4	44	4	46
4.5	55	4.5	56

Permeability coefficient (k) of raw silica monoliths calculated from Darcy pressure-flow relation (Equation 3.5) was equal to 5.9 10^{-12} m^2. Other authors have reported the same order of magnitude of permeability (11 10^{-12} m^2) (Ciemięga et al., 2017) but with monoliths with pore size of 30–50 µm. After enzyme immobilization, no change was observed for the value of permeability coefficient; which means that enzyme grafting does not affect the mass transfer.

4.3.2 Tetracycline degradation tests in continuous recycled mode

TC degradation tests were carried out with an aqueous solution of 20 ppm of TC in the lab-scale set-up as discussed in section. 3.3.7.3. The results are displayed in Figure 4-5. Control experiments (blank tests) were carried out to study the effect of TC self-degradation or adsorption on the evolution of TC concentration. For these control tests, enzymatic monoliths

were first thermally deactivated by heating in oven at 100°C for 2 hours. The results of control experiments show that less than 2% of initial TC was removed. The evolution of TC concentration with enzymatic monoliths shows that laccase-activated monoliths were able to degrade 40% of initial TC in first 5 hours and then the degradation rate decreased dramatically. From this point the TC concentration decreased slowly up to 50% at 24 hours of reaction. Many hypotheses can be done to explain this behaviour; they include the decrease of substrate concentration, if the kinetics obeys to a Michaelis-Menten equation. However, the diminution of the oxygen content, or even the formation of inhibiting by-products can also be considered.

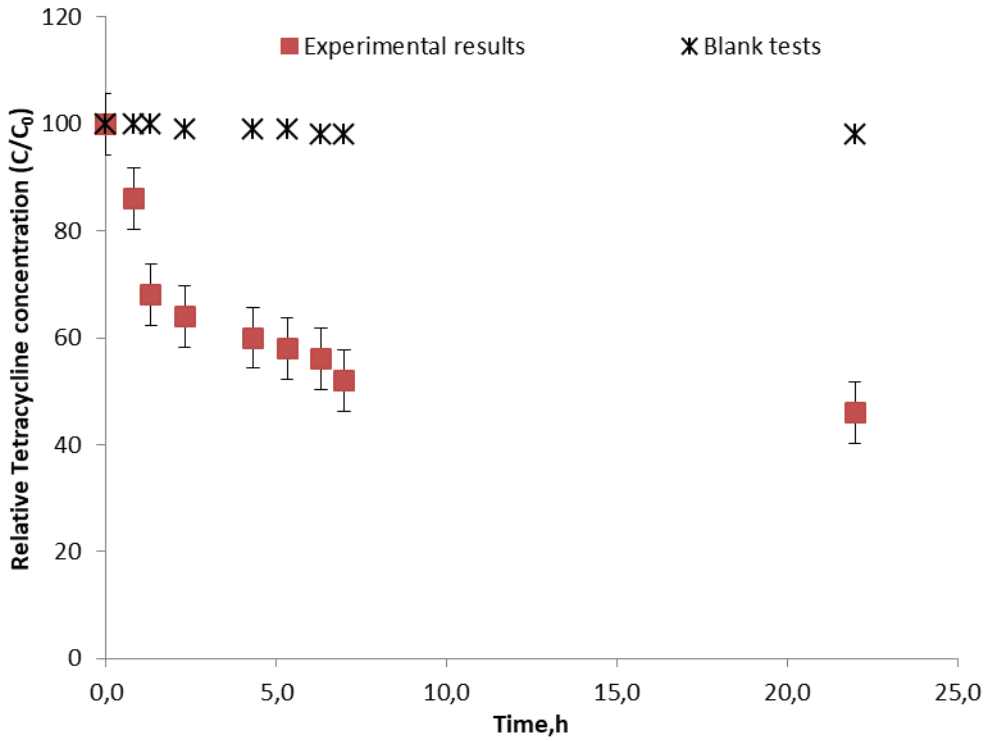

Figure 4-5. Degradation of TC. C/C_0: variation of the TC concentration respect to the initial TC concentration (20 ppm). Activity (0.5 U mL^{-1}); Total TC volume (30 mL)

Some authors (Kurniawati and Nicell, 2007; Ortner et al., 2015) have noticed that the velocity of oxidation of substrates by laccases can decrease very rapidly during the first hours of reaction because of the oxygen concentration depletion near catalytic sites. Indeed, the conversion can be improved by stirring on air atmosphere or reach 100% oxygen saturation by using pure oxygen (Ortner et al., 2015). In the case of experiments carried out in the monolithic system in continuous configuration, no stirring under air or oxygen was done. In addition, the concentration of immobilized enzyme was relatively high (15.0 U for 30 mL of

20 ppm of TC solution) and even if the calculated total initial amount of oxygen ($7.7\ 10^{-7}$ mol) was 5.5 times the initial amount of TC ($1.4\ 10^{-7}$ mol) it is possible that the oxygen depletion near the catalytic sites caused the observed decrease of the degradation rate. This effect has already been demonstrated in the literature (Kurniawati and Nicell, 2007; Ortner et al., 2015). Moreover, TC degradation results in many different by-products that can also be oxidized by laccases (Llorca et al., 2015; Yang et al., 2017b) and sometimes, first oxidation products are more reactive than the initial substrate. Indeed, the oxygen necessary for the degradation of TC can also be consumed by these side reactions. This point is certainly critical for the conversion reached with enzymatic reaction within the porosity of the monoliths.

4.3.3 Operational stability of laccase-activated monoliths

As well as storage stability, operational stability of the immobilized laccase is also a prerequisite for the economic viability of the process.

The operational stability of enzymatic monoliths was studied during 75 hours with the cyclical procedure described in section 3.3.7.4; the results are displayed in Figure 4-6. It can be observed that the evolution of TC concentration is very similar for all the cycles. As it is discussed in section 4.6, TC concentration decreases very rapidly during the first minutes of operation and then the degradation rate slows down. When the solution is replaced by a fresh one containing the same initial TC and oxygen concentration the same pattern of TC depletion is obtained. Indeed, it can be concluded that the enzymes immobilized in monoliths are stable during at least 75 hours of operation. The slowdown of the reaction rate observed can be explained by the lack of oxygen and could be avoided by using air or oxygen bubbling in the reservoir.

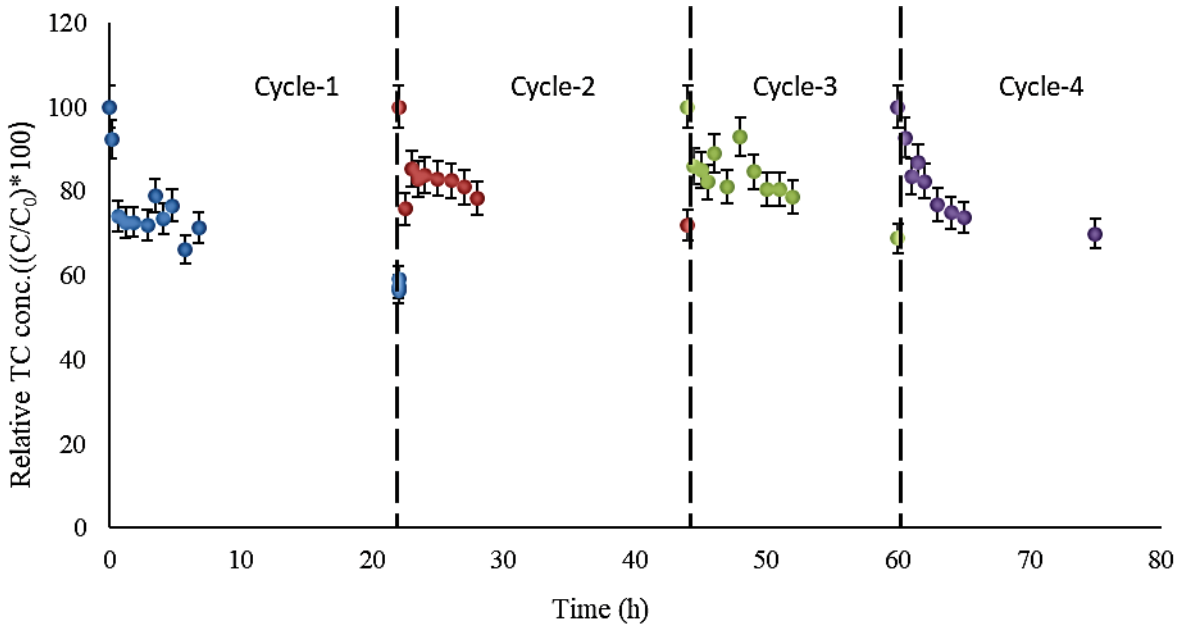

Figure 4-6. Operational stability of monoliths for 75 hours of sequential operation. Activity (0.5 U mL^{-1}); Total TC volume (30 mL); Initial TC concentration (20 ppm); Flow rate (1 mL min^{-1}).

4.3.4 Effect of recirculation flow rate on TC degradation.

The effect of recirculation flow rate was studied as explained in section 3.3.7.5, to obtain the optimal flow for the lab scale set up. The results obtained for TC degradation at different flow rates are shown in Figure 4-7.

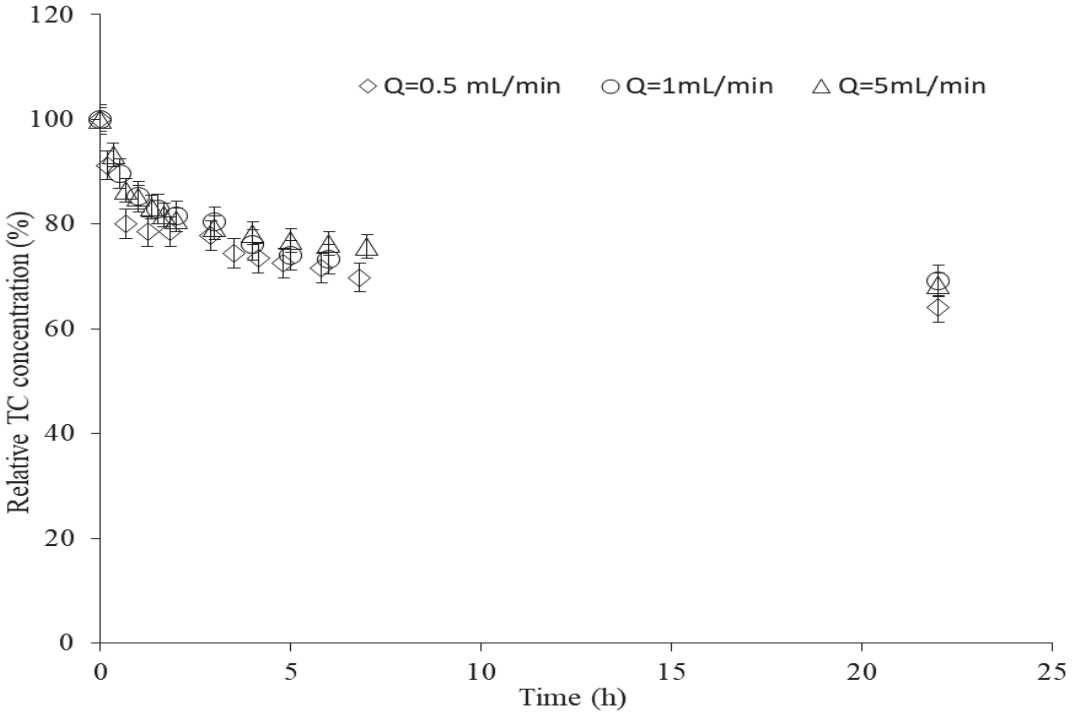

Figure 4-7. TC degradation at different recirculation flow rates at 25 °C; Initial concentration of TC (20ppm); activity (0.5 U mL^{-1}).

It can be seen from Figure 4-7 that, for each flow rate the TC degraded 30% in first five hours. After first five hours, the degradation rate was extremely low (about 10% in next 20 hours). This effect was observed with all the recirculation flow rates tested, i-e, by changing the flow rate the degradation rate was not changed. This result confirmed that within this range of flow rate tested, the overall TC degradation was controlled by reaction rates. The increase in the flow rate did not allow modifying the hydrodynamic flow regime. Indeed, the Reynolds number (Re) (discussed in more details in chapter 5) for the range of recirculation flow rates (0.5 mL min^{-1} to 5 mL min^{-1}) was ranged between 0.01 - 0.1. Indeed, even the value of Re for maximum flow rate (5 mL min^{-1}) tested in this research work is 0.1 and falls under laminar flow regime. (limit of the laminar flow regime (Re<1) (Agnaou et al., 2016). Therefore, it can be concluded that the increase in flow rate was not high enough to decrease possible external mass transfer resistances (decrease of boundary layers). The effect of external mass transfer is explained in more detail in chapter 5. Moreover, the TC conversion limitations observed, could be the result of internal diffusion limitations within the meso-porous skeleton or due to limitations of oxygen within the meso-pores which could limit the reaction rate. Therefore, a theoretical analysis considering the Thiele modulus in order to know if the overall mass transport is controlled by reaction rate or diffusion was carried out and is presented in chapter 5.

4.4 Effect of process parameters

4.4.1 Effect of enzyme concentration on TC degradation

For enzymatic catalytic reactions, the amount of enzyme to maintain appropriate ratio between substrate and enzyme concentration is important for the effective degradation of the substrate. TC degradation tests were carried out at different enzyme concentrations (0.05-0.6 U mL^{-1}) for 24 h in batch reactor with crushed activated monoliths as discussed in section 3.3.8.

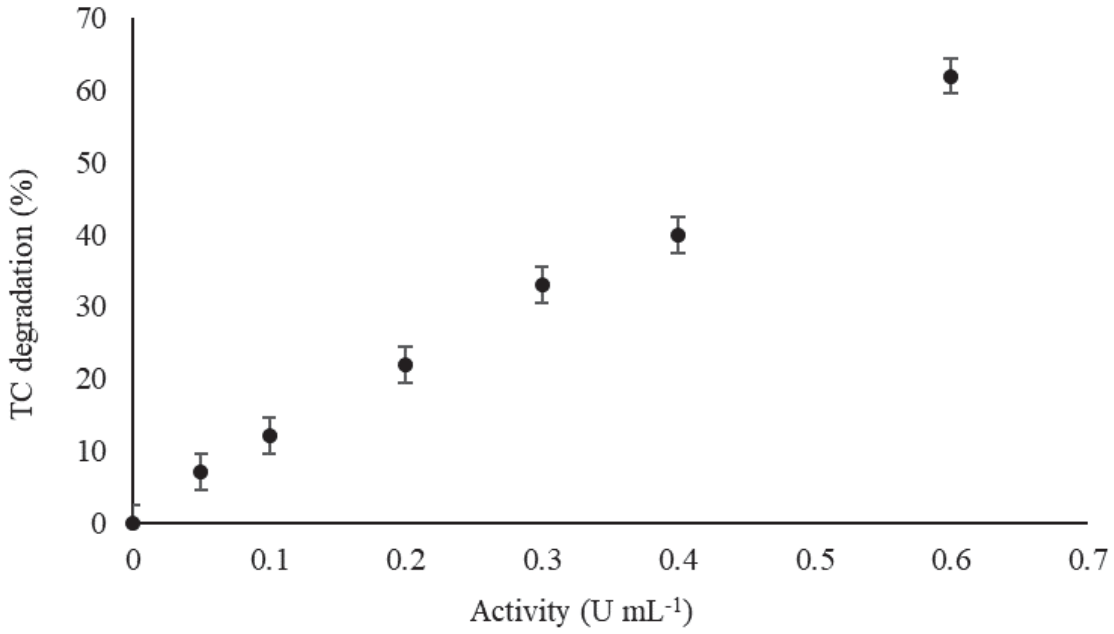

Figure 4-8. Effect of immobilized enzyme activity on TC degradation (crushed monoliths) in batch reactors with continuous stirring (150 rpm) at 25°C, Initial TC concentration (20 ppm) in osmosed water, total volume (10 mL).

From the results presented in Figure 4-8, it can be observed that with an increase in enzymatic activity from 0.05-0.6 (U mL ^{1}) TC degradation was increased from 7 to 60%. The results concluded that TC degradation was dependent on enzymatic activity within the range tested.

4.4.2 Effect of dissolved oxygen on TC degradation

Oxygen effects were studied in a stirred tank reactor using crushed monoliths and by bubbling air inside the TC solution as described in section 3.3.8.1. Results can be seen in Figure 4-9. Control experiments (blank tests) were also carried out to study the effect of TC self-degradation or adsorption on the evolution of TC concentration as explained in section 4.3.2.

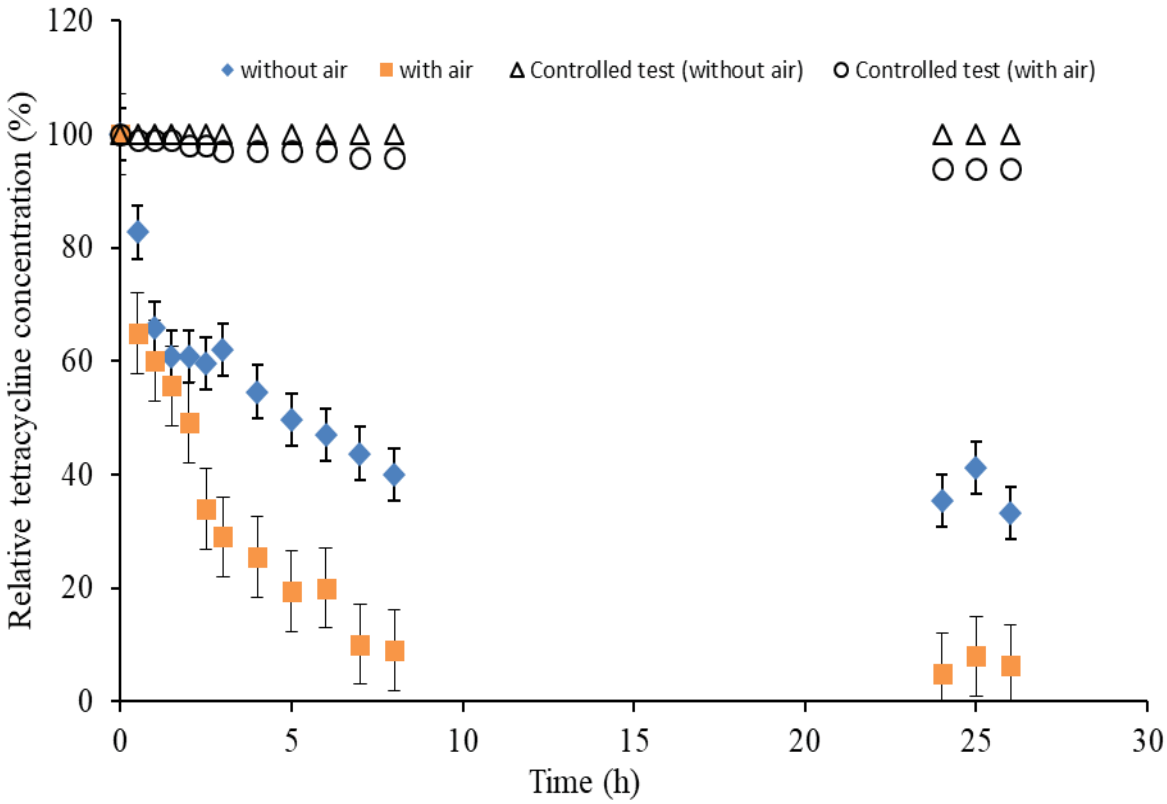

Figure 4-9. TC degradation in case of activated crushed monoliths in a stirred tank reactor: with and without air bubbling at 25°C. Initial TC concentration (20ppm) in osmosed water; Activity (0.6 U mL^{-1}); Total volume (30 mL).

In order to highlight the effect of dissolved oxygen, these experiments were carried out with a relatively high amount of enzymes (0.8 U mL-1). From Figure 4-9, it can be observed that without air bubbling, the TC degradation reached only 55% in the first six hours, while in case of air bubbling the degradation reached more than 90% in the same period. These results seem to confirm that oxygen was a limiting substrate in case of TC tests carried out without air bubbling. In the case of air bubbling experiments, oxygen was always at saturation value (8.3 mg L-1 at 25 °C) as can be seen in Figure 4-10, while without air bubbling, a decrease on oxygen concentration (DO) of about 20% was observed. After six hours of reaction, DO concentration was not further reduced and reached asteady-state concentration of 6 mg L^{-1}. However, the calculation of the number of moles of TC and oxygen at the end of experiments without air bubbling, indicates that we have final a ratio of 4 moles of oxygen/moles of TC (5.6 10^{-6} and 1.35 10^{-6} respectively).

It is well known that laccases catalyze theoretically the conversion of four –OH groups concomitant with the reduction of one molecule of oxygen to water (Shraddha et al 2011; Chea et al, 2012). Therefore, as far as TC presents four –OH groups (Figure 3-1) the final number of moles of oxygen reached without bubbling seems to be enough to oxidize all TC. Nevertheless, enzymatic oxidations with laccases can also produce oxygen-centered free radicals which are certainly not selective (Thurson, 1994). Without doubt, oxygen is certainly consumed by other parallel or consecutive reactions like oxidation in C4, dehydration, hydroxylation etc. In fact, many of these by-products have been detected in experiments of TC oxidation with the same laccase used in this work (Llorca et al., 2015). Indeed, the oxygen necessary to completely degrade TC seems to be much higher than the theoretical ratio of 4 moles of oxygen/moles of TC reached at the end of the reaction without air bubbling. This explanation above can be completed with possible mass transfer limitations at the level of mesopores where the majority of the enzyme is grafted, this aspect will be discussed later.

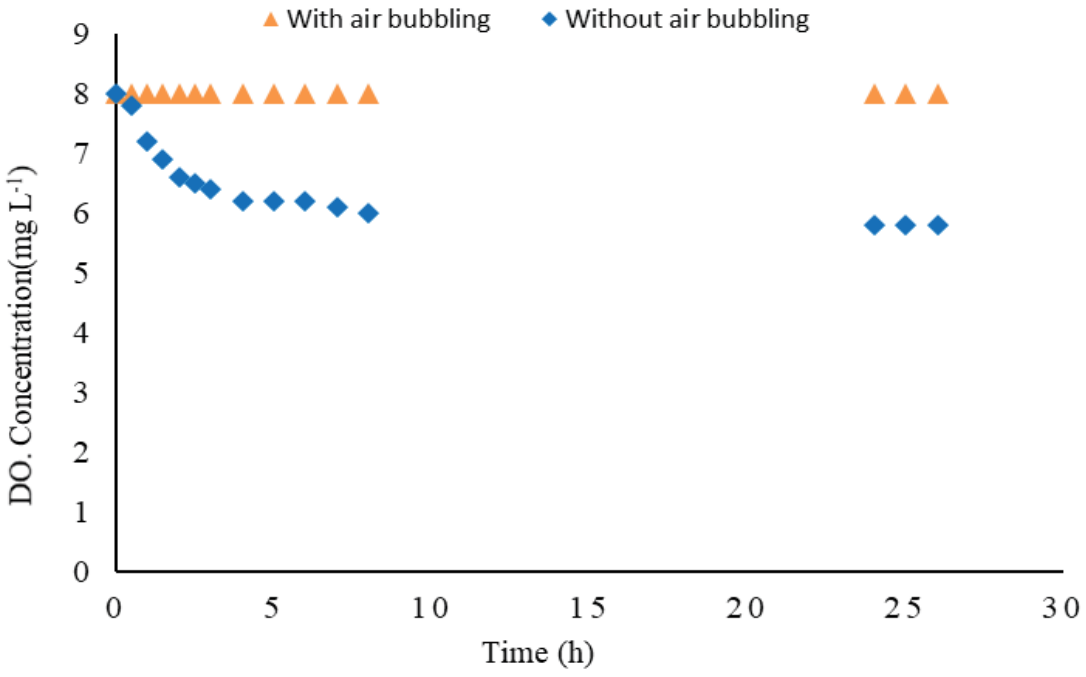

Figure 4-10. Dissolved oxygen (DO) concentration verse time in case of TC degradation test with or without air bubbling. Initial TC concentration (20ppm); Activity (0.6 U mL^{-1}); Total volume (30 mL).

The coupled effect of air bubbling and recirculating flow was also studied by bubbling or not bubbling air inside the supply tank under the flow-through monolithic reactor configuration while the recirculating flow rate was set at 1 mL min^{-1} or 5 mL min^{-1}. Initial tetracycline concentration for each experiment was 20 ppm, total volume of 30 mL and enzyme

concentration was 0.4 U mL^{-1}. The results are shown in Figure 4-11. It can be observed that for a flow rate of 5 mL min^{-1}, the degradation is higher (about 50 %) with air bubbling while it is only 30% without air bubbling. Similarly, for 1 mL min^{-1}, the TC degradation is higher (40%) in case of air bubbling compared to the TC degradation without air bubbling (30%). It should be noted that during air bubbling in controlled test, TC degradation was about (5%) as can be seen in Figure 4-9. Therefore, it can be concluded that air bubbling within the feed tank enhanced the TC degradation only by 10% after 24h of operation, but still complete degradation was not achieved. In comparison, the air bubbling during the batch experiments allowed more than 90% degradation (Figure 4-9). The reason for lower degradation in case of continuous recycled mode system could be the diffusional limitations, non-accessibility to the active sites or oxygen limitations near bio-catalytic sites inside the mesoporosity.

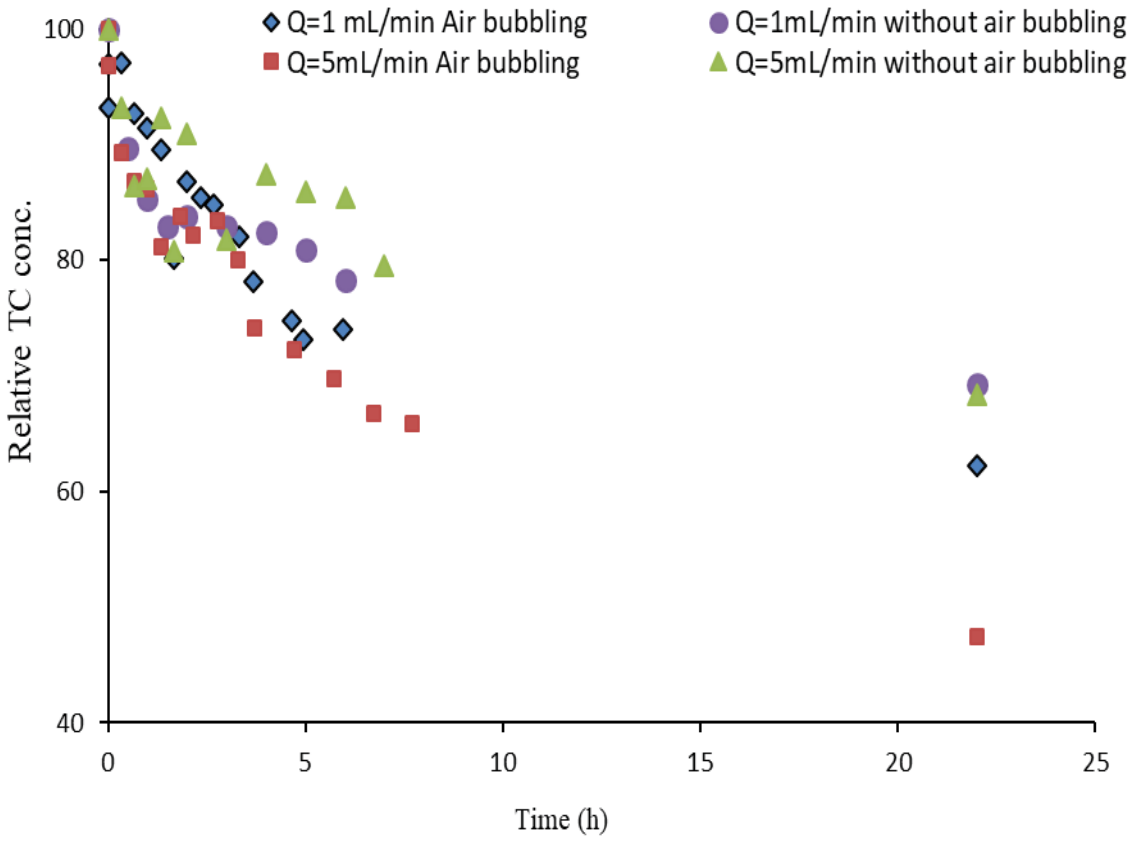

Figure 4-11. Tetracycline degradation rate in the reservoir tank under flow-through monolithic reactor configuration.at different flow rates with or without air bubbling at 25°C; Conditions: Initial TC conc. (20ppm) in osmosed water; Total volume of TC solution (30mL); Activity (0.4 U mL^{-1}).

4.4.3 Effect of degradation products

Effect of degradation products on the degradation of TC was studied as explained in section 3.3.4.2. The results are presented in Figure 4-12. Although the enzyme concentration was the same (0.2 U mL^{-1}) for all experiments, the TC degradation increased with the concentration of degradation products. Indeed, when the concentration of degradation products is increased from 50 to 90 %, the TC degradation was enhanced by two times. These results confirmed that the TC degradation products do not affect the degradation rate, on the contrary their presence at high concentration can enhance TC removal. According to the radical reaction mechanism of substrates with laccase and molecular oxygen described above, it is possible that reaction products which are still reactive enhance the concentration of radicals that can contribute to a better conversion of TC. However, this first study has to be deepened to better understand the role of the degradation products. Moreover, for this purpose, it is important to know their structure, their lifetime during the reaction and the reaction mechanisms involved.

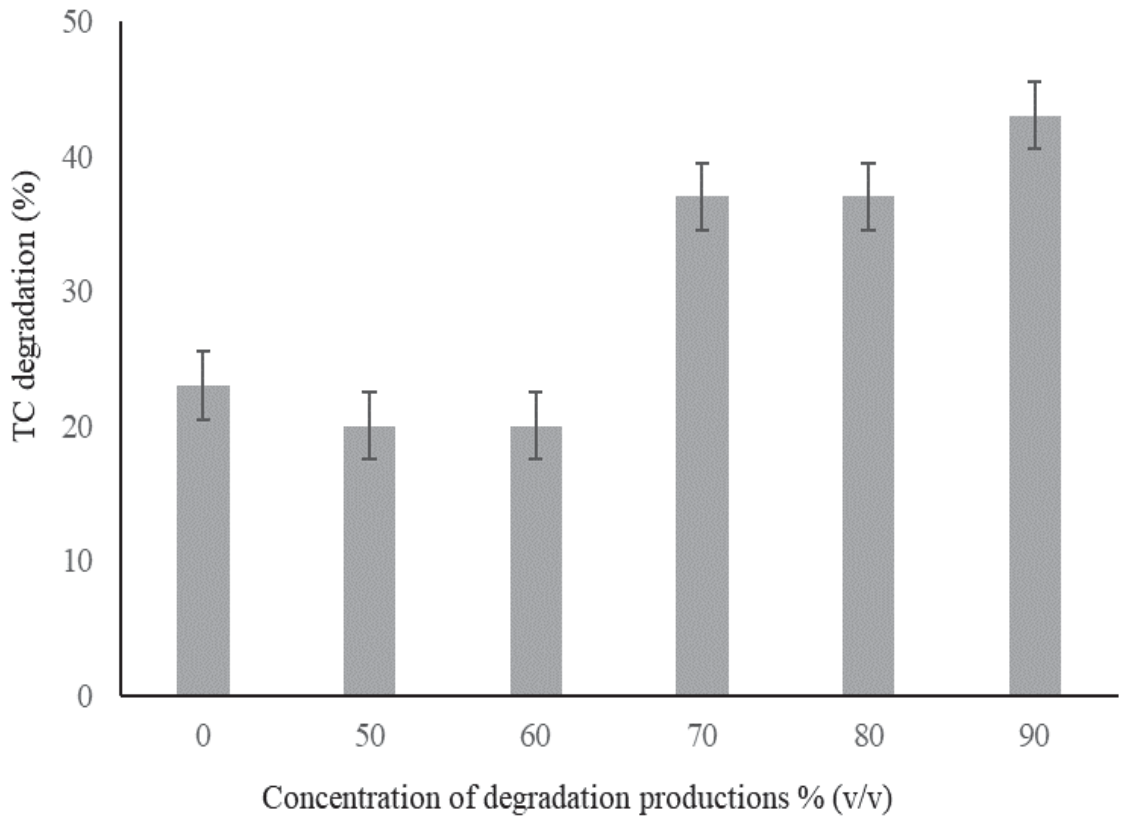

Figure 4-12. Effect of TC degradation products on TC degradation. Initial TC concentration (20ppm); Activity (0.2 U mL^{-1}). Total TC volume for each experiment (10 mL).

Chapter 5

Modelling and simulation of monoliths for enzymatic degradation of tetracycline degradation.

5. MODELLING AND SIMULATION OF MONOLITHS FOR THE ENZYMATIC DEGRADATION OF TETRACYCLINE

Summary

This chapter is divided into two parts; first part is devoted to the model development for the TC degradation in water by enzymatic monolithic reactors considering the flow-through reactor configuration with recycling. Simulation results of the developed model are presented in second part of the chapter. The building of the model was carried out in two parts: in the first part, steady-state as well as time-dependent CFD model was developed in COMSOL MULTIPHYSICS® 5.3. Some model parameters, like reaction kinetics and permeability coefficient were obtained from experimental results (chapter 3). The modelling was based on the reaction kinetic model of Michaelis-Menten (V_{max} and K_M) and considers a homogenized geometry of monoliths. Indeed, the TC degradation in a single pass was computed. In the second part, a dynamic mass transport balance model was developed in MATLAB® 2017 to compute TC concentration change with time in the feed tank. Both models were coupled via COMSOL-MATLAB Live-link feature and run simultaneously. This modelling coupling allowed determining the computation of TC concentration evolution in the feed tank. External and internal mass transfer limitations were also studied. The model developed was validated with the experimental results, but only during first 5 hours of reaction, it means during initial reaction times when TC and oxygen concentration are not limiting, After 5 hours of reaction, experimental TC concentration reaches a plateau, indicating there are certainly kinetic or mass transfer limitations that are not considered in model equations.

The second part of this chapter is devoted to study the simulations considering only the initial reaction times, like a single pass through monolithic reactors, it means under conditions where the model has been validated. Indeed, the simulation of TC concentration distribution through monoliths is presented for steady-state as well as time-dependent conditions. The influence of internal and external diffusion limitations within the monoliths structure is also considered. Finally, results of simulated large-scale enzymatic monoliths for complete TC degradation as well as their implementation for wastewater treatment are presented.

5.1 Introduction

In chapter 2 which concerns the state of the art, it has been reported that few models of mass transport through monoliths consider the microscopic structure and develop approaches for simulation of velocity fields, diffusion and dispersion of chemical species within the porous structure. These models which are based on morphology and real structure of porous monoliths, requires complex image processing techniques as well as very high computing times. Therefore, these simulation approaches can be costly to simulate large scale geometries required for practical engineering problems. Moreover, in literature, there is no specific modelling study, which simulates the reaction kinetics coupled with transport of species within macroporous silica monoliths.

In this work the modelling approach is different; firstly, it is not microscopic and do not consider the real fine structure or morphology of monoliths (complex internal 3D geometry, communicating and blind pores) but takes the assumption of a homogenous structure which is only related to macroscopic structural measurable parameters (porosity, tortuosity, pore size distribution) and flow (permeability). Secondly, the mass transport through this homogenous structure is coupled with the experimental enzymatic kinetics. Similar modeling approaches have been reported for enzymatic membranes (Abejón et al., 2015b; Ameur et al., 2014).

Schematically the model presented here was developed in two parts (Figure 5-1). In a first part, the degradation of TC during the flowing of the aqueous solution through the monolith was computed by COMSOL MULTIPHYSICS® 5.3 software. Initially, the TC concentration (C_{in}^{n+1}) at the inlet of the monolith was considered equivalent to the TC concentration in the tank. As the TC flowed through the monoliths, the degradation occurred due to enzymatic reactions within the activated monolith. Finally, the computed TC concentration (C_{out}^{n+1}) at the outlet of the monolith was then calculated by the average integration over the outlet surface of the monolith.

In a second part, the recycling of the TC solution in the feed tank was considered. Indeed, the TC concentration in the tank changes continuously with time. Then transient mass transport conditions occurring are simulated through a model built in MATLAB® 2017. Both the modelling parts are explained in detail in next section.

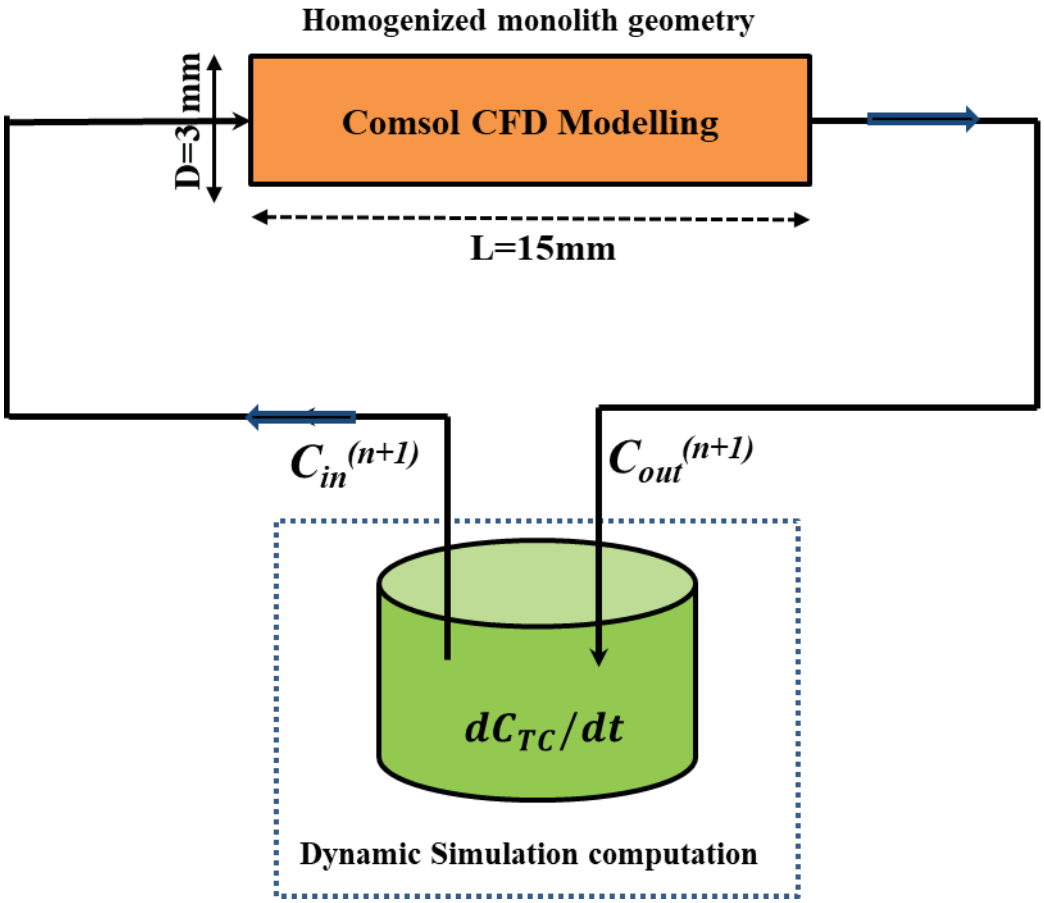

Figure 5-1. Modelling scheme of the monolith system in closed loop system.

For the global simulation of the evolution of TC concentration in the feed tank, both models were coupled and run together via COMSOL-MATLAB live link feature available in COMSOL MULTIPHYSICS® 5.3. In this procedure, COMSOL model was built and opened in MATLAB® code window via MPH commands and then the overall modelling steps were run in the MATLAB® programming window.

5.2 Modelling in COMSOL MULTIPHYSICS®

5.2.1 Reactor geometry and homogenization

As explained above, the objective of the COMSOL model was to study the concentration and velocity distribution at the reactor length scale and not on the pore scale; therefore, the monoliths were considered as a homogenized porous structure having the same dimensions as the monoliths used in experiments (three monoliths of 5 length and 6 mm diameter connected in series). This approach considers the whole geometry as a porous material having an average porosity and permeability. Then the reaction kinetics was applied on the porous geometry. Likewise, the flow within the porous domain was computed with the help of

Brinkman equation (presented later). Homogenization is a relatively simple approach; it is cost effective and requires less simulation time to solve complex porous geometries. This approach can be applied to complex porous geometries/reactors like packed bed or pellet bed reactors where reactions takes place at micro/macro level and the reactor geometry is about 10^3-10^5 larger than the pores size. The Figure 5-2 shows further illustration of homogenization approach, where a porous monolithic structure is drawn in COMSOL® 5.3 geometry builder feature (CAD kernel). The homogenization as well as meshing, (explained later) were carried out considering the real dimensions. It should be noted that for modelling purposes, the length of monolith considered here, was equivalent of the sum of the length of the three monoliths connected in series in experiments. (for instance, see the experimental setup in Figure 3-4).

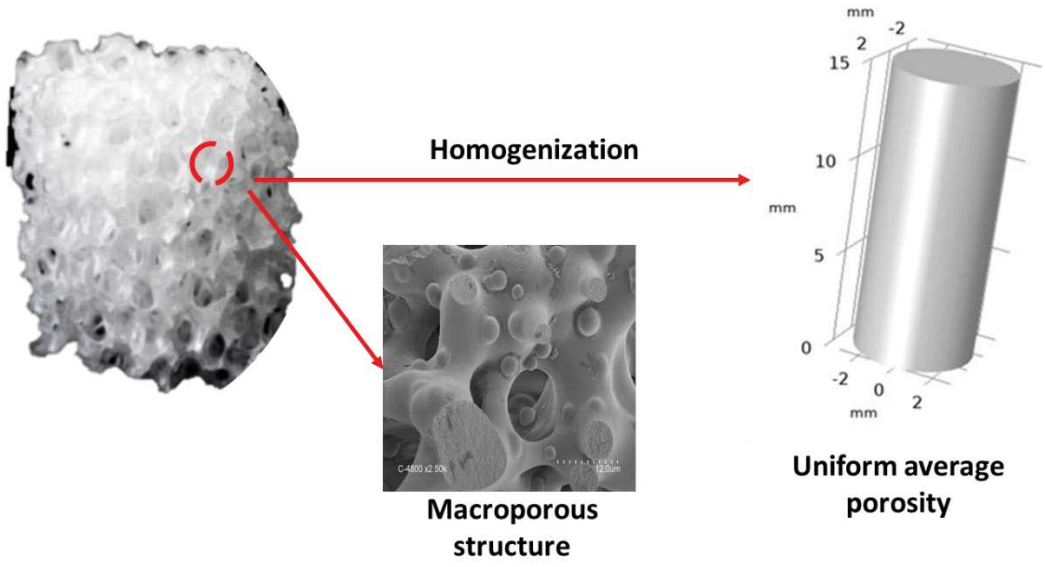

Figure 5-2. Homogenization of monolith geometry considering average porosity and permeability.

5.2.2 Model Assumptions

- Uniform temperature within the reactor and in the feed tank
- The assembly of degradation products were considered as a single product formation without any side reactions
- Homogenous porous structure (porosity-0.6)
- Plug flow conditions
- Uniform flow and concentration distribution within the porous structure

5.2.3 Model Inputs

Table 5-1 summarizes all the input parameters required for the model equations, many of these inputs were measured experimentally (Chapter 3). It is important to notice that some

parameters like diffusion coefficient of TC in water and tortuosity were not measured experimentally their values were taken from literature or calculated by correlations taken from literature. To our knowledge the diffusion coefficient of TC in water has not been measured or reported in the literature. Soriano et al. (2017) determined the diffusion coefficient of five different kinds of antibiotics; Amtyl (M_w: 365.4 g mol^{-1}), Ciprotyl (M_w: 331.34 g mol^{-1}), Doxylak Forte (M_w: 545g mol^{-1}), Trisullak (M_w: 543 g mol^{-1}), and Vetracin Gold in the temperature range of 293.15 to 313.15 K. Vetracin Gold is a commercial name of a mixture containing in majority Doxycycline (M_w: 444.43 g mol-1), that is a cycline of the same family of TC having a similar molecular weight. Therefore, the diffusion coefficient of Vetracin Gold reported by Soriano et al. (2017) was then considered as a good approximation for TC diffusion coefficient (Table 5-1).

The tortuosity is the property of the porous structure and is defined as the ratio of the actual diffusion path travelled by fluid in porous media to the straight path travelled in the absence of any porous media. In case of monoliths, having macroporous structure as well as mesoporous skeleton, two types of tortuosity are possible, i-e; macroporous or external tortuosity and mesoporous/skeleton tortuosity. Macroporous tortuosity is applicable where the convection flow streamline distribution within the macroporous structure needs to be studied, while mesoporous tortuosity is applicable to determine the effective diffusion coefficient (as the case in this study). Since, homogenized structure for the monolith is considered in this study (no streamline flow distribution) therefore, macroporous tortuosity is not applicable for this modelling approach. For meso porosity with average meso-porous (0.2-0.3); tortuosity can be calculated by Equation (1) which is theoretically found for freely overlapping spheres (Weissberg, 1963) and experimentally verified for non-overlapping spheres and some other shapes (Comiti and Renaud, 1989).

$$\tau = 1 - p * ln\varepsilon_{meso} \quad (5\text{-}1)$$

Where, τ is the tortuosity, ε_{meso} is the meso porosity, p is the topological factor its value depends on the pore topology with proposed values of p= 0.41-0.49 for spheres, p=0.53 for cubes and p=0.86-3.2 for plate (Mauret and Renaud, 1997).

Table 5-1. Input parameters for the model building in COMSOL MULTIPHYSICS®.

Parameters	Units	Expression/value	
Maximum Reaction rate (V_{max})	µmol $L^{-1}min^{-1}$	2.6 10^{-2}	Measured experimentally
Michaelis-Menten Constant (K_M)	µmol L^{-1}	20	Measured experimentally
Permeability coefficient (k) (m^2)	m^2	9.5 10^{-12}	Measured experimentally
Average macro-porosity(εp)	---	0.6	Measured experimentally
Average meso-porosity	---	0.2	Measured experimentally
Macroporous specific surface area S_A^{macro} (m^2)	m^2 g^{-1}	1	Measured experimentally
Meso-porous specific surface area after laccase immobilization: S_A^{meso} (m^2)	m^2 g^{-1}	164	Measured experimentally
Diffusion Coefficient of TC in water (m^2 s^{-1})	m^2 s^{-1}	9.9 10^{-9}	From literature (Soriano et al., 2017)
Tortuosity	---	2.7-3.3	Calculated – Eq. (5-1)
Temperature	K	298	Measured experimentally

Recently, Nguyen et al., (2020) determined experimentally the p value for silica monoliths having meso-pore diameter (d_{meso} = 12-16 µm). The p value for the monolith was 1.4.

The meso-porous skeleton tortuosity was then calculated from Equation 1, using p value of 1.4 and meso porosity of 0.2-0.3. The value of tortuosity is given in Table 5-1.

5.2.4 CFD modelling of homogenized porous monolithic structure

The modelling of the monoliths carried out in steady-state as well as in transient conditions was built in COMSOL MULTIPHYSICS®, by coupling reaction kinetics and Brinkman flow (equations presented later). As explained above, homogenized porous structure was considered, keeping in view a global porosity and permeability through all monolith volume. Ideal plug-flow behavior was assumed because of large macropores (20µm) and small skeleton thickness (5µm). The plug flow behavior can be illustrated using typical Bodenstein number (Bo) characterizing reactor-based liquid-phase transport by flow relative to hydrodynamic dispersion occurring simultaneously along the macroscopic flow direction as shown in Equation 2.

$$B_o = \frac{u_{ave} L_{bed}}{D_L} \tag{5-2}$$

Where u_{ave} is the average velocity (m s^{-1}) (Darcy velocity) (1-3 mm s^{-1}), L_{bed} is the length of monolith (5 mm), D_L is the dispersion coefficient ($1.5*10^{-9}$ m^2 s^{-1}). The values of dispersion coefficient were taken from literature for the macro-porous silica monoliths (Haas et al. 2017). The values of B_o calculated from Equation 5.2 were in the range of 10^3-10^4 which revealed extremely plug-flow conditions.

The other parameters like structure properties of the monoliths, permeability (*k*) and reaction kinetics parameters (K_M and V_{max}) used in modelling were measured experimentally as discussed in chapter 3. For convective-diffusive transport model development in COMSOL MULTPHYSICS®, two conditions were considered i-e; time-dependent and steady-state conditions as can be seen from Equation 5.3 and 5.4 respectively. The purpose of time-dependent model ($\frac{\partial C_{TC}}{\partial t} \neq 0$) was to study TC concentration distribution along the reactor length at different times, this type of model also help calculating the residence time within the monoliths, while steady-state model ($\frac{\partial C_{TC}}{\partial t} = 0$) computed TC concentration along the length of reactor at steady-state conditions (single pass). TC concentration at the outlet in both cases (time-dependent as well as steady-state) was then calculated by average integration over the outlet surface of the monolith.

In order to set up the model, a general time-dependent convective-diffusive transport equation (Equation 5.3) was applied on the homogenized monolith geometry shown in Figure 5-2.

$$\frac{\partial C_{TC}}{\partial t} + \nabla(-D_e \nabla c_{TC}) + u\nabla c_i = R_{TC} \quad (5\text{-}3)$$

Similarly, the steady-state convective-diffusive transport equation is shown in (Equation 5.4)

$$\nabla(-D_e \nabla c_{TC}) + u\nabla c_{TC} = R_{TC} \quad (5\text{-}4)$$

Equations (5-3) and (5-4) are the basic mass transport equations in time-dependent and steady-state conditions. They couple the reaction rate with the flow within the monolith geometry, and are applied to simulate the TC concentration gradient (∇c_{TC}) along the length of the monolith geometry as well as TC concentration change with time $\frac{\partial C_{TC}}{\partial t}$ (in case of time-dependent equation). It includes the TC effective diffusion coefficient (D_e) (calculated from Equation ($D_e = \frac{\varepsilon}{\tau} D$), the velocity within porous domain (u), and the enzymatic reaction rate (R_{TC}). Velocity was calculated within the monolithic porous geometry by applying Brinkman equation (Equation 5.11, described later).

Following boundary conditions were applied at the inlet and outlet of the monolith:

In flow boundary condition:

$$C_{TC_{inlet}} = Constant \quad (5\text{-}5)$$

Out flow boundary condition:

$$-D_e \frac{\partial C_{TC}}{\partial x} = 0 \quad (5\text{-}6)$$

5.2.5 Enzymatic kinetics

To model the enzymatic reaction, only the disappearance of TC in the solution was considered, therefore reaction rate was considered based on a reactant converted into a single product. An enzymatic reaction based on Michaelis-Menten model (as shown in Equation 5.8) for TC degradation was then defined throughout the geometry volume using the COMSOL MULTIPHYSICS® 5.3 chemistry physics feature. Reaction rate equation (5.8) represents the TC disappearance with reaction kinetic parameters (K_M and V_{max}) were determined in batch experiments with crushed activated monolith under continuous stirring as explained in section (3.3.6.2). Under these conditions diffusional limitations are certainly reduced. On the contrary when TC solution is flowed through activated monoliths the mesoporosity is certainly less accessible because the majority of flow takes place through the macroporosity. From Table 5-1, large surface area of the monolith is mainly due to mesopores (164 $m^2\ g^{-1}$) in comparison to

macropore surface area (0.6 m^2 g^{-1}), which means that most of the activity is available in the mesoporosity. Furthermore, experimental results obtained in the frame of the PhD thesis of Sebai Wassim (under way) have demonstrated that laccase was mainly immobilized into mesopores. He found very small activity (0.8-1 U g^{-1}) when monoliths with only macropores were used for laccase immobilization. In comparison the immobilized laccase activity found in this work with macro/mesopores was 15 U g^{-1}, these results confirmed that most of the laccase can only be immobilized in the mesopores.

Since the in actual TC degradation takes place only in the mesoporosity, however in case of simulated geometry we have only considered a single porosity (average), therefore, the reaction rate equation (5.8) was modified before applying to homogenized geometry (Figure 5-2). To incorporate the effects of reaction rate only takes place within mesoporosity, a ratio of meso-porosity (0.2) of the monolith to the total porosity (0.86) was multiplied to the reaction rate determined in batch conditions ($\frac{\varepsilon_{meso}}{\varepsilon_{total}}$) as shown in Equation 5.9. This factor illustrates that the reaction rate is only considered in the mesoporosity and not in the whole porosity.

$$TC \xrightarrow{E} TC^* \tag{5-7}$$

Where, TC and TC^* are respectively the tetracycline and the assembly of degradation products considered as a single compound.

$$R_{actual} = \frac{V_{max} * C_{TC}}{K_M + C_{TC}} \tag{5-8}$$

$$R_{adjusted} = \left(\frac{V_{max} * C_{TC}}{K_M + C_{TC}}\right) * \frac{\varepsilon_{meso}}{\varepsilon_{total}} \tag{5-9}$$

Here, C_{TC} is the concentration of TC, V_{max} is the maximum reaction rate, K_M is the Michaelis-Menten constant, ε_{meso} is the meso porosity and ε_{total} is the overall porosity (macro and meso). R_{actual} is the reaction rate determined by experimental data. $R_{adjusted}$ is the adjusted reaction rate which indicates that the reaction occurs only within the meso porosity.

5.2.6 Porous media flow

To simulate the velocity within the homogenized geometry of the monolith, Brinkman equation was applied (Equation 5.11), this equation has demonstrated to give a good description of flowing fluids through porous materials under laminar conditions (Auriault, 2009; Vasin and Filippov, 2009; Yao et al., 2013, Ameur et al., 2014b). From experimental

data of flow rate vs pressure drop (Table 4-2) it can be seen a linear relationship which means that for the range of flow rates used in this study (0.5 mL min^{-1} to 5 mL min^{-1}), the flow behavior falls in the Darcy's regime (laminar flow conditions). For porous media, Darcy's regime is applicable for Re less than 1 (Agnaou et al., 2016) however some studies suggested that Darcy's flow is applicable at Re up to 10 (Mauret and Renaud, 1997). Indeed, Re calculated from equation (5.10) for the flow rates (0.5 mL min^{-1} to 5 mL min^{-1}) was between 0.001 to 0.01, ensuring Darcy's flow conditions (less than 1) (Agnaou et al., 2016) and then allowing the use of Brinkman equation (Yao et al., 2013) to compute the velocity within porous monoliths:

$$Re = \frac{\rho u d_{macro}}{\mu} \tag{5-10}$$

$$\nabla \left[-PI + \mu \frac{1}{\varepsilon_p} (\nabla u + (\nabla u)^T) - \frac{2}{3} \mu \frac{1}{\varepsilon_p} (\nabla . u) I \right] - (\mu k^{-1}) = 0 \tag{5-11}$$

where ε_p is the global porosity of the domain; k (m^2) is the permeability of the domain; u (m s^{-1}) is the Darcy's velocity (the ratio of flow rate to monolith cross section) and μ (mPa s) the viscosity of the solution; P is the Pressure (Pa). Reference pressure and temperature were 10^5 Pa and 298 K respectively.

The boundary conditions defined in order solve the Brinkman equation are the following:

Inlet boundary conditions: fully developed flow with porous media entry (Hamdan, 1994).

Outer wall boundary: No slip conditions.

Outlet boundary conditions: P=0 with suppress backflow.

5.2.7 Meshing and post-processing

COMSOL MULTIPHYSICS® is based on Finite Element method. In this technique, the whole geometry is divided into finite element size and then the equations are solved for each element of definite size. These small elements creation on whole large geometry is called meshing. The accuracy of modelling results depends on mesh size. In this study, Fine physics-controlled mesh was applied on the homogenized geometry calibrated for fluid dynamics. Further refining the mesh structure had no effect on TC concentration distribution profile and outlet TC concentration.

Table 5-2. Details of the mesh applied on monolith geometry for computation.

Description	Value	Description	Value
Calibrate for	Fluid dynamics	Minimum element quality	0.03011
Maximum element size	0.222	Average element quality	0.6303
Minimum element size	0.024	Tetrahedron	223750
Curvature factor	0.4	Prism	41448
Resolution of narrow regions	0.9	Triangle	15716
Predefined size	Finer	Quad	528

The details of the meshing used can be seen in Table 5-2. Similarly, the fine meshed-monolith geometry is shown in Figure 5-3. Near the outer boundaries of the monolith, adaptive meshing can be seen; the purpose of this kind of meshing was to obtain more accurate results at the boundaries, due to no slip velocity condition at walls. Apart from outer boundaries, a uniform meshing throughout the geometry was considered keeping in view the homogenized geometry.

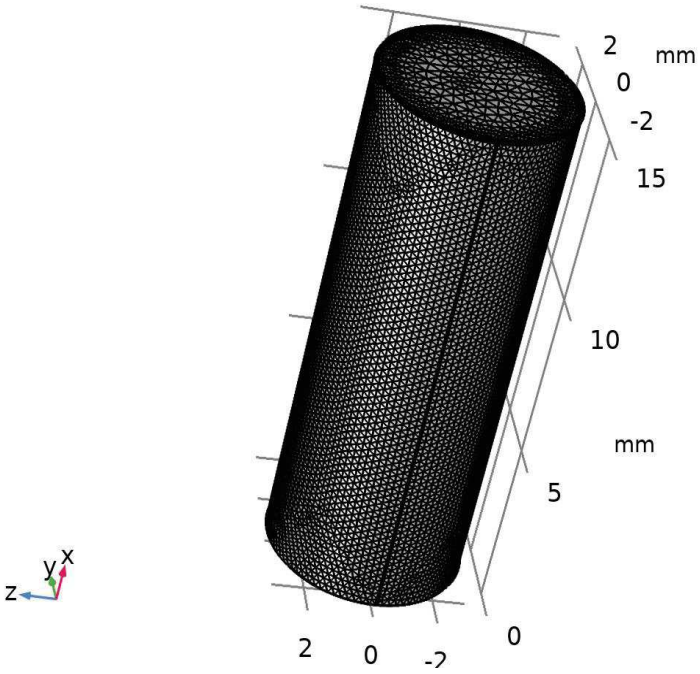

Figure 5-3. Mesh of homogenized monolith geometry built in COMSOL MULTIPHYSICS® software.

5.3 Dynamic Feed tank modelling

Transient mass balance was applied on the feed tank in order to simulate TC degradation rate in the feed tank. The TC inlet concentration in the tank was calculated from the TC concentration at the outlet of the monolith. The schematic can be seen in Figure 5-4.

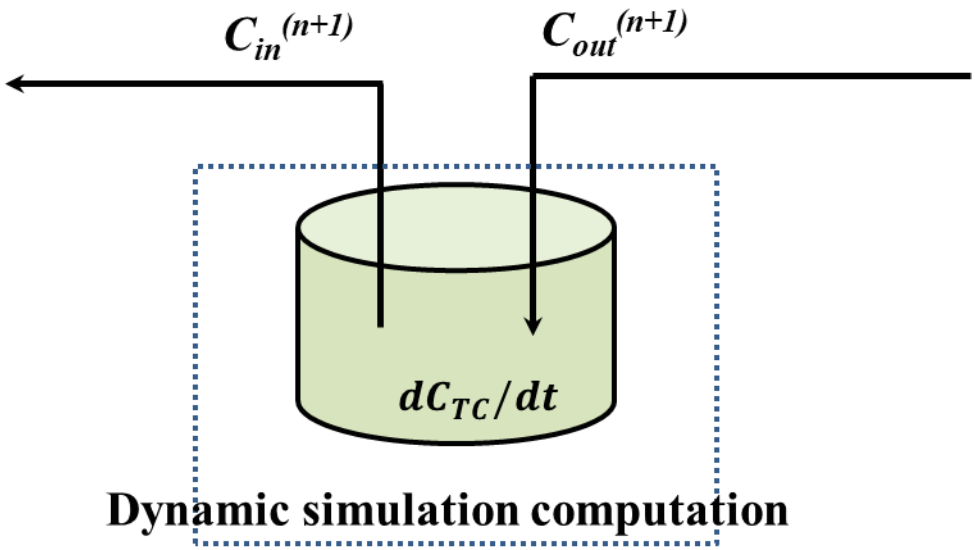

Figure 5-4. Dynamic mass transfer modelling in the feed tank a close-loop system for TC degradation.

Applying the transient mass balance for tetracycline on the feed tank:

Inlet – outlet = Accumulation

$$V\frac{dC_{TC}}{dt} = Q\left({C_{in}}^{n+1} - {C_{out}}^{n+1}\right) \quad (5\text{-}12)$$

Where,

V= Volume of the TC solution in the tank (mL),

Q = Flow rate (mL/min)

$\frac{dC_{TC}}{dt}$ = TC degradation rate

${C_{in}}^{n+1}$= Inlet TC concentration for a loop (n+1)

${C_{out}}^{n+1}$= Outlet TC concentration for a loop (n+1)

n= number of loops

5.4 Coupling of steady-state modelling with dynamic modelling

Steady-state model built in COMSOL MULTIPHYSICS® environment was imported into MATLAB® 2017 script window with the help of COMSOL-MATLAB Livelink feature of COMSOL®. Then the steady-state model was coupled to transient mass balance on feed tank in order to run the steady-state model in recycled loops. The loop was initiated with initial TC concentration (C_{TCi}) at t=0, and for each cycle the input was updated with the help of transient balance. The closed loop was ended once the given number of iterations (n) was reached. The closed loop is illustrated in the Figure 5-5.

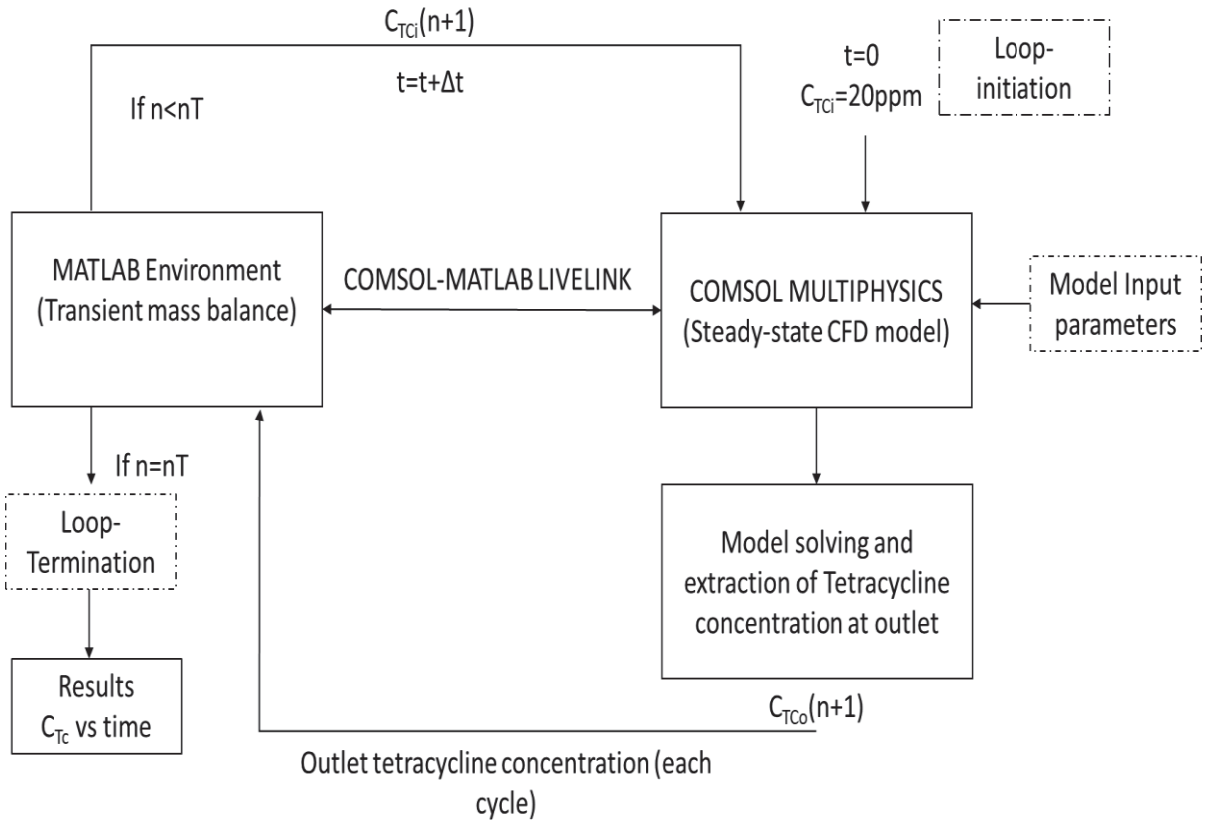

Figure 5-5. Simulation closed loop coupling COMSOL®-MATLAB® software for computing rate of tetracycline concentration change in the feed tank.

5.5 Mass transfer within the porous silica monoliths

Mass transfer mechanism in the macro-meso porous reactor can be explained with the help of the Figure 5-6. Inside the macro-pores the flow occurs mainly by convection, while inside the mesoporous skeleton the mass transport is certainly dominated by diffusion. As the reactive sites are in majority in the meso-porous skeleton; therefore, it is obvious that concentration boundary layers along the skeleton are present. Indeed, it is obvious that in this system we are probably in presence of internal and external mass transfer resistances or limitations. In the case of external mass transfer limitations, we can consider a boundary layer.

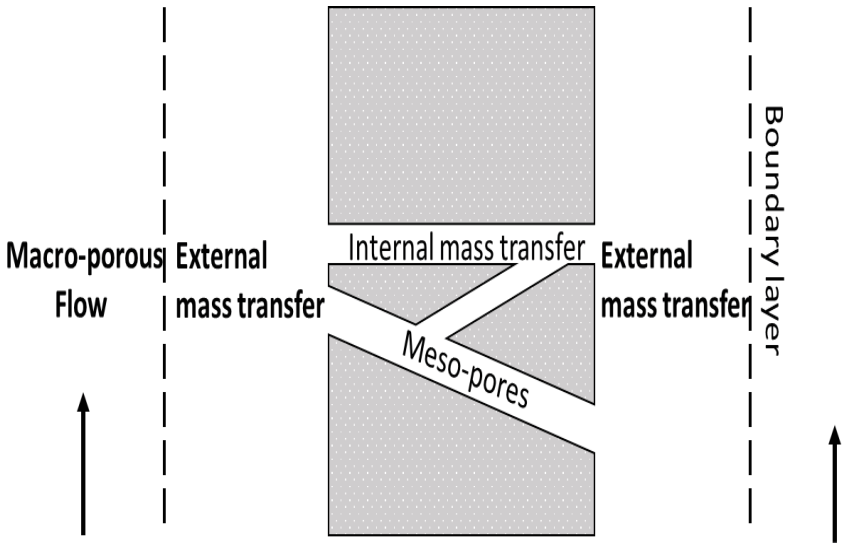

Figure 5-6. External and internal mass transport mechanism inside the meso-porous structure of the monolith.

For the design of catalytic reactors, the knowledge of the relationship between surface reaction rates and mass transfer resistances (both external and internal) is fundamental in order to try to limit these resistances through operating conditions (Levenspiel, 1999). Therefore, both external and internal mass transfer limitations were studied for enzymatic monoliths. To study the external mass transfer limitations, TC degradation tests were carried out at different flow rates. No effect of varying flow rates on degradation rates was observed. From classical reaction engineering practices, it is well known that if the relationship between Reynolds' number and reaction rate inside the reactor is linear then the overall mass transfer is limited by external mass transfer coefficient, and if the reaction rate does not change with flow rate, then reaction rate constant limits the overall mass transfer (Levenspiel, 1999). Indeed, the Re calculated in section 5.3 suggested that flow was always under laminar regime; it is then possible that a mass transfer boundary layer formation takes place in the vicinity of the reactive sites, limiting the overall mass transfer.

Internal diffusional mass transfer limitations were studied by calculating the Thiele modulus for monolithic mesoporous structure. The monolith skeleton exhibited variable thickness 5-15 μm, having meso-porosity (0.2-0.3) and tortuosity of 5-10. For enzymatic reactions inside the porous materials, the relationship between reaction rate and diffusional mass transfer has been studied by well-known dimensionless number, Thiele modulus (φ) and Effectiveness factor of the catalyst as shown in Equation (5.13) and Equation (5.14). (Haas et al., 2017),(Salai Mathi Selvi et al., 2018).

$$\varphi = L\sqrt{\frac{V_{max}}{K_M D_e}} \quad (5\text{-}13)$$

$$\eta = \frac{tanh\,(\varphi)}{(\varphi)} \quad (5\text{-}14)$$

Where,

L= half the length of the meso-pores, in this study as the skeleton thickness varies from 5 μm-15 μm, therefore values between this range were tested for calculation.

V_{max} = Maximum reaction rate (mol m^{-3} s^{-1})

K_M = Michaelis-Menten constant (mol m^{-3})

D_e = Effective diffusivity of the tetracycline solution inside the meso-pores (m^2 s^{-1})

$$D_e = \frac{\varepsilon}{\tau} D \quad (5\text{-}15)$$

D = Diffusion coefficient of antibiotics in water at 298 K ($0.99*10^{-8}$ m^2 s^{-1}) (Soriano et al., 2017).

ε = porosity of the meso-pores (0.2)

τ=1/ε; tortuosity inside the meso-pores.

5.6 Model application for TC degradation at actual wastewater concentration and proposed scale up of the system.

Considering the model developed above as valid, it should be interesting to study its application for the simulation of real cases. For this purpose, we carried out a scale up and considered the TC degradation at real TC concentrations found in municipal wastewaters (2.8-5.6 * 10^{-4} ppm). TC values were taken from literature according to Danner et al. (2019) and (Abejón et al., 2015b).

The scale up of the monoliths was proposed at two levels:

1. Single monolith required for complete degradation of TC under lab-scale conditions: For this purpose, monoliths with large size (10-50 cm in length; 1-5 cm in diameter)

were built in COMSOL MULTIPHYSICS®. The idea of this proposed scale up was to calculate the size of monolith required for the complete degradation of TC in a single pass under the lab scale conditions (5 mL min^{-1}).

2. A large-scale implementation considering a configuration of monoliths in parallel and real fluxes, for this case again we consider a complete TC degradation in a single pass. Here, three case studies of wastewater were considered: i.e, municipal wastewater, hospital wastewater and industrial wastewater as reported previously by (Abejón et al. (2015b) for large-scale membrane process. Indeed, large scale enzymatic monoliths were implemented in parallel configuration as shown in Figure 5-7. The calculations were based on a single monolith which allowed complete TC degradation with capacity of 7.2 10^{-3} m^3/day. Then by applying the total mass balance, the total number of the monoliths required for the TC degradation in a wastewater treatment plant was calculated.

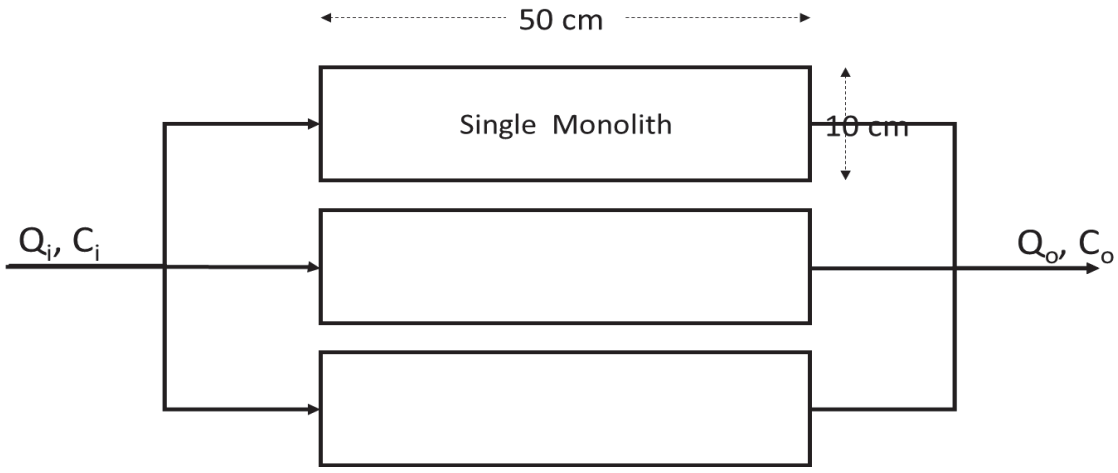

Figure 5-7. A general scheme of parallel combination of large-scale monoliths for a real implementation. (Single monolith able to degrade more than 90% of initial TC concentration having capacity of (7.2 10^{-3} m^3/day). Qi (Wastewater Inlet Flow rate (m3/day)); Ci (TC concentration at Inlet (µg L^{-1}); (Q_o (Outlet flow rate(m^3/day); Co (outlet concentration (µg L^{-1}).

5.7 Model validation

CFD model coupled with transient feed tank mass balance allowed computing the TC degradation with time inside the feed tank. Simulation results obtained for the TC concentration evolution inside the feed tank were compared with the experimental results in the range of different flow rates used for simulation. The results can be seen in Figure 5-8. The simulation results showed the cumulated conversion is strongly dependent on the flow rate, this result is completely different to the results obtained in experiments where no dependence of degradation with the flowrate is observed. We can notice a relatively good agreement but only during the first hours of operation and for the flow rate range between 0.6-0.8 mL min^{-1}. Moreover, it can be observed that after first five hours of operation, the experimental TC concentration reaches steady-state state while simulated TC concentration decreases continuously. The deviation between experimental and simulation results would be explained by different phenomena that may occur in the system and that are not considered in the homogenized model (uniform porosity). First of all, for modelling purposes, the kinetics used was the kinetics obtained during experiments with crushed monoliths (almost all porosity is accessible) and under agitation which means all the active sites were able without any diffusion limits. While in case of continuous flow, due to relatively high convective flow in compared to diffusion within the meso porosity all the active sites may not be available. It is also possible that during first hour of reaction, the mesopores are not filled with TC solution but after few minutes the mesopores are filled with TC solution/degradation products hence the access to active sites is reduced and then steady-state condition is achieved.

Another reason can be the oxygen limitation within the mesopores. Oxidoreductases enzymes like laccases uses oxygen to degrade their substrates and thus degradation rate is dependent of oxygen concentration. However, reaction kinetic equation applied to model is based on Michaelis-Menten apparent kinetics and the effect of oxygen concentration was not considered on the kinetic equation because they were carried out under agitation at saturated oxygen conditions (As usual for enzymatic kinetics, experiments were carried out at initial conversion times and low TC concentration). Nevertheless, experimental results showed the importance of oxygen bubbling and agitation on the conversion during all experiments carried out with the stirred tank or monolithic reactor. In monolithic reactors connected in series and operating in continuous recycled mode, even if the feed solution was saturated with oxygen in the reservoir, it is possible that the necessary oxygen to complete the TC degradation was

rapidly consumed near catalytic sites and was then depleted drastically inside the mesopores or near pores' mouth. Indeed, it could result in a local lack of one essential substrate of the reaction.

Moreover, as explained above silica monoliths have interconnected mesoporous structure with thickness ranges from (5-15µm). The reactive sites are mainly inside the mesoporous structure which is only accessible through diffusion. Therefore, the diffusion mechanism of TC and oxygen molecules into mesoporous can also limit the transport and ultimately the real conversion.

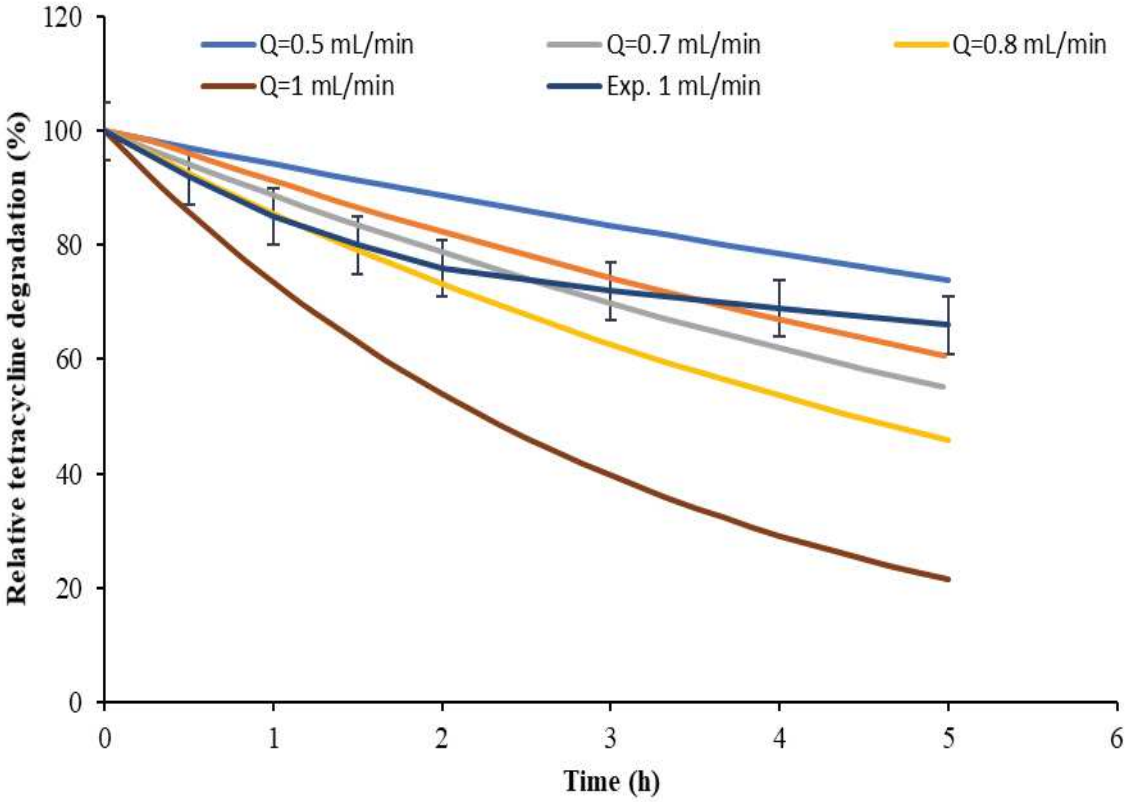

Figure 5-8. TC degradation computed through modelling and simulation at flow rates (0.5-1 mL min^{-1}) and comparison with experimental TC degradation at Flow rate (1mL min^{-1}); Simulation conditions: Temperature: 25°C; TC initial concentration (20ppm); Total volume of TC solution (30 mL).

The limitations described above can explain different experimental results like the independence of conversion with the flow rate as well as the threshold observed for TC degradation after 5 hours of reaction. Nevertheless, it is important to notice that the TC conversion given here (experimental and simulated) are cumulated conversions because the single-pass conversion is very low, indeed, it was necessary to recycle the solution in the tank in order to cumulate the decrease of TC concentration and then allow its measurement. Indeed, this cumulative process certainly highlights the phenomena of lack of co-substrate. Therefore,

in the next section which concerns the simulation, all of the results were calculated considering only a single pass of TC solution through the monoliths, then a very low TC conversion (~0.2%). Indeed, it implies initial enzymatic velocity and then probably no-lack of co-factor (for instance see Figure 5-10).

5.8 TC concentration distribution along the length of the reactor

5.8.1 Transient TC concentration distribution

Transient transport equation coupled with Brinkman equation allowed the simulation of TC degradation along the length of monolith at different time intervals, just after the feed of a fresh TC solution into the considered activated monolith (three monoliths in series). The simulation results of the distribution of degradation products along the length of the monolith can be seen in Figure 5-9. Initially, at the inlet conditions (t=0 sec), the TC concentration is zero throughout the reactor, except at the reactor inlet (45µmol L^{-1}) (dark red color). As the TC flowed through the activated monolith (red color maximum concentration), TC degraded and then its concentration decreases (color shift from red to light blue). It can be noted that reactants reached the reactor outlet in 16-20 seconds and then the maximum concentration change which is very low (0.2%) is achieved after 20 seconds. These results suggest that simulated residence time inside reactor is around 20 seconds. While based on single monolith volume (0.18 mL) and flow rate of 1 mL min^{-1}; the residence time for 3 monoliths connected in series is 35 seconds. This difference in residence time between simulated and theoretically calculated residence time may be due to homogenization approach, and this can be one of the reason why experimental and simulated results matched well when simulation runs were performed in the range of flow rate range of 0.6 mL min^{-1} to 0.8 mL min^{-1}. It can be further noticed that initial TC concentration (45 µmol L^{-1}) is higher in comparison to reaction rate ($4.4x10^{-5}$ µmol L^{-1} min^{-1}), therefore in order to completely degrade the TC for single pass large size reactor should be required.

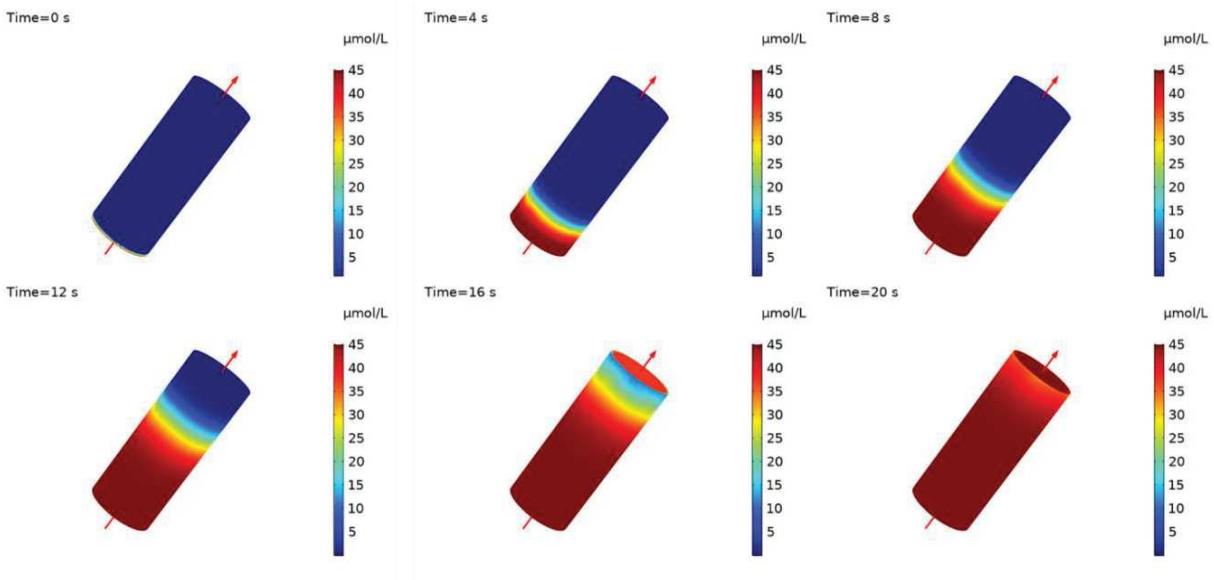

Figure 5-9. TC concentration distribution along the length of the reactor at different time from t=0-20 s; Flow: 1 mL min^{-1}; TC initial concentration 45 µmol L^{-1} (20ppm); Brinkman velocity 5.9x10^{-4} m s^{-1}; Reaction rate: 4.4x10^{-5} µmol L^{-1} min^{-1}; Reactor size (L=15 mm; D= 6mm).

5.8.2 Steady-state TC concentration distribution

Steady-state modeling for TC concentration distribution provided the results for TC conversion in a single pass through activated monoliths. The computing of steady-state transport equation (Equation 5.4) coupled with Brinkman equation provided the steady-state concentration distribution along the length of the reactor as shown in Figure 5-10. The TC concentration change along the length of the reactor can be seen from the color change from red (Inlet of the reactor) to dark blue (outlet of the reactor). However, it should be noted that difference in concentration between inlet and outlet is very small (1.5x10^{-3} µmol L^{-1}**)** as explained above. This was due to very slow reaction kinetics (4.4x10^{-5} µmol L^{-1} min^{-1}) in comparison to convective flow velocity (5.9x10^{-4} m s^{-1}). From these results, it can be concluded that due to very low TC reaction kinetics, it was not practically possible to study experimentally the monolithic system in a single pass in continuous mode. Therefore, to observe concentration change during the experiments, the monolithic system was operated in continuous recycled mode (Figure 3-4) in order to make possible the analysis of the variation of TC concentration. Furthermore, other factors like internal diffusion limitations might have impact on TC conversion, therefore internal and external mass transfer diffusion were studied and explained in the next section.

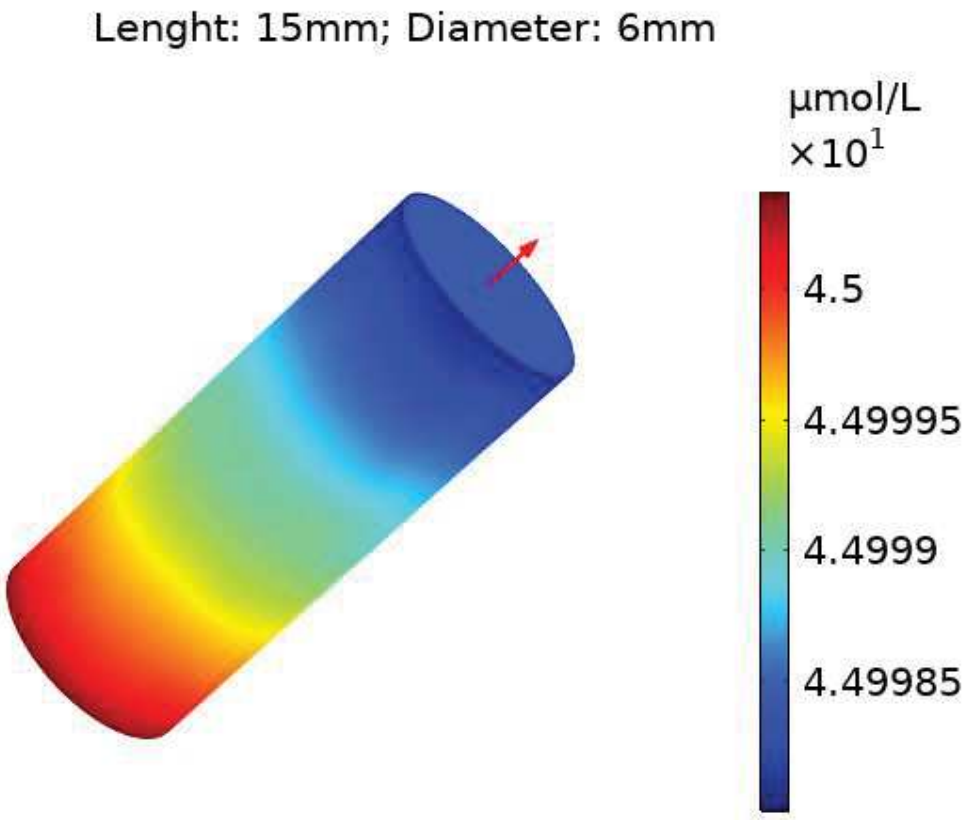

Figure 5-10. Steady-state TC concentration distribution along the length of the reactor. Flow: 1 mL min^{-1}; TC inlet concentration 45 µmol L^{-1} (20ppm); Brinkman velocity 5.9x10^{-4} m s^{-1}; Reaction rate: 4.4x10^{-5} µmol L^{-1} min^{-1}.

5.9 Mass transfer limitations within porous monoliths

Effect of both Internal and external mass transfer on reaction rates were studied in order to know the overall mass transfer controlling mechanism within the porous monoliths.

For internal mass transfer limitations, Thiele-modulus and effectiveness factor were calculated for the monoliths studied here (mesoporous thickness ranged between 5 to 15µm. These parameters are very useful to predict the performance of the porous catalysts and provide information that whether the TC degradation is controlled by kinetics or internal diffusion. The meso-porous skeleton thickness range was selected based on SEM analysis of the monolith as can be seen in Figure 4-1. The results of the relationship between Thiele-modulus and effectiveness factor of the monolith are plotted in Figure 5-11. For all the values of mesoporous thickness, shown the evolution of the Effectiveness factor versus the Thiele-modulus. It can be noticed that for the range of the considered mesoporous skeleton thickness, an effectiveness factor of 1-0.99 was reached for a Thiele number of 0.016-0.12. These values correspond to a

process controlled by the reaction kinetics. These results conclude that even for the maximum thickness of skeleton (15 µm) the overall TC degradation was controlled by reaction rate and there even if limitations of internal skeleton mass transport through diffusion could exist, they are not controlling the global process. Thiele-modulus for silica monoliths with very small skeleton thickness of 0.22 µm was previously studied by Haas et al.(2017) and obtained Thiele-modulus values between 0.0012-0.0016 for the Knoevenagel reaction at different temperatures. The results obtained by Haas et al.(2017) were also in the region controlled by reaction rate. This analysis is in good agreement with the experimental observation concerning the limitation of co-substrate (oxygen) which limits the reaction rate.

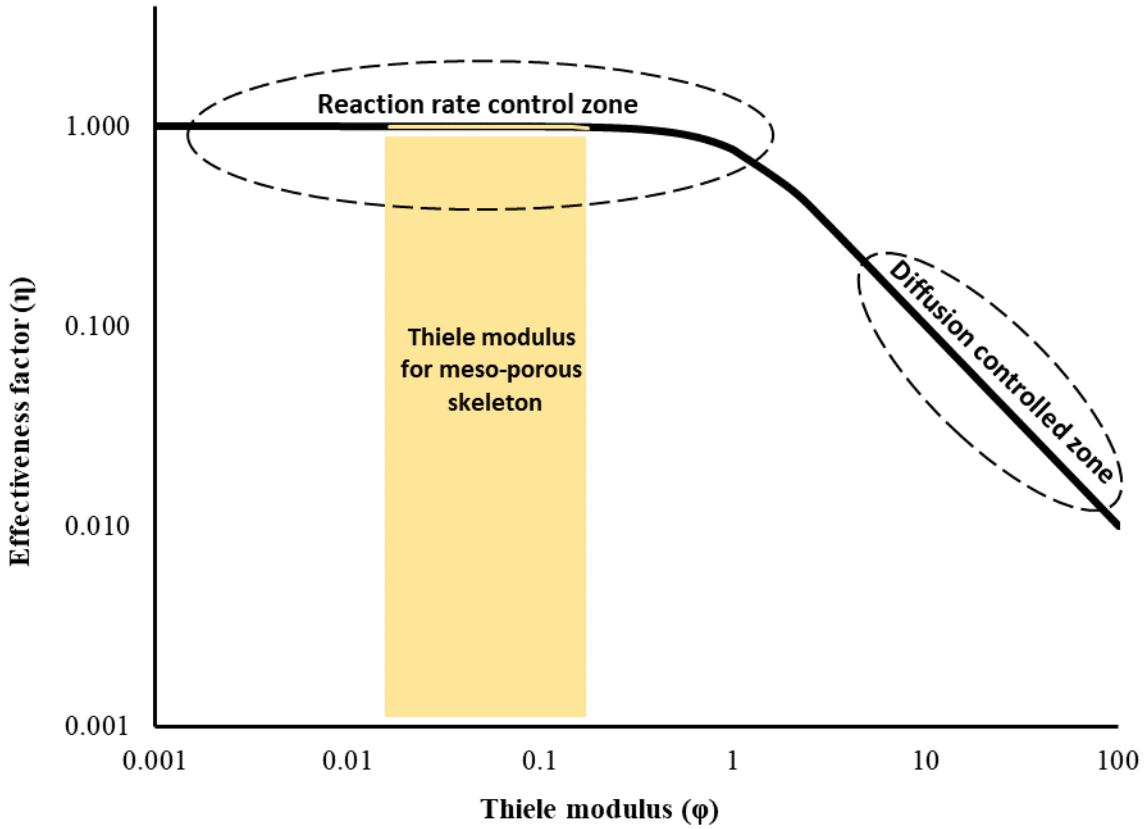

Figure 5-11. Effectiveness factor (η) vs Thiele modulus (φ) plot for the silica monoliths meso porous skeleton range (5-15µm).

External mass transfer means the transfer of reactants from moving fluid to the reaction site and the transfer back of products from reaction site to the moving fluid. External mass transfer can be studied with the help of experiments as well as by the development of classical correlations of Sherwood or Damköhler number (Burghardt, 1986; Levenspiel, 1999).

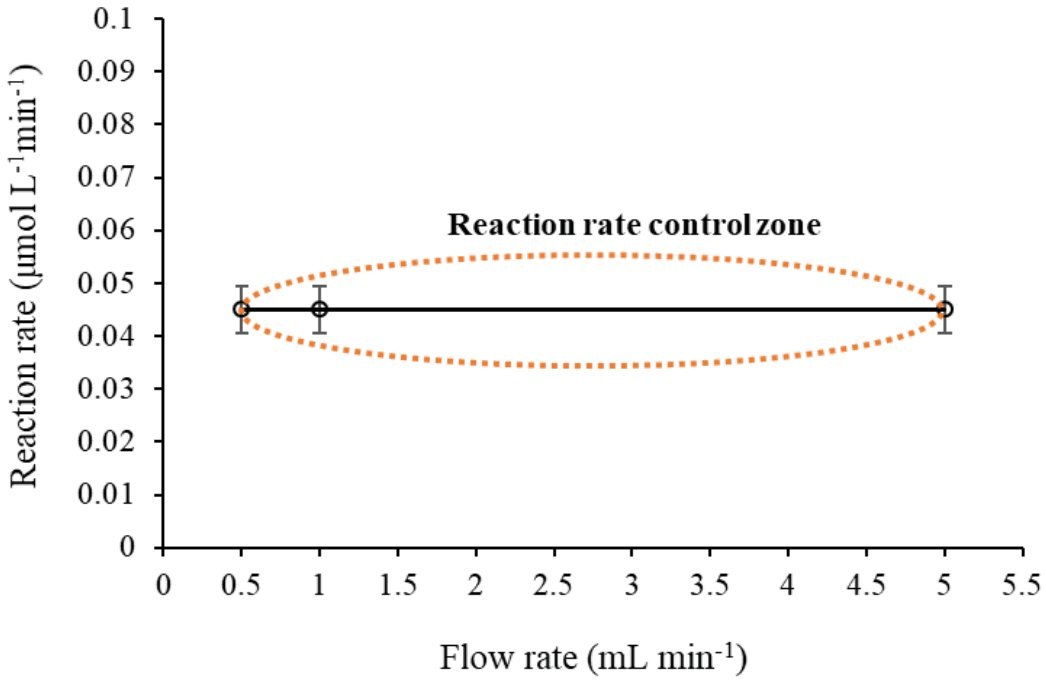

Figure 5-12. Relationship between Reaction rate and Recirculation flow rate tested during experiments carried under continuous recycled mode. Total volume of TC (30 mL), Initial TC concentration (20 ppm), Laccase activity used (0.3 U mL).

In case of experiments with flow through monoliths, if the relationship between the flow rate through the reactor and the reaction rate (calculated based on 30% of initial TC degraded in first 5 hours) is linear then it is considered that overall mass transfer is limited by external mass transfer, and if the flow rate variation doesn't affect the reaction rate then it is the case of reaction rate controlling the overall mass transfer within the reaction. External mass transfer limitations were studied by performing TC degradation experiments at different recirculation flow rates (0.5-5 mL min^{-1}). The results for TC degradation vs recirculation flow rate are shown in Figure 5-12. The results revealed that there was negligible effect of recirculation flow rate on TC degradation rate tested in these experiments; the reaction rate was constant for all the flow rates tested. Furthermore, it should be noted that the Re number calculated in section 5.3 for the flow range (0.5 mL min^{-1} to 5 mL min^{-1}) was between 0.001 to 0.01, which corresponds to laminar flow in porous media even with the maximum flow rate (5 mL min^{-1}) used in this work. Therefore, the flow regime was always under laminar flow and then the effect of external mass transfer cannot be neglected. Indeed, even if mass transfer limitations are certainly occurring in this system, the global process is controlled by the reaction kinetics as it has been explained above.

5.10 Application of model for the actual wastewater concentrations and proposed scale up of monolith system

During experimental study, relatively high initial TC concentration was used (20 ppm), however for practical implementation of the monolith system it was necessary to study the TC degradation in the range of actual TC concentrations found in wastewater. For this purpose, modelled monoliths (as discussed in section 5.13) were considered to degrade TC at a concentration of 0.28 µg L^{-1} which is currently encountered in wastewaters as suggested by Danner et al. (2019) and (Abejón et al., 2015b).

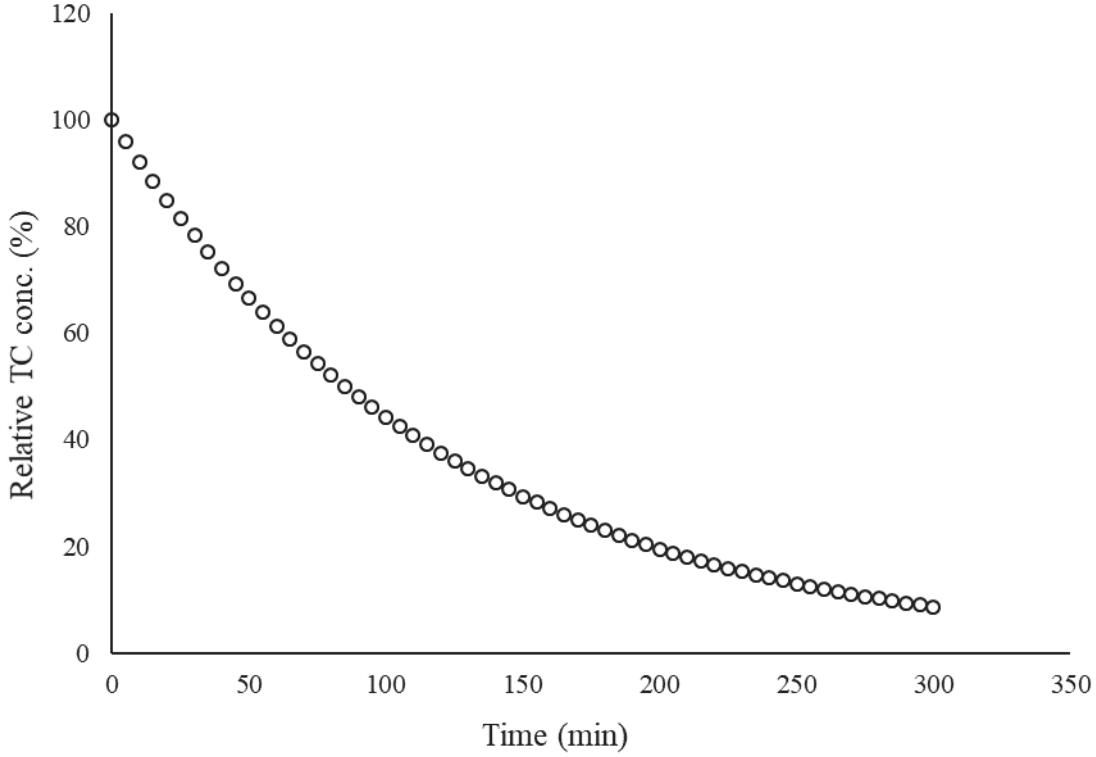

Figure 5-13. Simulated degradation of TC applied to actual initial TC concentration (0.28 µg L^{-1}) found in wastewater; Simulation conditions: Flow rate (1 mL min^{-1}) continuous recycled mode; Temperature (25 °C); Activity (0.5 U mL^{-1}).

It is important to notice that this TC concentration is very low (2.8 10^{-4} ppm) when compared to 20 ppm used for experimental studies in this work or with 8.3 ppm of dissolved oxygen at 25°C. The model applied to actual TC concentration found in wastewater, was able to degrade more than 90 % of initial TC during first 5 hours under laboratory conditions (total volume of TC: 30 mL) as can be seen from Figure 5-13. It should be noted that the model used the reaction kinetics and reactor dimensions based on the lab scale. These results are promising even if the simulated results were validated with the experimental results only during the first 5 hours of

reaction (Figure 5-13); it can be used as a basis for scaling up the monolith system for the degradation of micropollutants from wastewater.

Table 5-3. Single pass TC conversion for different monolith sizes: simulation-based results; Flow rate: 1 mL min^{-1}.

Length (cm)	Diameter (cm)	Inlet TC concentration ($\mu mol\ L^{-1}$) $x10^{-4}$	Outlet TC concentration ($\mu mol\ L^{-1}$) $x10^{-4}$	TC conversion in a single pass (%)
0.15	0.06	6.34	6.34	≤ 0.01
5	2	6.34	6.31	0.5
10	4	6.34	6.06	4
15	6	6.34	5.46	13
20	8	6.34	4.47	28
25	10	6.34	3.22	52
50	**20**	**6.34**	**0**	**100**

The scale up of the activated monoliths and the TC conversion reached in a single pass was then proposed by increasing their geometrical dimensions. For this purpose, monoliths with different size (Length and diameter ranged in between 5-25 cm and 1-5 cm respectively) were considered for simulations, the results are summarized in Table 5-3. Indeed, it was important here to increase the size of the activated monoliths in order to reach a complete TC degradation in a single pass (without recycling). From Table 5-3, we can notice that when the size of monoliths and conversion are enhanced simultaneously. For example, when the monolith geometry was set at 5cm of length and 1cm of diameter only 0.5% of initial TC was converted. However, with monoliths of 50 cm of length and 20cm of diameter it was possible to complete deplete the TC in a single pass. These theoretical "large-scale monoliths" were then used for further simulations.

5.11 TC concentration distribution in « large-scale monoliths » (L= 50cm; D= 20cm)

TC concentration distribution along the length of "large-scale monoliths" for different flow rates (1-5 mL min^{-1}) are shown in Figure 5-14. From these results, it can be seen that at inlet, TC concentration (red color) is maximum ($6.3x10^{-4}$ µmol L^{-1} ≈0.28 µg L^{-1}); then, as the TC flows through the reactor, the concentration decreases along the length of the reactor due to the enzymatic reaction. The TC concentration distribution profile is different in case of different flow rates. For example, at a flow rate of 1 mL min^{-1}, the TC concentration changes rapidly as can be observed from color changes and 90-100% of TC is converted when TC reaches one-third of the reactor length, (dark blue color shows zero concentration). At 2 mL min^{-1}, the TC concentration changes along the length of the reactor in the first half of the reactor and at 3-4 mL min^{-1}, the concentration distribution is larger; and only 60-70 % conversion is reached with these flow rates. Similarly, at 5 mL min^{-1}, a greater concentration distribution was observed with only 50% of TC conversion.

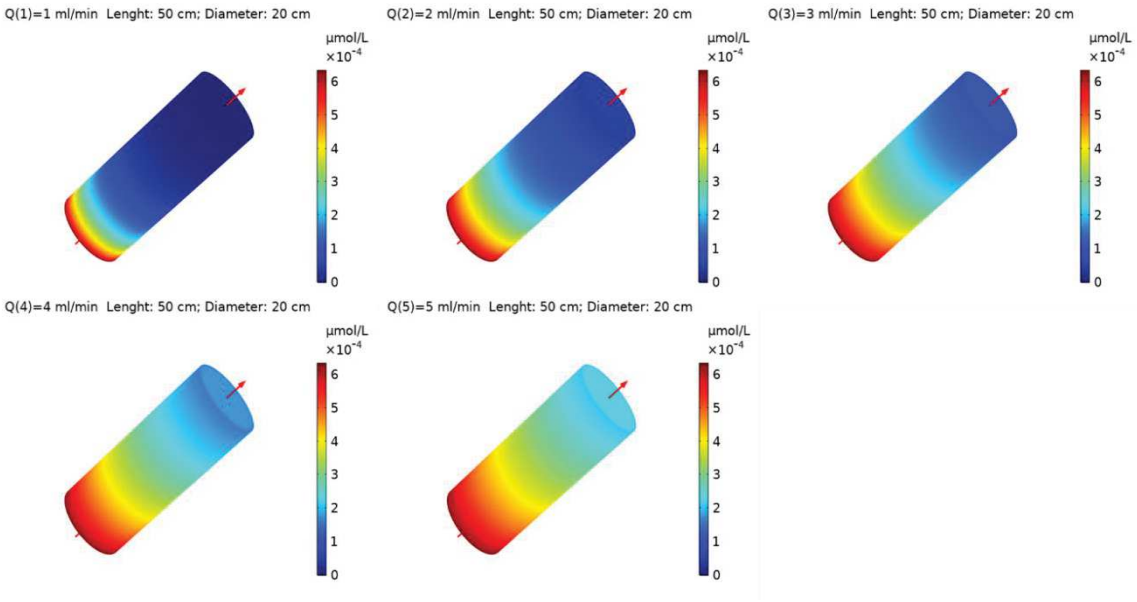

Figure 5-14. Steady-state TC concentration along the length of the "large scale monolioth" in single pass at different TC flow rates. Total reactor length: 50 cm, diameter: 20 cm; Inlet TC concentration: 0.28 µg L^{-1}; Reaction rate: $4.4x10^{-5}$ µmol L^{-1} min^{-1}.

In terms of TC conversion along the length of the reactor at different flow rates, a line graph was plotted as can be seen from Figure 5-15. Complete TC degradation is achieved at the flow rate of 1 mL min^{-1}. However, it can be observed that the rate of TC depletion in the last 15 cm relatively very low, and then this last section of the monolith is not enough efficient. For flow rates higher than 1 mL min^{-1}, TC conversion decreases and values between 50-90% are reached. In fact, the global process is controlled by reaction kinetics and at high flow rates, the

residence time is too low to reach a complete TC depletion. However, as far as real wastewater fluxes are very high (600-70.000 m^3/day, for instance see next section 5.12) a compromise has to be reached in between the level of TC depletion, the contact time and process effectiveness, for this an optimization has to be carried out with multi-objective programming like Pareto optimality, this analysis has to be coupled with the cost of the process (Abejón et al., 2015a).

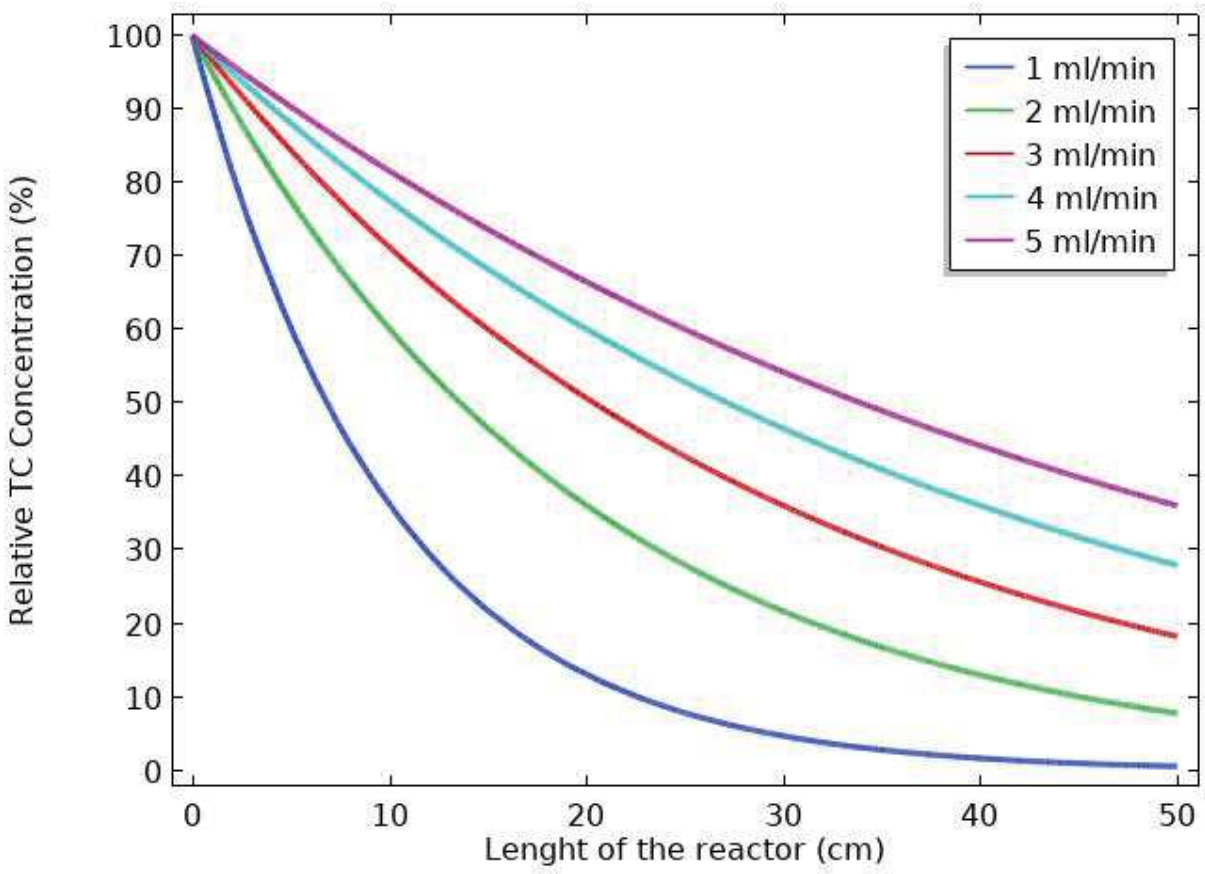

Figure 5-15. Relative tetracycline concentration along the length of the reactor from Inlet to outlet at different TC flow rates. Total reactor length: 50 cm, diameter: 20 cm; Inlet TC concentration: 0.28 µg L^{-1}; Reaction rate: 4.4x10^{-5} µmol L^{-1} min^{-1}.

5.12 A case study of enzymatic monolithic system for TC degradation in wastewater treatment plants (WWTPs).

Large scale enzymatic monolithic system was applied for TC degradation in wastewaters. For this purpose, three case studies were considered, i-e; municipal wastewater, hospital wastewater and industrial wastewater. TC concentration values found in those wastewater were taken from literature as suggested by (Abejón et al., 2015b).

5.12.1 Enzymatic monolithic system for Municipal wastewater Treatment

For the case of municipal wastewater treatment, TC concentration considered was of 0.28 µg $L^{-1} \approx 6.3x10^{-4}$ µmol L^{-1} and the effluent flow was 70.000 m^3/day based on inhabitant population of 220.000 and specific wastewater production 0.32 m^3/(day-inh).

To propose an enzymatic monolithic system for municipal wastewater treatment, a single large-scale monolith (L=50 cm; D=20 cm) was first simulated based on inlet TC concentration found in municipal wastewater. As far as an optimization study has not been carried out in this work, and considering two facts: firstly at a flowrate of 1 mL min^{-1} the last section of the enzymatic monolith is not enough efficient. Secondly, the real flows of wastewaters are very high; it was decided to double the flowrate up to 2 mL min^{-1} for the rest of simulations. The simulation results for TC degradation along the length of the large-scale monolith are shown in Figure 5-16. It can be seen from the results that a single large-scale enzymatic monolith (L=50 cm; D=20 cm) is able to degrade approximately 90% of inlet TC concentration. It should be noted; then to treat 70.000 m^3/day of wastewater, a large number of monoliths. Moreover, to maintain the same contact time, these monoliths have to be connected in parallel configuration. The total number of monoliths required to treat 70.000 m^3/day of municipal wastewater were calculated from the total flow rate of effluents divided by the capacity of a single monolith.

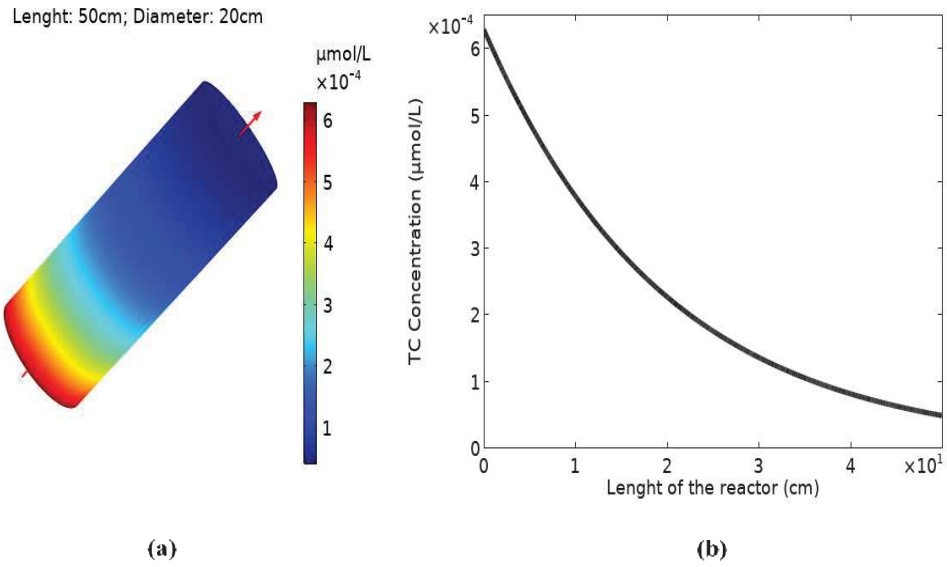

Figure 5-16. Simulation of a single large-scale monolith for municipal wastewater treatment. (a) 3D TC concentration profile along the length of the large-scale monolith (b) 2-D plot of TC degradation along the length of the large-scale monolith. Flow rate: 2 mL min^{-1}). Inlet TC concentration: $6.3x10^{-4}$ µmol L^{-1}. Brinkman velocity: $1.2x10^{-3}$ m s^{-1}; Reaction rate: $4.4x10^{-5}$ µmol L^{-1} min^{-1}.

Each large-scale monolith has the capacity of 2.9 x 10^{-3} m^3/day (2 mL min^{-1}). Therefore, the calculated number of the monoliths required to degrade TC in municipal wastewater are 24.305.000. The cross-sectional area of the single monolith with diameter 0.2 m was 0.0314 m^2 (circular area of inlet). Therefore, the total area required for all the monolith was 763.660 m^2 (no. of monoliths x Area of single monolith). Indeed, this enzymatic monolithic process is certainly not adapted to be implemented on large-scale for municipal wastewater treatment. However, even if an economical study needs to be carried out, only in terms of foot-print, the enzymatic monolithic process based on lab-scale reaction kinetics seems to be non-realistic for the degradation of TC. Higher reaction kinetics are certainly required in order to reduce the number of the monoliths.

5.12.2 Enzymatic monolithic system for hospital wastewater treatment

For the hospital wastewater with TC concentration of 0.4 µg L^{-1} as suggested by (Abejón et al., 2015b), the single large-scale monolith simulated results for TC degradation along the length of the reactor are shown in Figure 5-17. The simulation results show that single monolith having TC treatment capacity (3.5 x 10^{-3} m^3/day) can degrade more than 99% of the initial TC concentration (0.4 µg L^{-1} ≈ 9 µmol L^{-1}) found in hospital wastewater. Based on the capacity of the single large-scale monolith, the total number of the monoliths required to treat hospital wastewater flowing at the rate of 600 m^3/day is 171.400 (hospital having 1000 beds capacity and specific wastewater production of 0.6 m^3/bed hospital wastewater).

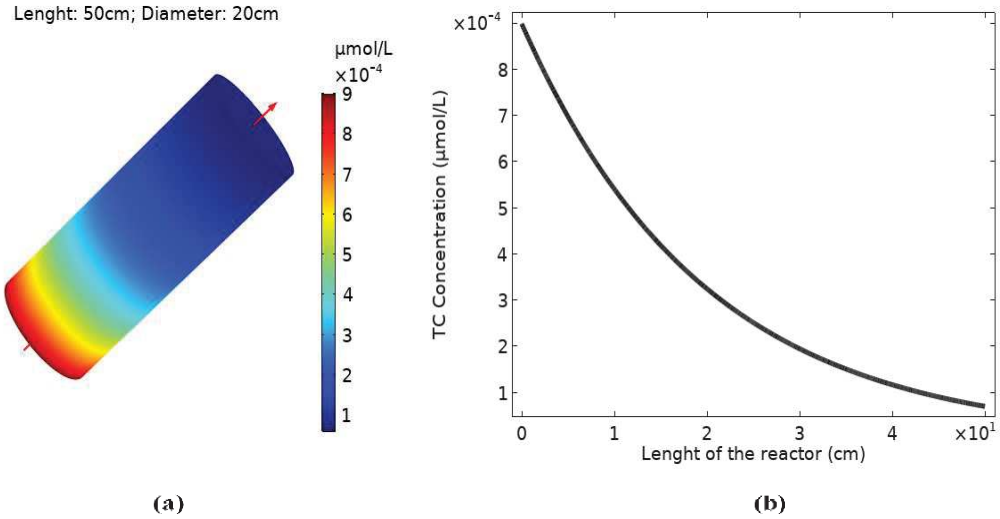

Figure 5-17. Simulation of a single large-scale monolith for hospital wastewater treatment. (a) 3D TC concentration profile along the length of the large-scale monolith (b) 2-D plot of TC degradation along the length of the large-scale monolith. Flow rate :2 mL min^{-1}. Inlet TC concentration: 9x10^{-4} µmol L^{-1}. Brinkman velocity: 1.2x10^{-3} m s^{-1}; Reaction rate: 4.4x10^{-5} µmol L^{-1} min^{-1}.

5.12.3 Enzymatic monolithic system for Industrial wastewater treatment

For industrial wastewater, the design parameters were based on initial TC concentration of 11.000 µg L^{-1} as suggested (Abejón et al., 2015b) and an effluent flow rate of 5000 m^3/day. The final concentration of TC was considered as below 1 µg L^{-1}. This TC concentration can be discharged into public sewage for further treatment into municipal WWTP. The simulated TC degradation profile for a single large-scale monolith implemented for industrial wastewater is shown in Figure 5-18. The results show that a single large-scale monolith is able to degrade more than 99 % of initial TC. The TC treatment capacity of the single monolith based initial concentration of (11.000 µg L^{-1} ≈ 25 µmol L^{-1}) is 2.88 x 10^{-3} m^3/day (2 mL min^{-1}). Hence, the required number of the monoliths to treat industrial wastewater at the rate of 5000 m^3/day is 1.736.100.

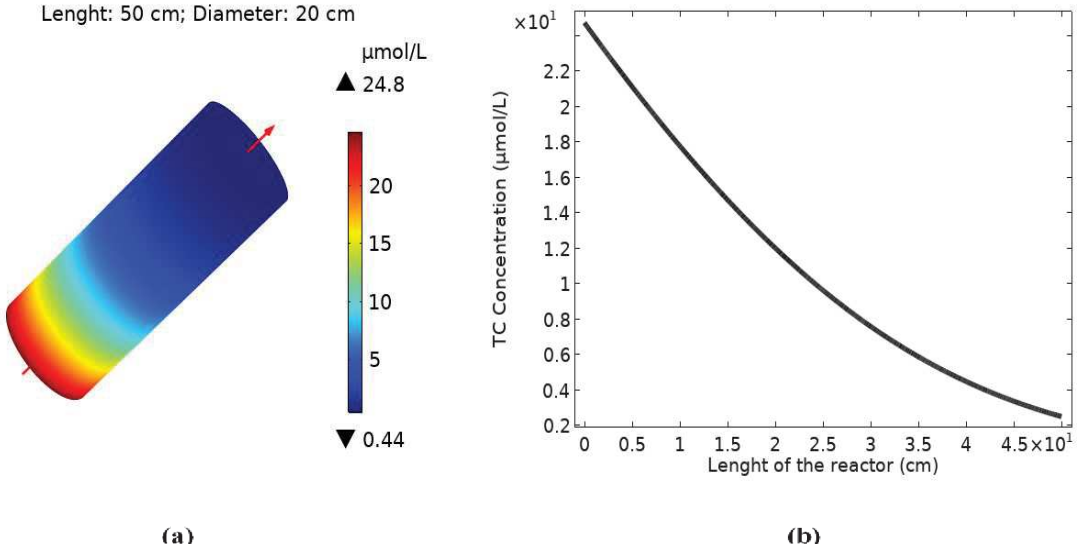

Figure 5-18. Simulation of a single large-scale monolith for industrial wastewater treatment. (a) 3D TC concentration profile along the length of the large-scale monolith (b) 2-D plot of TC degradation along the length of the large-scale monolith. Flow rate :1 mL min^{-1}. Inlet TC concentration: 25 µmol L^{-1}. Brinkman velocity: 6x10^{-4} m s^{-1}; Reaction rate: 4.4x10^{-5} µmol L^{-1} min^{-1}.

It is important to notice that in this last case the initial concentration is relatively high (11 ppm) and then the results of the model are only an approximation, because in such conditions it is possible to reach limitations on oxygen concentration it has been explained previously.

From above results it can be concluded that enzymatic monolithic system applied to degrade TC treatment in municipal wastewater, hospital wastewater and industrial wastewater requires an extremely large number of enzymatic monoliths. This large number of monoliths

needs also very large foot-print space, for example in case of municipal wastewater, enzymatic monolithic system will require approximately 763.660 m^2 on the site. Indeed, the enzymatic monolithic process is neither practical nor economical to be implemented at large-scale. Therefore, improvements in the enzymatic process are required firstly at the lab scale. These improvements include the immobilization of a much more active laccase on the surface of monoliths. It is well known that one of the most important factors which enhance the enzymatic activity is the V_{max} which depends not only on the intrinsic activity of the enzyme but also on the enzyme concentration (Abejon et al. 2015a). Another possible solution for the application of this process is the treatment of concentrates obtained from nanofiltration of waters containing antibiotics. In such case, the volumes to be treated are certainly much lower but antibiotics concentration is relatively high and then as far as Michaelis-Menten kinetics depends on substrate concentration the conversion will be certainly enhanced but oxygen limitations could be also present and need to be resolved.

The TC depletion reached by immobilizing a very active laccase on the surface of the monolith was studied through the model. For this purpose, the actual value of V_{max} experimentally measured, was increased in rage in between 5 to 100 times and injected into the calculation software.

For this purpose, were considered the examples of municipal wastewater (MWW), hospital wastewater (HWW) and industrial wastewater (IWW) described previously. The flow rates and initial TC concentration were, MWW flow rate: 70.000 m^3/day containing 0.28 µg $L^{-1} \approx 6.3x10^{-4}$ µmol L^{-1} of TC; HWW flow rate : 600 m^3/day containing 0.4 µg L^{-1} ≈ 9 µmol L^{-1} of TC; IWW flow rate: 5000 m^3/day containing 11.000 µg $L^{-1} \approx 25$ µmol L^{-1} of TC as well as active monoliths formerly scaled up (L=50 cm; D=20 cm).

Simulations for were carried out increasing V_{max} and calculating flow rates necessary to reach a complete degradation of TC in only one pass through the monolith. Then from the flow rates, the number of enzymatic monoliths in parallel required to deplete TC from MWW, HWW and IWW were calculated.

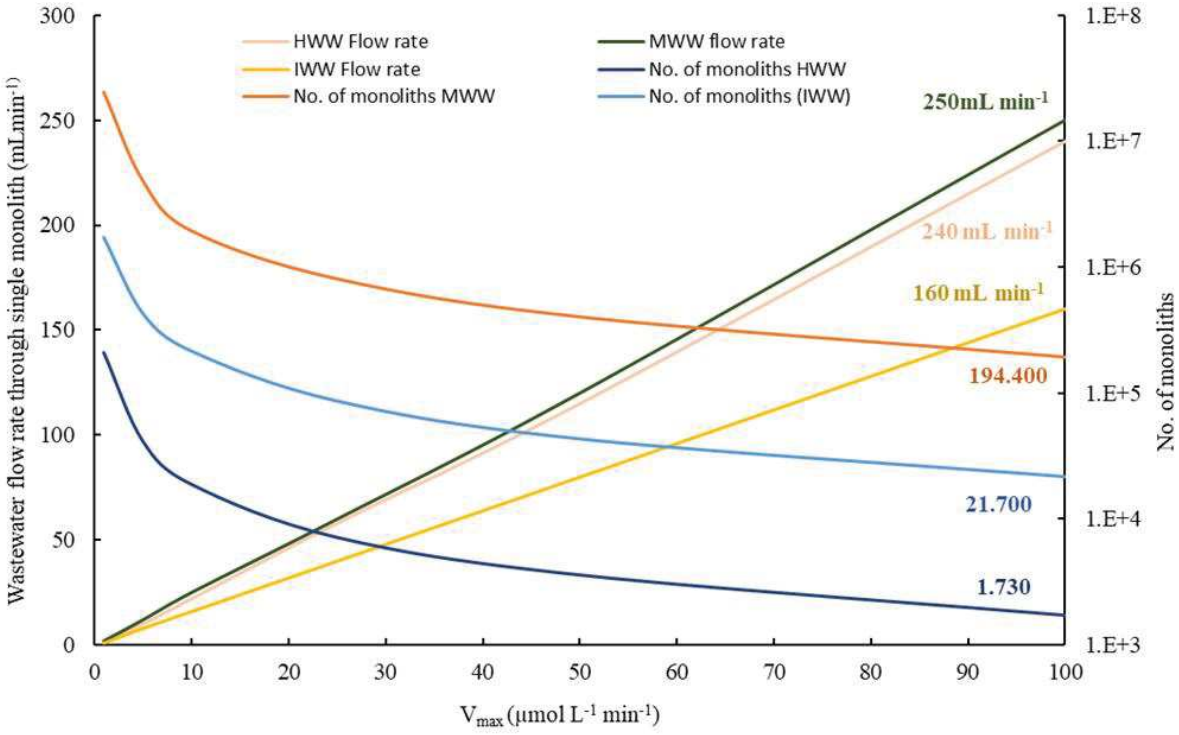

Figure 5-19. Simulations of the V_{max} enhancement on wastewater flow rate (mL.min^{-1}) though one monolith (total TC degradation) and the number of monoliths necessary to treat municipal wastewater (MWW) flow rate: 70.000 m^3/day containing 0.28 µg L^{-1} ≈ 6.3x10^{-4} µmol L^{-1} of TC; hospital wastewater (HWW) flow rate : 600 m^3/day containing 0.4 µg L^{-1} ≈ 9 µmol L^{-1} of TC and industrial wastewater (IWW) flow rate: 5000 m^3/day containing 11.000 µg L^{-1} ≈ 25 µmol L^{-1} of TC.

The results are presented in Figure 5-19. It can be seen that increasing V_{max}, the wastewater flow rate to reach total depletion of TC is enhanced too. Indeed, the wastewater treating capacity of a single monolith is improved. Moreover, V_{max} enhancement results also on a decrease of the number of monoliths required to treat wastewater. For example, in case of MWW and HWW by increasing the V_{max} 100 times, the flow rate through single monolith for complete TC degradation linearly increased from 2 mL min^{-1} to 250 mL min^{-1} and 240 mL min^{-1} respectively. Similarly, in case of IWW, which presents a relatively high initial TC concentration (11.000 µg L^{-1}) the flow rate was increased from 1 mL min^{-1} to 160 mL min^{-1}. The required number of monoliths for highest V_{max} and flows were 194.400, 21.700 and 1.730 for MWW, IWW and HWW respectively. To comparison purposes if we consider the actual experimentally measured kinetics the number of monoliths were 24.305.000, 1.736.100 and 171.400 for MWW, IWW and HWW respectively. From the results it can be seen that the number of monoliths were reduced approximately 100 times for maximum V_{max} used in this simulation.

These results confirmed that by immobilizing a very active laccase on the surface of the monoliths, enzymatic monoliths can be promising in the wastewater treatment applications.

Nevertheless, we have to take into account that such improvement on the V_{max} could result on a lack of oxygen, for this further improvement of the process, like manufacturing shorter monoliths and bubbling air in between are certainly necessary.

Chapter 6

Conclusions and future prospective.

6. CONCLUSIONS AND PROSPECTIVE

The objective of this research work was to study the feasibility of enzymatic monoliths for the degradation of PPs in wastewater. For this purpose, enzymatic monoliths were applied for the degradation of TC as a model PPs molecule. The research was developed through experimental and modelling approaches. For experimental studies, highly porous silica monoliths (support material prepared at ICGM) presenting a double pore size distribution (mesopores and macropores) were activated by immobilizing a laccase from *Trametes versicolor* via covalent bonds with glutaraldehyde. High immobilization yields were achieved due to large meso porous surface area and interconnected macropores. Immobilization efficiency and expressed activity showed that the activity of immobilized laccase towards ABTS oxidation was enhanced in comparison to initial activity of free enzyme. Immobilized laccase on monoliths presented also a decrease in the Michaelis-Menten constant (K_M) value for ABTS and TC degradation compared to free laccase indicating that the affinity towards both substrates was enhanced. Storage stability of the immobilized laccase on silica monoliths confirmed that laccase immobilized monoliths can be stored for longer period of time. These results confirmed that silica monoliths can be considered as a promising support material for enzymes immobilization and can be used for PPs degradation.

Water permeability tests carried out with silica monoliths in a pilot unit showed that monoliths present a very high permeability together with a low pressure drop and then can be promising supports to be used in a “Flow through reactor” configuration.

TC degradation tests were carried out in a tubular reactor under a continuous flow and recirculation configuration. It is important to notice that the TC conversion was based on cumulated conversions because a single-pass conversion was very low and impossible to be measured experimentally. Therefore, it was necessary to recycle the TC solution in the tank in order to cumulate the decrease of TC concentration and then allowed its measurement. The results showed that only 30-40% TC was degraded during the first 5 hours of reaction, after that the conversion decreased arriving to a threshold. The decrease of reaction rate with time could be explained through various hypotheses: lack of dissolved oxygen near catalytic sites limiting the overall reaction rate, TC degradation products inhibition, inaccessibility of all the active sites as the convective flow was relatively higher than the diffusive flow, external or internal mass transfer limitations.

The effect of different parameters like dissolved oxygen concentration, TC degradation products and recirculation flow rates on TC degradation rate were studied. The results of these studies showed that dissolved oxygen concentration as well as TC degradation products enhanced TC degradation rate; while, the recirculation flow rate had no significant effect.

Operational stability tests carried out during 75 hours of sequential tests showed that laccase-activated monoliths retained more than 90% of their activity after several cycles of TC degradation tests, which means first that laccase was firmly attached to the surface via covalent bonds and secondly, that the loss of enzymatic activity is almost negligible during the time of experiences. Nevertheless, long-term operation stability tests need to be carried out to determine the maximum time of enzymatic activity of monoliths.

A model was developed in order to simulate the evolution of TC concentration inside a monolith or in the pilot unit. The building of the model was carried out in two parts: in the first part, steady-state as well as time-dependent CFD model was developed in COMSOL MULTIPHYSICS® 5.3. Some model parameters, like reaction kinetics and permeability coefficient were obtained from experimental results. The modelling was based on the reaction kinetic model of Michaelis-Menten (V_{max} and K_M) and considers a homogenized geometry of monoliths. Indeed, the TC degradation in a single pass was computed. In the second part, a dynamic mass transport balance model was developed in MATLAB® 2017 to compute TC concentration change with time in the feed/recycling tank. Both models were coupled via COMSOL-MATLAB Live-link feature and run simultaneously. Modelling and simulations were carried out with two main objectives: first, to evaluate the TC conversion in a single pass through enzymatic monoliths based on lab-scale conditions (measured reaction kinetics, monoliths dimensions and flow rates) and secondly to simulate the evolution of the TC conversion in the reservoir were the TC solution is recycled. Finally, the model was applied to evaluate the TC degradation at actual wastewater concentrations and then to propose the scale up of enzymatic monolith reactors on large scale. Simulation results for TC degradation matched well with experimental results for the initial five hours of reaction, after this time, experimental TC concentration reached steady-state while simulated TC concentration decreased continuously. As it was explained above, TC conversion was cumulative in order to allow TC concentration evolution measurement. Indeed, it is possible that this cumulative process certainly highlights the phenomena of lack of oxygen as co-substrate. This phenomenon as well as the fact that the kinetics depends on two substrates (oxygen and TC) are not taken into account in the model developed in this work. Indeed, in order to avoid this

decrease of the reaction rate CFD simulations were carried out considering a single pass of TC solution through a monolith. The conversion reached in such conditions is very low (0.2%) and corresponds to the small monolith geometry and low reaction rates measured. The TC conversion was then simulated by varying the size of monoliths. It was observed that a simulated enzymatic monolith with 50 cm of length and 20 cm of diameter was able to completely degrade TC in a single pass. It should be noted that flow rates used for simulation were similar to lab-scale flow rates (1-5 mL min^{-1}). Furthermore, these enzymatic monoliths were then considered for TC degradation at large scale. For this purpose, three case studies from literature were considered and the required number of monoliths was calculated for each case. The cases of study were: 1-municipal wastewater (flow rate of 70.000 m^3/day and initial TC concentrations of 0.28 μg L^{-1}), 2-hospital wastewater (flow rate of 600 m^3/day and TC concentration of 0.4 μg L^{-1}) and finally 3- industrial wastewater (flow rate of 5000 m^3/day and TC concentration of 11.000 μg L^{-1}). The simulations allowed calculating a required number of monoliths of 24.305.000, 171.400 and 1.736.100 for the three cases of study respectively. This very large number of monoliths is not realistic and would require large area at site therefore, the enzymatic monolithic process is neither practical nor economical to be implemented at large-scale.

Other simulations were carried out considering immobilizing much more active enzymes than the laccase studied experimentally in this work. For this purpose, the experimental value of V_{max} was arbitrarily increased in between 5 to 100 times and injected into the model for simulations. The results revealed that increasing the V_{max} the number of monoliths was considerably reduced. For example, enhancing V_{max} 100 times, the number of monoliths were reduced in the same number.

These results confirmed that immobilization of a very active laccase on the surface of monoliths can be interesting in wastewater treatment applications at large scale. Nevertheless, we have to take into account that such improvement on the V_{max} could result also on a lack of oxygen. However, technical solutions like manufacturing shorter monoliths and bubbling air in between will probably be effective.

Another possible solution for the application of this process is the treatment of concentrates obtained from nanofiltration of waters containing antibiotics. In such case, the volumes to be treated will certainly be much lower. Nevertheless, in such case, antibiotics concentration will be relatively high and then as far as Michaelis-Menten kinetics depends on

substrate concentration, the conversion will certainly be enhanced but oxygen limitations may also be present and will need to be resolved.

Future recommendations and prospects

Based on the results obtained in this research work, some future work is recommended to improve the degradation efficiency of enzymatic monoliths.

1. Optimization of immobilization effecting parameters, such as the concentration of laccase and glutaraldehyde solutions used for immobilization, the reaction times for the monolith activation with glutaraldehyde and laccase. Moreover, the immobilization of monoliths in continuous flow will ensure that glutaraldehyde/laccase solutions reach all the active sites. By optimizing all these parameters, immobilization yield as well as immobilization efficiency could be further enhanced.
2. Optimization of monoliths pore size (macro as well as meso pore diameter) for laccase immobilization as well as for TC degradation in flow-through monoliths. In fact, the mesopores contain most of the active sites and then mesopore diameter can affect the reaction kinetics during the process due to internal diffusional limitations or steric hindrance effects.
3. Actual reaction kinetics study but considering a kinetics depending on two substrates TC and oxygen in order to determine the substrate limitations during the TC degradation in flow through monoliths.
4. Experiments should be carried out on actual wastewater concentrations that are very low in comparison to the concentrations used in this research study. Such study needs special analysis methods and devices for very low concentrations or traces (Orbitrap™ for example).
5. Using monoliths with different sizes and oxygen bubbling within the monoliths could be a solution to limitations of dissolved oxygen within the meso porosity.
6. Immobilization of monoliths with more active laccases in order to improve the reaction rates. The improved reaction rates can make enzymatic process feasible on large scale because of the smaller number of monoliths required to treat large flows.
7. Enzymatic monoliths can be utilized for other enzymatic reactions like preparation of high value chemicals.

8. As real wastewater fluxes are very high (600-70.000 m^3/day), a compromise has to be found between the level of TC depletion, the contact time and the process effectiveness, for this an optimization has to be carried out with multi-objective programming like Pareto optimality, this analysis has to be coupled with the cost of the process.

References

Abejón, R., Belleville, M.P., Sanchez-Marcano, J., 2015a. Design, economic evaluation and optimization of enzymatic membrane reactors for antibiotics degradation in wastewaters. Separation and Purification Technology 156, 183–199. https://doi.org/10.1016/j.seppur.2015.09.072

Abejón, R., De Cazes, M., Belleville, M.P., Sanchez-Marcano, J., 2015b. Large-scale enzymatic membrane reactors for tetracycline degradation in WWTP effluents. Water Research 73, 118–131. https://doi.org/10.1016/j.watres.2015.01.012

Agnaou, M., Lasseux, D., Ahmadi, A., 2016. From steady to unsteady laminar flow in model porous structures: an investigation of the first Hopf bifurcation. Computers & Fluids 136, 67–82. https://doi.org/10.1016/j.compfluid.2016.05.030

Alalm, M.G., Tawfik, A., Ookawara, S., 2015. Degradation of four pharmaceuticals by solar photo-Fenton process: Kinetics and costs estimation. Journal of Environmental Chemical Engineering 3, 46–51. https://doi.org/10.1016/j.jece.2014.12.009

Al-Ansari, M.M., Steevensz, A., Al-Aasm, N., Taylor, K.E., Bewtra, J.K., Biswas, N., 2009. Soybean peroxidase-catalyzed removal of phenylenediamines and benzenediols from water. Enzyme and Microbial Technology 45, 253–260. https://doi.org/10.1016/j.enzmictec.2009.07.004

Al-Khateeb, L.A., Almotiry, S., Salam, M.A., 2014. Adsorption of pharmaceutical pollutants onto graphene nanoplatelets. Chemical Engineering Journal 248, 191–199. https://doi.org/10.1016/j.cej.2014.03.023

Almomani, F.A., Shawaqfah, M., Bhosale, R.R., Kumar, A., 2016. Removal of emerging pharmaceuticals from wastewater by ozone-based advanced oxidation processes. Environmental Progress & Sustainable Energy 35, 982–995. https://doi.org/10.1002/ep.12306

Alotaibi, M., C. Manayil, J., M. Greenway, G., J. Haswell, S., M. Kelly, S., F. Lee, A., Wilson, K., Kyriakou, G., 2018. Lipase immobilised on silica monoliths as continuous-flow microreactors for triglyceride transesterification. Reaction Chemistry & Engineering 3, 68–74. https://doi.org/10.1039/C7RE00162B

Altinkaynak, C., Tavlasoglu, S., Kalin, R., Sadeghian, N., Ozdemir, H., Ocsoy, I., Özdemir, N., 2017. A hierarchical assembly of flower-like hybrid Turkish black radish peroxidase-Cu2+ nanobiocatalyst and its effective use in dye decolorization. Chemosphere 182, 122–128. https://doi.org/10.1016/j.chemosphere.2017.05.012

Altmann, J., Ruhl, A.S., Zietzschmann, F., Jekel, M., 2014. Direct comparison of ozonation and adsorption onto powdered activated carbon for micropollutant removal in advanced wastewater treatment. Water Research 55, 185–193. https://doi.org/10.1016/j.watres.2014.02.025

Alvarino, T., Lema, J., Omil, F., Suárez, S., 2018. Trends in organic micropollutants removal in secondary treatment of sewage. Rev Environ Sci Biotechnol 17, 447–469. https://doi.org/10.1007/s11157-018-9472-3

Ameur, S.B., Luminiţa Gîjiu, C., Belleville, M.-P., Sanchez, J., Paolucci-Jeanjean, D., 2014. Development of a multichannel monolith large-scale enzymatic membrane and

application in an immobilized enzymatic membrane reactor. Journal of Membrane Science 455, 330–340. https://doi.org/10.1016/j.memsci.2013.12.026

Arca-Ramos, A., Kumar, V. V, Eibes, G., Moreira, M.T., Cabana, H., 2016. Recyclable cross-linked laccase aggregates coupled to magnetic silica microbeads for elimination of pharmaceuticals from municipal wastewater. Environmental Science and Pollution Research 23, 8929–8939. https://doi.org/10.1007/s11356-016-6139-x

Archer, E., Petrie, B., Kasprzyk-hordern, B., Wolfaardt, G.M., 2017. The fate of pharmaceuticals and personal care products (PPCPs), endocrine disrupting contaminants (EDCs), metabolites and illicit drugs in a WWTW and environmental waters. Chemosphere 174, 437–446. https://doi.org/10.1016/j.chemosphere.2017.01.101

Arnold, K.E., Brown, A.R., Ankley, G.T., Sumpter, J.P., 2014. Medicating the environment: assessing risks of pharmaceuticals to wildlife and ecosystems. Philosophical Transactions of the Royal Society B: Biological Sciences 369, 20130569. https://doi.org/10.1098/rstb.2013.0569

Auriault, J.-L., 2009. On the Domain of Validity of Brinkman's Equation. Transp Porous Med 79, 215–223. https://doi.org/10.1007/s11242-008-9308-7

Baker, D.R., Barron, L., Kasprzyk-Hordern, B., 2014. Illicit and pharmaceutical drug consumption estimated via wastewater analysis. Part A: Chemical analysis and drug use estimates. Science of The Total Environment 487, 629–641. https://doi.org/10.1016/j.scitotenv.2013.11.107

Barbosa, M.O., Moreira, N.F.F., Ribeiro, A.R., Pereira, M.F.R., 2016. Occurrence and removal of organic micropollutants: An overview of the watch list of EU Decision 2015/495. Water Research 94, 257–279. https://doi.org/10.1016/j.watres.2016.02.047

Barbosa, O., Ortiz, C., Berenguer-Murcia, Á., Torres, R., C. Rodrigues, R., Fernandez-Lafuente, R., 2014. Glutaraldehyde in bio-catalysts design: a useful crosslinker and a versatile tool in enzyme immobilization. RSC Advances 4, 1583–1600. https://doi.org/10.1039/C3RA45991H

Barbosa, O., Torres, R., Ortiz, C., Berenguer-Murcia, Á., Rodrigues, R.C., Fernandez-Lafuente, R., 2013. Heterofunctional Supports in Enzyme Immobilization: From Traditional Immobilization Protocols to Opportunities in Tuning Enzyme Properties. Biomacromolecules 14, 2433–2462. https://doi.org/10.1021/bm400762h

Barrios-Estrada, C., de Jesús Rostro-Alanis, M., Muñoz-Gutiérrez, B.D., Iqbal, H.M.N., Kannan, S., Parra-Saldívar, R., 2018a. Emergent contaminants: Endocrine disruptors and their laccase-assisted degradation – A review. Science of The Total Environment 612, 1516–1531. https://doi.org/10.1016/J.SCITOTENV.2017.09.013

Barrios-Estrada, C., Rostro-Alanis, M. de J., Parra, A.L., Belleville, M.-P., Sanchez-Marcano, J., Iqbal, H.M.N., Parra-Saldívar, R., 2018b. Potentialities of active membranes with immobilized laccase for Bisphenol A degradation. International Journal of Biological Macromolecules 108, 837–844. https://doi.org/10.1016/j.ijbiomac.2017.10.177

Barth, M., Oeser, T., Wei, R., Then, J., Schmidt, J., Zimmermann, W., 2015. Effect of hydrolysis products on the enzymatic degradation of polyethylene terephthalate nanoparticles by a polyester hydrolase from Thermobifida fusca. Biochemical Engineering Journal 93, 222–228. https://doi.org/10.1016/j.bej.2014.10.012

Batt, A.L., Kim, S., Aga, D.S., 2007. Comparison of the occurrence of antibiotics in four full-scale wastewater treatment plants with varying designs and operations. Chemosphere 68, 428–435. https://doi.org/10.1016/j.chemosphere.2007.01.008

Bebić, J., Banjanac, K., Ćorović, M., Milivojević, A., Simović, M., Marinković, A., Bezbradica, D., 2020. Immobilization of laccase from Myceliophthora thermophila on functionalized silica nanoparticles: Optimization and application in lindane degradation. Chinese Journal of Chemical Engineering 28, 1136–1144. https://doi.org/10.1016/j.cjche.2019.12.025

Becker, D., Varela Della Giustina, S., Rodriguez-Mozaz, S., Schoevaart, R., Barceló, D., de Cazes, M., Belleville, M.P., Sanchez-Marcano, J., de Gunzburg, J., Couillerot, O., Völker, J., Oehlmann, J., Wagner, M., 2016. Removal of antibiotics in wastewater by enzymatic treatment with fungal laccase – Degradation of compounds does not always eliminate toxicity. Bioresource Technology 219, 500–509. https://doi.org/10.1016/j.biortech.2016.08.004

Biggelaar, L. van den, Soumillion, P., Debecker, D., 2019. Continuous Flow Mode Biocatalytic Transamination Using Macrocellular Silica Monoliths: Optimizing Support Functionalisation and Enzyme Grafting. https://doi.org/10.26434/chemrxiv.7853552.v1

Bilal, M., Iqbal, H.M.N., 2019. Lignin peroxidase immobilization on Ca-alginate beads and its dye degradation performance in a packed bed reactor system. Biocatalysis and Agricultural Biotechnology 20, 101205. https://doi.org/10.1016/j.bcab.2019.101205

Bilal, M., Rasheed, T., Nabeel, F., Iqbal, H.M.N., Zhao, Y., 2019. Hazardous contaminants in the environment and their laccase-assisted degradation – A review. Journal of Environmental Management 234, 253–264. https://doi.org/10.1016/j.jenvman.2019.01.001

Björlenius, B., Ripszám, M., Haglund, P., Lindberg, R.H., Tysklind, M., Fick, J., 2018. Pharmaceutical residues are widespread in Baltic Sea coastal and offshore waters – Screening for pharmaceuticals and modelling of environmental concentrations of carbamazepine. Science of The Total Environment 633, 1496–1509. https://doi.org/10.1016/j.scitotenv.2018.03.276

Blair, B., Nikolaus, A., Hedman, C., Klaper, R., Grundl, T., 2015. Evaluating the degradation, sorption, and negative mass balances of pharmaceuticals and personal care products during wastewater treatment. Chemosphere 134, 395–401. https://doi.org/10.1016/j.chemosphere.2015.04.078

Blasco, J., Chapman, P.M., Campana, O., Hampel, M., 2016. Marine Ecotoxicology: Current Knowledge and Future Issues. Academic Press.

Boudrant, J., Woodley, J.M., Fernandez-Lafuente, R., 2020a. Parameters necessary to define an immobilized enzyme preparation. Process Biochemistry 90, 66–80. https://doi.org/10.1016/j.procbio.2019.11.026

Boudrant, J., Woodley, J.M., Fernandez-Lafuente, R., 2020b. Parameters necessary to define an immobilized enzyme preparation. Process Biochemistry 90, 66–80. https://doi.org/10.1016/j.procbio.2019.11.026

Boulard, L., Dierkes, G., Schlüsener, M.P., Wick, A., Koschorreck, J., Ternes, T.A., 2020. Spatial distribution and temporal trends of pharmaceuticals sorbed to suspended

particulate matter of German rivers. Water Research 171, 115366. https://doi.org/10.1016/j.watres.2019.115366

Brodin, T., Fick, J., Jonsson, M., Klaminder, J., 2013. Dilute Concentrations of a Psychiatric Drug Alter Behavior of Fish from Natural Populations. Science 339, 814–815. https://doi.org/10.1126/science.1226850

Bruce, G.M., Pleus, R.C., Snyder, S.A., 2010. Toxicological Relevance of Pharmaceuticals in Drinking Water. Environ. Sci. Technol. 44, 5619–5626. https://doi.org/10.1021/es1004895

Brun, N., Ungureanu, S., Deleuze, H., Backov, R., 2011. Hybrid foams, colloids and beyond: From design to applications. Chemical Society Reviews 40, 771–788. https://doi.org/10.1039/B920518G

Bu, Q., Wang, B., Huang, J., Deng, S., Yu, G., 2013. Pharmaceuticals and personal care products in the aquatic environment in China: A review. Journal of Hazardous Materials 262, 189–211. https://doi.org/10.1016/j.jhazmat.2013.08.040

Burch, K.D., Han, B., Pichtel, J., Zubkov, T., 2019. Removal efficiency of commonly prescribed antibiotics via tertiary wastewater treatment. Environ Sci Pollut Res 26, 6301–6310. https://doi.org/10.1007/s11356-019-04170-w

Burghardt, A., 1986. Transport phenomena and chemical reactions in porous catalysts for multicomponent and multireaction systems. Chemical Engineering and Processing: Process Intensification 20, 229–244. https://doi.org/10.1016/0255-2701(86)80016-2

Burns, E.E., Carter, L.J., Kolpin, D.W., Thomas-Oates, J., Boxall, A.B.A., 2018. Temporal and spatial variation in pharmaceutical concentrations in an urban river system. Water Research 137, 72–85. https://doi.org/10.1016/j.watres.2018.02.066

Cabana, H., Alexandre, C., Agathos, S.N., Jones, J.P., 2009. Immobilization of laccase from the white rot fungus Coriolopsis polyzona and use of the immobilized biocatalyst for the continuous elimination of endocrine disrupting chemicals. Bioresource Technology 100, 3447–3458. https://doi.org/10.1007/s10103-009-0744-6

Cabana, H., Jiwan, J.L.H., Rozenberg, R., Elisashvili, V., Penninckx, M., Agathos, S.N., Jones, J.P., 2007. Elimination of endocrine disrupting chemicals nonylphenol and bisphenol A and personal care product ingredient triclosan using enzyme preparation from the white rot fungus Coriolopsis polyzona. Chemosphere 67, 770–778. https://doi.org/10.1016/j.chemosphere.2006.10.037

Calza, P., Zacchigna, D., Laurenti, E., 2016. Degradation of orange dyes and carbamazepine by soybean peroxidase immobilized on silica monoliths and titanium dioxide. Environ Sci Pollut Res 23, 23742–23749. https://doi.org/10.1007/s11356-016-7399-1

Carlsson, C., Johansson, A.-K., Alvan, G., Bergman, K., Kühler, T., 2006. Are pharmaceuticals potent environmental pollutants?: Part I: Environmental risk assessments of selected active pharmaceutical ingredients. Science of The Total Environment 364, 67–87. https://doi.org/10.1016/j.scitotenv.2005.06.035

Castiglioni, S., Zuccato, E., Fattore, E., Riva, F., Terzaghi, E., Koenig, R., Principi, P., Di Guardo, A., 2020. Micropollutants in Lake Como water in the context of circular economy: A snapshot of water cycle contamination in a changing pollution scenario. Journal of Hazardous Materials 384, 121441. https://doi.org/10.1016/j.jhazmat.2019.121441

Catherine, H., Penninckx, M., Frédéric, D., 2016. Product formation from phenolic compounds removal by laccases: A review. Environmental Technology & Innovation 5, 250–266. https://doi.org/10.1016/j.eti.2016.04.001

Charuaud, L., Jardé, E., Jaffrézic, A., Liotaud, M., Goyat, Q., Mercier, F., Le Bot, B., 2019. Veterinary pharmaceutical residues in water resources and tap water in an intensive husbandry area in France. Science of The Total Environment 664, 605–615. https://doi.org/10.1016/j.scitotenv.2019.01.303

Cho, H.-H., Huang, H., Schwab, K., 2011. Effects of Solution Chemistry on the Adsorption of Ibuprofen and Triclosan onto Carbon Nanotubes. Langmuir 27, 12960–12967. https://doi.org/10.1021/la202459g

Choi, P.M., Tscharke, B.J., Donner, E., O'Brien, J.W., Grant, S.C., Kaserzon, S.L., Mackie, R., O'Malley, E., Crosbie, N.D., Thomas, K.V., Mueller, J.F., 2018. Wastewater-based epidemiology biomarkers: Past, present and future. TrAC Trends in Analytical Chemistry 105, 453–469. https://doi.org/10.1016/j.trac.2018.06.004

Comiti, J., Renaud, M., 1989. A new model for determining mean structure parameters of fixed beds from pressure drop measurements: application to beds packed with parallelepipedal particles. Chemical Engineering Science 44, 1539–1545. https://doi.org/10.1016/0009-2509(89)80031-4

Coutu, S., Wyrsch, V., Wynn, H.K., Rossi, L., Barry, D.A., 2013. Temporal dynamics of antibiotics in wastewater treatment plant influent. Science of The Total Environment 458–460, 20–26. https://doi.org/10.1016/j.scitotenv.2013.04.017

Dai, Y., Yao, J., Song, Y., Wang, S., Yuan, Y., 2016. Enhanced adsorption and degradation of phenolic pollutants in water by carbon nanotube modified laccase-carrying electrospun fibrous membranes. Environmental Science: Nano 3, 857–868. https://doi.org/10.1039/C6EN00148C

Danner, M.-C., Robertson, A., Behrends, V., Reiss, J., 2019. Antibiotic pollution in surface fresh waters: Occurrence and effects. Science of The Total Environment 664, 793–804. https://doi.org/10.1016/j.scitotenv.2019.01.406

Dantas Renato F., Sans Carme, Esplugas Santiago, 2011. Ozonation of Propranolol: Transformation, Biodegradability, and Toxicity Assessment. Journal of Environmental Engineering 137, 754–759. https://doi.org/10.1061/(ASCE)EE.1943-7870.0000377

Davididou, K., Monteagudo, J.M., Chatzisymeon, E., Durán, A., Expósito, A.J., 2017. Degradation and mineralization of antipyrine by UV-A LED photo-Fenton reaction intensified by ferrioxalate with addition of persulfate. Separation and Purification Technology 172, 227–235. https://doi.org/10.1016/j.seppur.2016.08.021

De Cazes, M., Abejón, R., Belleville, M.-P., Sanchez-Marcano, J., 2014. Membrane Bioprocesses for Pharmaceutical Micropollutant Removal from Waters. Membranes 4, 692–729. https://doi.org/10.3390/membranes4040692

de Cazes, M., Belleville, M.-P., Mougel, M., Kellner, H., Sanchez-Marcano, J., 2015. Characterization of laccase-grafted ceramic membranes for pharmaceuticals degradation. Journal of Membrane Science 476, 384–393. https://doi.org/10.1016/j.memsci.2014.11.044

de Cazes, M., Belleville, M.-P., Petit, E., Llorca, M., Rodríguez-Mozaz, S., de Gunzburg, J., Barceló, D., Sanchez-Marcano, J., 2014. Design and optimization of an enzymatic

membrane reactor for tetracycline degradation. Catalysis Today, Proceedings of the 11th International Conference on Catalysis in Membrane Reactors 236, 146–152. https://doi.org/10.1016/j.cattod.2014.02.051

de Jongh, C.M., Kooij, P.J.F., de Voogt, P., ter Laak, T.L., 2012. Screening and human health risk assessment of pharmaceuticals and their transformation products in Dutch surface waters and drinking water. Science of The Total Environment 427–428, 70–77. https://doi.org/10.1016/j.scitotenv.2012.04.010

Debecker, D.P., 2018. Innovative Sol-Gel Routes for the Bottom-Up Preparation of Heterogeneous Catalysts. The Chemical Record 18, 662–675. https://doi.org/10.1002/tcr.201700068

Demarche, P., Junghanns, C., Nair, R.R., Agathos, S.N., 2012. Harnessing the power of enzymes for environmental stewardship. Biotechnology Advances 30, 933–953. https://doi.org/10.1016/j.biotechadv.2011.05.013

Directive, W.F., 2000. Directive 2000/60/EC of the European Parliament and of the Council of 23 October 2000 establishing a framework for Community action in the field of water policy. Official journal of the European communities 22, 2000.

Durán, N., Rosa, M.A., D'Annibale, A., Gianfreda, L., 2002. Applications of laccases and tyrosinases (phenoloxidases) immobilized on different supports: a review. Enzyme and Microbial Technology 31, 907–931. https://doi.org/10.1016/S0141-0229(02)00214-4

Ebele, A.J., Abou-Elwafa Abdallah, M., Harrad, S., 2017. Pharmaceuticals and personal care products (PPCPs) in the freshwater aquatic environment. Emerging Contaminants 3, 1–16. https://doi.org/10.1016/j.emcon.2016.12.004

Faccio, G., Kruus, K., Saloheimo, M., Thöny-Meyer, L., 2012. Bacterial tyrosinases and their applications. Process Biochemistry 47, 1749–1760. https://doi.org/10.1016/j.procbio.2012.08.018

Fairhead, M., Thöny-Meyer, L., 2012. Bacterial tyrosinases: old enzymes with new relevance to biotechnology. New Biotechnology, Industrial Biotechnology 29, 183–191. https://doi.org/10.1016/j.nbt.2011.05.007

Fletcher, P.D.I., Haswell, S.J., He, P., Kelly, S.M., Mansfield, A., 2011. Permeability of silica monoliths containing micro- and nano-pores. J Porous Mater 18, 501–508. https://doi.org/10.1007/s10934-010-9403-3

Galarneau, A., Sachse, A., Said, B., Pelisson, C.-H., Boscaro, P., Brun, N., Courtheoux, L., Olivi-Tran, N., Coasne, B., Fajula, F., 2016a. Hierarchical porous silica monoliths: A novel class of microreactors for process intensification in catalysis and adsorption. Comptes Rendus Chimie, Emerging Chemistry in France 19, 231–247. https://doi.org/10.1016/j.crci.2015.05.017

Galarneau, A., Sachse, A., Said, B., Pelisson, C.-H., Boscaro, P., Brun, N., Courtheoux, L., Olivi-Tran, N., Coasne, B., Fajula, F., 2016b. Hierarchical porous silica monoliths: A novel class of microreactors for process intensification in catalysis and adsorption. Comptes Rendus Chimie, Emerging Chemistry in France 19, 231–247. https://doi.org/10.1016/j.crci.2015.05.017

Gamallo, M., Moldes-Diz, Y., Eibes, G., Feijoo, G., Lema, J.M., Moreira, M.T., 2018. Sequential reactors for the removal of endocrine disrupting chemicals by laccase

immobilized onto fumed silica microparticles. Biocatalysis and Biotransformation 36, 254–264. https://doi.org/10.1080/10242422.2017.1316489

Gao, N., Liu, C.X., Xu, Q.M., Cheng, J.S., Yuan, Y.J., 2018. Simultaneous removal of ciprofloxacin, norfloxacin, sulfamethoxazole by co-producing oxidative enzymes system of Phanerochaete chrysosporium and Pycnoporus sanguineus. Chemosphere 195, 146–155. https://doi.org/10.1016/j.chemosphere.2017.12.062

García Galán, M.J., Díaz-Cruz, M.S., Barceló, D., 2012. Removal of sulfonamide antibiotics upon conventional activated sludge and advanced membrane bioreactor treatment. Anal Bioanal Chem 404, 1505–1515. https://doi.org/10.1007/s00216-012-6239-5

García-Morales, R., García-García, A., Orona-Navar, C., Osma, J.F., Nigam, K.D.P., Ornelas-Soto, N., 2018. Biotransformation of emerging pollutants in groundwater by laccase from P. sanguineus CS43 immobilized onto titania nanoparticles. Journal of Environmental Chemical Engineering 6, 710–717. https://doi.org/10.1016/j.jece.2017.12.006

Gasser, C.A., Ammann, E.M., Shahgaldian, P., Corvini, P.F.X., 2014. Laccases to take on the challenge of emerging organic contaminants in wastewater. Applied Microbiology and Biotechnology 98, 9931–9952. https://doi.org/10.1007/s00253-014-6177-6

George, A., Radhakrishnan, G.A., Joseph, K.T., 1984a. Grafting of Acrylonitrile onto Gelatin in Zinc Chloride Medium. Journal of Macromolecular Science: Part A - Chemistry 21, 179–191. https://doi.org/10.1080/00222338408056547

George, A., Radhakrishnan, G.A., Joseph, K.T., 1984b. Grafting of Acrylonitrile onto Gelatin in Zinc Chloride Medium. Journal of Macromolecular Science: Part A - Chemistry 21, 179–191. https://doi.org/10.1080/00222338408056547

Gerrity, D., Trenholm, R.A., Snyder, S.A., 2011. Temporal variability of pharmaceuticals and illicit drugs in wastewater and the effects of a major sporting event. Water Research 45, 5399–5411. https://doi.org/10.1016/j.watres.2011.07.020

Ghosh, G.C., Okuda, T., Yamashita, N., Tanaka, H., 2009. Occurrence and elimination of antibiotics at four sewage treatment plants in Japan and their effects on bacterial ammonia oxidation. Water Sci Technol 59, 779–786. https://doi.org/10.2166/wst.2009.067

Giger, W., Alder, A.C., Golet, E.M., Kohler, H.-P.E., McArdell, C.S., Molnar, E., Siegrist, H., Suter, M.J.-F., 2003. Occurrence and Fate of Antibiotics as Trace Contaminants in Wastewaters, Sewage Sludges, and Surface Waters. chimia (aarau) 57, 485–491. https://doi.org/10.2533/000942903777679064

Giraldo-Aguirre, A.L., Serna-Galvis, E.A., Erazo-Erazo, E.D., Silva-Agredo, J., Giraldo-Ospina, H., Flórez-Acosta, O.A., Torres-Palma, R.A., 2018. Removal of β-lactam antibiotics from pharmaceutical wastewaters using photo-Fenton process at near-neutral pH. Environ Sci Pollut Res 25, 20293–20303. https://doi.org/10.1007/s11356-017-8420-z

Göbel, A., McArdell, C.S., Joss, A., Siegrist, H., Giger, W., 2007. Fate of sulfonamides, macrolides, and trimethoprim in different wastewater treatment technologies. Science of The Total Environment 372, 361–371. https://doi.org/10.1016/j.scitotenv.2006.07.039

Goi, A., 2005. Advanced oxidation processes for water purification and soil remediation, Thesis on chemistry and chemical engineering. TTU Press, Tallinn.

Golet, E.M., Xifra, I., Siegrist, H., Alder, A.C., Giger, W., 2003. Environmental Exposure Assessment of Fluoroquinolone Antibacterial Agents from Sewage to Soil. Environ. Sci. Technol. 37, 3243–3249. https://doi.org/10.1021/es0264448

Gómez-Canela, C., Pueyo, V., Barata, C., Lacorte, S., Marcé, R.M., 2019. Development of predicted environmental concentrations to prioritize the occurrence of pharmaceuticals in rivers from Catalonia. Science of The Total Environment 666, 57–67. https://doi.org/10.1016/j.scitotenv.2019.02.078

Grandclément, C., Seyssiecq, I., Piram, A., Wong-Wah-Chung, P., Vanot, G., Tiliacos, N., Roche, N., Doumenq, P., 2017. From the conventional biological wastewater treatment to hybrid processes, the evaluation of organic micropollutant removal: A review. Water Research 111, 297–317. https://doi.org/10.1016/j.watres.2017.01.005

Gulkowska, A., Leung, H.W., So, M.K., Taniyasu, S., Yamashita, N., Yeung, L.W.Y., Richardson, B.J., Lei, A.P., Giesy, J.P., Lam, P.K.S., 2008. Removal of antibiotics from wastewater by sewage treatment facilities in Hong Kong and Shenzhen, China. Water Research 42, 395–403. https://doi.org/10.1016/j.watres.2007.07.031

Guo, X.L., Zhu, Z.W., Li, H.L., 2014. Biodegradation of sulfamethoxazole by Phanerochaete chrysosporium. Journal of Molecular Liquids 198, 169–172. https://doi.org/10.1016/j.molliq.2014.06.017

Haas, C.P., Müllner, T., Kohns, R., Enke, D., Tallarek, U., 2017. High-performance monoliths in heterogeneous catalysis with single-phase liquid flow. React. Chem. Eng. 2, 498–511. https://doi.org/10.1039/C7RE00042A

Hai, F.I., Li, X., Price, W.E., Nghiem, L.D., 2011. Removal of carbamazepine and sulfamethoxazole by MBR under anoxic and aerobic conditions. Bioresource Technology 102, 10386–10390. https://doi.org/10.1016/j.biortech.2011.09.019

Halling-Sørensen, B., Nors Nielsen, S., Lanzky, P.F., Ingerslev, F., Holten Lützhøft, H.C., Jørgensen, S.E., 1998. Occurrence, fate and effects of pharmaceutical substances in the environment- A review. Chemosphere 36, 357–393. https://doi.org/10.1016/S0045-6535(97)00354-8

Hamdan, M.H., 1994. Single-phase flow through porous channels a review of flow models and channel entry conditions. Applied Mathematics and Computation 62, 203–222. https://doi.org/10.1016/0096-3003(94)90083-3

Hlushkou, D., Bruns, S., Tallarek, U., 2010. High-performance computing of flow and transport in physically reconstructed silica monoliths. Journal of Chromatography A 1217, 3674–3682. https://doi.org/10.1016/j.chroma.2010.04.004

Hoarau, M., Badieyan, S., Marsh, E.N.G., 2017. Immobilized enzymes: understanding enzyme – surface interactions at the molecular level. Org. Biomol. Chem. 15, 9539–9551. https://doi.org/10.1039/C7OB01880K

Homem, V., Santos, L., 2011. Degradation and removal methods of antibiotics from aqueous matrices - A review. Journal of Environmental Management 92, 2304–2347. https://doi.org/10.1016/j.jenvman.2011.05.023

Hong, S.-G., Kim, B.C., Na, H.B., Lee, J., Youn, J., Chung, S.-W., Lee, C.-W., Lee, B., Kim, H.S., Hsiao, E., Kim, S.H., Kim, B.-G., Park, H.G., Chang, H.N., Hyeon, T., Dordick, J.S., Grate, J.W., Kim, J., 2017. Single enzyme nanoparticles armored by a thin silicate network: Single enzyme caged nanoparticles. Chemical Engineering Journal 322, 510–515. https://doi.org/10.1016/j.cej.2017.04.022

Hörsing, M., Ledin, A., Grabic, R., Fick, J., Tysklind, M., Jansen, J. la C., Andersen, H.R., 2011. Determination of sorption of seventy-five pharmaceuticals in sewage sludge. Water Research 45, 4470–4482. https://doi.org/10.1016/j.watres.2011.05.033

Hospido, A., Carballa, M., Moreira, M., Omil, F., Lema, J.M., Feijoo, G., 2010. Environmental assessment of anaerobically digested sludge reuse in agriculture: Potential impacts of emerging micropollutants. Water Research 44, 3225–3233. https://doi.org/10.1016/j.watres.2010.03.004

Hou, C., Ghéczy, N., Messmer, D., Szymańska, K., Adamcik, J., Mezzenga, R., Jarzębski, A.B., Walde, P., 2019. Stable Immobilization of Enzymes in a Macro- and Mesoporous Silica Monolith. ACS Omega 4, 7795–7806. https://doi.org/10.1021/acsomega.9b00286

Hu, J., Zhou, J., Zhou, S., Wu, P., Tsang, Y.F., 2018. Occurrence and fate of antibiotics in a wastewater treatment plant and their biological effects on receiving waters in Guizhou. Process Safety and Environmental Protection 113, 483–490. https://doi.org/10.1016/j.psep.2017.12.003

Hubbert, M.K., 1956. Darcy's Law and the Field Equations of the Flow of Underground Fluids. Transactions of the AIME 207, 222–239. https://doi.org/10.2118/749-G

Ikehata, K., Naghashkar, N.J., El-Din, M.G., 2006. Degradation of Aqueous Pharmaceuticals by Ozonation and Advanced Oxidation Processes: A Review. Ozone: Science & Engineering 28, 353–414. https://doi.org/10.1080/01919510600985937

Inoue, Y., Hata, T., Kawai, S., Okamura, H., Nishida, T., 2010. Elimination and detoxification of triclosan by manganese peroxidase from white rot fungus. Journal of Hazardous Materials 180, 764–767. https://doi.org/10.1016/j.jhazmat.2010.04.024

Ivanová, L., Mackuľak, T., Grabic, R., Golovko, O., Koba, O., Staňová, A.V., Szabová, P., Grenčíková, A., Bodík, I., 2018. Pharmaceuticals and illicit drugs – A new threat to the application of sewage sludge in agriculture. Science of The Total Environment 634, 606–615. https://doi.org/10.1016/j.scitotenv.2018.04.001

Iyer, P.V., Ananthanarayan, L., 2008. Enzyme stability and stabilization—Aqueous and non-aqueous environment. Process Biochemistry, Metabolic Engineering 43, 1019–1032. https://doi.org/10.1016/j.procbio.2008.06.004

J. Carter, L., Chefetz, B., Abdeen, Z., A. Boxall, A.B., 2019. Emerging investigator series: towards a framework for establishing the impacts of pharmaceuticals in wastewater irrigation systems on agro-ecosystems and human health. Environmental Science: Processes & Impacts 21, 605–622. https://doi.org/10.1039/C9EM00020H

Jelic, A., Gros, M., Ginebreda, A., Cespedes-Sánchez, R., Ventura, F., Petrovic, M., Barcelo, D., 2011. Occurrence, partition and removal of pharmaceuticals in sewage water and sludge during wastewater treatment. Water Research 45, 1165–1176. https://doi.org/10.1016/j.watres.2010.11.010

Ji, C., Hou, J., Chen, V., 2016a. Cross-linked carbon nanotubes-based biocatalytic membranes for micro-pollutants degradation: Performance, stability, and regeneration. Journal of Membrane Science 520, 869–880. https://doi.org/10.1016/j.memsci.2016.08.056

Ji, C., Hou, J., Wang, K., Zhang, Y., Chen, V., 2016b. Biocatalytic degradation of carbamazepine with immobilized laccase-mediator membrane hybrid reactor. Journal of Membrane Science 502, 11–20. https://doi.org/10.1016/j.memsci.2015.12.043

Ji, C., Hou, J., Wang, K., Zhang, Y., Chen, V., 2016c. Biocatalytic degradation of carbamazepine with immobilized laccase-mediator membrane hybrid reactor. Journal of Membrane Science 502, 11–20. https://doi.org/10.1016/j.memsci.2015.12.043

Ji, C., Nguyen, L.N., Hou, J., Hai, F.I., Chen, V., 2017. Direct immobilization of laccase on titania nanoparticles from crude enzyme extracts of P. ostreatus culture for micro-pollutant degradation. Separation and Purification Technology 178, 215–223. https://doi.org/10.1016/j.seppur.2017.01.043

Ji, L., Chen, W., Zheng, S., Xu, Z., Zhu, D., 2009. Adsorption of Sulfonamide Antibiotics to Multiwalled Carbon Nanotubes. Langmuir 25, 11608–11613. https://doi.org/10.1021/la9015838

Ji, L., Liu, F., Xu, Z., Zheng, S., Zhu, D., 2010. Adsorption of Pharmaceutical Antibiotics on Template-Synthesized Ordered Micro- and Mesoporous Carbons. Environ. Sci. Technol. 44, 3116–3122. https://doi.org/10.1021/es903716s

Jing, X., Zhang, X., Bao, J., 2009. Inhibition Performance of Lignocellulose Degradation Products on Industrial Cellulase Enzymes During Cellulose Hydrolysis. Appl Biochem Biotechnol 159, 696. https://doi.org/10.1007/s12010-009-8525-z

Jones, H.E., Hickman, M., Kasprzyk-Hordern, B., Welton, N.J., Baker, D.R., Ades, A.E., 2014. Illicit and pharmaceutical drug consumption estimated via wastewater analysis. Part B: Placing back-calculations in a formal statistical framework. Science of The Total Environment 487, 642–650. https://doi.org/10.1016/j.scitotenv.2014.02.101

Jones, O.A., Lester, J.N., Voulvoulis, N., 2005. Pharmaceuticals: a threat to drinking water? Trends in Biotechnology 23, 163–167. https://doi.org/10.1016/j.tibtech.2005.02.001

Jung, C., Son, A., Her, N., Zoh, K.-D., Cho, J., Yoon, Y., 2015. Removal of endocrine disrupting compounds, pharmaceuticals, and personal care products in water using carbon nanotubes: A review. Journal of Industrial and Engineering Chemistry 27, 1–11. https://doi.org/10.1016/j.jiec.2014.12.035

Jungreuthmayer, C., Steppert, P., Sekot, G., Zankel, A., Reingruber, H., Zanghellini, J., Jungbauer, A., 2015. The 3D pore structure and fluid dynamics simulation of macroporous monoliths: High permeability due to alternating channel width. Journal of Chromatography A 1425, 141–149. https://doi.org/10.1016/j.chroma.2015.11.026

Kanakaraju, D., Glass, B.D., Oelgemöller, M., 2018a. Advanced oxidation process-mediated removal of pharmaceuticals from water: A review. Journal of Environmental Management 219, 189–207. https://doi.org/10.1016/j.jenvman.2018.04.103

Kanakaraju, D., Glass, B.D., Oelgemoller, M., 2018b. Advanced oxidation process-mediated removal of pharmaceuticals from water : A review. Journal of Environmental Management 219, 189–207. https://doi.org/10.1016/j.jenvman.2018.04.103

Karam, J., Nicell, J.A., 1997. Potential Applications of Enzymes in Waste Treatment. Chem. Tech. Biotechnol 69, 141–153. https://doi.org/10.1002/(SICI)1097-4660(199706)69

Karthikeyan, K.G., Meyer, M.T., 2006. Occurrence of antibiotics in wastewater treatment facilities in Wisconsin, USA. Science of The Total Environment 361, 196–207. https://doi.org/10.1016/j.scitotenv.2005.06.030

Kerrigan, J.F., Sandberg, K.D., Engstrom, D.R., LaPara, T.M., Arnold, W.A., 2018. Sedimentary record of antibiotic accumulation in Minnesota Lakes. Science of The Total Environment 621, 970–979. https://doi.org/10.1016/j.scitotenv.2017.10.130

Kidd, K.A., Paterson, M.J., Rennie, M.D., Podemski, C.L., Findlay, D.L., Blanchfield, P.J., Liber, K., 2014. Direct and indirect responses of a freshwater food web to a potent synthetic oestrogen. Philosophical Transactions of the Royal Society B: Biological Sciences 369, 20130578. https://doi.org/10.1098/rstb.2013.0578

Kim, M.-K., Zoh, K.-D., Kim, M.-K., Zoh, K.-D., 2016. Occurrence and removals of micropollutants in water environment. Environmental Engineering Research 21, 319–332. https://doi.org/10.4491/eer.2016.115

Kim, S., Eichhorn, P., Jensen, J.N., Weber, A.S., Aga, D.S., 2005. Removal of Antibiotics in Wastewater: Effect of Hydraulic and Solid Retention Times on the Fate of Tetracycline in the Activated Sludge Process. Environ. Sci. Technol. 39, 5816–5823. https://doi.org/10.1021/es050006u

Kıdak, R., Doğan, Ş., 2018. Medium-high frequency ultrasound and ozone based advanced oxidation for amoxicillin removal in water. Ultrasonics Sonochemistry, SI: ESS-15, 2016, Istanbul 40, 131–139. https://doi.org/10.1016/j.ultsonch.2017.01.033

Klatte, S., Schaefer, H., Hempel, M., 2017. Pharmaceuticals in the environment – A short review on options to minimize the exposure of humans, animals and ecosystems. Sustainable Chemistry and Pharmacy 5, 61–66. https://doi.org/10.1016/j.scp.2016.07.001

Kumar, V.V., Cabana, H., 2016. Towards high potential magnetic biocatalysts for on-demand elimination of pharmaceuticals. Bioresource Technology 200, 81–89. https://doi.org/10.1016/J.BIORTECH.2015.09.100

Kurniawati, S., Nicell, J.A., 2007. Variable Stoichiometry during the Laccase-Catalyzed Oxidation of Aqueous Phenol. Biotechnology Progress 23, 389–397. https://doi.org/10.1021/bp060312r

Kyzas, G.Z., Koltsakidou, A., Nanaki, S.G., Bikiaris, D.N., Lambropoulou, D.A., 2015. Removal of beta-blockers from aqueous media by adsorption onto graphene oxide. Science of The Total Environment 537, 411–420. https://doi.org/10.1016/j.scitotenv.2015.07.144

Legrini, O., Oliveros, E., Braun, A.M., 1993. Photochemical processes for water treatment. Chem. Rev. 93, 671–698. https://doi.org/10.1021/cr00018a003

Levenspiel, O., 1999. Chemical reaction engineering, 3. ed. ed. Wiley, Hoboken, NJ.

Li, B., Zhang, T., 2011. Mass flows and removal of antibiotics in two municipal wastewater treatment plants. Chemosphere 83, 1284–1289. https://doi.org/10.1016/j.chemosphere.2011.03.002

Li, W., Shi, Y., Gao, L., Liu, J., Cai, Y., 2013. Occurrence, distribution and potential affecting factors of antibiotics in sewage sludge of wastewater treatment plants in China. Science of The Total Environment 445–446, 306–313. https://doi.org/10.1016/j.scitotenv.2012.12.050

Li, X., He, Q., Li, H., Gao, X., Hu, M., Li, S., Zhai, Q., Jiang, Y., Wang, X., 2017. Bioconversion of non-steroidal anti-inflammatory drugs diclofenac and naproxen by chloroperoxidase. Biochemical Engineering Journal 120, 7–16. https://doi.org/10.1016/j.bej.2016.12.018

Liang, S., Wu, X.-L., Xiong, J., Zong, M.-H., Lou, W.-Y., 2020. Metal-organic frameworks as novel matrices for efficient enzyme immobilization: An update review.

Coordination Chemistry Reviews 406, 213149. https://doi.org/10.1016/j.ccr.2019.213149

Lin, A.Y.-C., Tsai, Y.-T., 2009. Occurrence of pharmaceuticals in Taiwan's surface waters: Impact of waste streams from hospitals and pharmaceutical production facilities. Science of The Total Environment, Thematic Issue - BioMicroWorld Conference 407, 3793–3802. https://doi.org/10.1016/j.scitotenv.2009.03.009

Lindberg, R.H., Olofsson, U., Rendahl, P., Johansson, M.I., Tysklind, M., Andersson, B.A.V., 2006. Behavior of Fluoroquinolones and Trimethoprim during Mechanical, Chemical, and Active Sludge Treatment of Sewage Water and Digestion of Sludge. Environ. Sci. Technol. 40, 1042–1048. https://doi.org/10.1021/es0516211

Liu, F., Zhao, J., Wang, S., Du, P., Xing, B., 2014. Effects of Solution Chemistry on Adsorption of Selected Pharmaceuticals and Personal Care Products (PPCPs) by Graphenes and Carbon Nanotubes. Environ. Sci. Technol. 48, 13197–13206. https://doi.org/10.1021/es5034684

Liu, J., Luo, Q., Huang, Q., 2016. Removal of 17 β-estradiol from poultry litter via solid state cultivation of lignolytic fungi. Journal of Cleaner Production 139, 1400–1407. https://doi.org/10.1016/j.jclepro.2016.09.020

Liu, Z., Kanjo, Y., Mizutani, S., 2009. Removal mechanisms for endocrine disrupting compounds (EDCs) in wastewater treatment — physical means, biodegradation, and chemical advanced oxidation: A review. Science of The Total Environment 407, 731–748. https://doi.org/10.1016/j.scitotenv.2008.08.039

Llorca, M., Rodríguez-Mozaz, S., Couillerot, O., Panigoni, K., de Gunzburg, J., Bayer, S., Czaja, R., Barceló, D., 2015. Identification of new transformation products during enzymatic treatment of tetracycline and erythromycin antibiotics at laboratory scale by an on-line turbulent flow liquid-chromatography coupled to a high resolution mass spectrometer LTQ-Orbitrap. Chemosphere 119, 90–98. https://doi.org/10.1016/j.chemosphere.2014.05.072

Lloret, L., Eibes, G., Feijoo, G., Moreira, M.T., Lema, J.M., 2012. Continuous operation of a fluidized bed reactor for the removal of estrogens by immobilized laccase on Eupergit supports. Journal of Biotechnology, Current research and future perspectives of Applied Biotechnology 162, 404–406. https://doi.org/10.1016/j.jbiotec.2012.04.007

Lloret, L., Eibes, G., Lú-Chau, T.A., Moreira, M.T., Feijoo, G., Lema, J.M., 2010. Laccase-catalyzed degradation of anti-inflammatories and estrogens. Biochemical Engineering Journal 51, 124–131. https://doi.org/10.1016/j.bej.2010.06.005

Lonappan, L., Rouissi, T., Laadila, M.A., Brar, S.K., Hernandez Galan, L., Verma, M., Surampalli, R.Y., 2017. Agro-industrial-Produced Laccase for Degradation of Diclofenac and Identification of Transformation Products. ACS Sustainable Chemistry and Engineering 5, 5772–5781. https://doi.org/10.1021/acssuschemeng.7b00390

Luo, Y., Guo, W., Ngo, H.H., Nghiem, L.D., Hai, F.I., Zhang, J., Liang, S., Wang, X.C., 2014. A review on the occurrence of micropollutants in the aquatic environment and their fate and removal during wastewater treatment. Science of The Total Environment 473–474, 619–641. https://doi.org/10.1016/j.scitotenv.2013.12.065

Mailler, R., Gasperi, J., Coquet, Y., Deshayes, S., Zedek, S., Cren-Olivé, C., Cartiser, N., Eudes, V., Bressy, A., Caupos, E., Moilleron, R., Chebbo, G., Rocher, V., 2015.

Study of a large scale powdered activated carbon pilot: Removals of a wide range of emerging and priority micropollutants from wastewater treatment plant effluents. Water Research, Occurrence, fate, removal and assessment of emerging contaminants in water in the water cycle (from wastewater to drinking water) 72, 315–330. https://doi.org/10.1016/j.watres.2014.10.047

Malato, S., Blanco, J., Vidal, A., Richter, C., 2002. Photocatalysis with solar energy at a pilot-plant scale: an overview. Applied Catalysis B: Environmental 37, 1–15. https://doi.org/10.1016/S0926-3373(01)00315-0

Mallozzi, M., Leone, C., Manurita, F., Bellati, F., Caserta, D., 2017. Endocrine Disrupting Chemicals and Endometrial Cancer: An Overview of Recent Laboratory Evidence and Epidemiological Studies. Int J Environ Res Public Health 14. https://doi.org/10.3390/ijerph14030334

Mao, L., Huang, Q., Luo, Q., Lu, J., Yang, X., Gao, S., 2010. Ligninase-mediated removal of 17β-estradiol from water in the presence of natural organic matter: Efficiency and pathways. Chemosphere 80, 469–473. https://doi.org/10.1016/j.chemosphere.2010.03.054

Margot, J., Copin, P.-J., von Gunten, U., Barry, D.A., Holliger, C., 2015. Sulfamethoxazole and isoproturon degradation and detoxification by a laccase-mediator system: Influence of treatment conditions and mechanistic aspects. Biochemical Engineering Journal 103, 47–59. https://doi.org/10.1016/j.bej.2015.06.008

Margot, J., Maillard, J., Rossi, L., Barry, D.A., Holliger, C., 2013. Influence of treatment conditions on the oxidation of micropollutants by Trametes versicolor laccase. New Biotechnology 30, 803–813. https://doi.org/10.1016/j.nbt.2013.06.004

Martin-Laurent, F., Topp, E., Billet, L., Batisson, I., Malandain, C., Besse-Hoggan, P., Morin, S., Artigas, J., Bonnineau, C., Kergoat, L., Devers-Lamrani, M., Pesce, S., 2019. Environmental risk assessment of antibiotics in agroecosystems: ecotoxicological effects on aquatic microbial communities and dissemination of antimicrobial resistances and antibiotic biodegradation potential along the soil-water continuum. Environ Sci Pollut Res 26, 18930–18937. https://doi.org/10.1007/s11356-019-05122-0

Martínez, A.T., 2002. Molecular biology and structure-function of lignin-degrading heme peroxidases. Enzyme and Microbial Technology, Recent Advances in Lignin Biodegradation 30, 425–444. https://doi.org/10.1016/S0141-0229(01)00521-X

Mauret, E., Renaud, M., 1997. Transport phenomena in multi-particle systems—I. Limits of applicability of capillary model in high voidage beds-application to fixed beds of fibers and fluidized beds of spheres. Chemical Engineering Science 52, 1807–1817. https://doi.org/10.1016/S0009-2509(96)00499-X

Medina, J.D.C., Woiciechowski, A.L., Guimarães, L.R.C., Karp, S.G., Soccol, C. R., 2017. 10 - Peroxidases, in: Pandey, A., Negi, S., Soccol, Carlos Ricardo (Eds.), Current Developments in Biotechnology and Bioengineering. Elsevier, pp. 217–232. https://doi.org/10.1016/B978-0-444-63662-1.00010-5

Meinel, F., Ruhl, A.S., Sperlich, A., Zietzschmann, F., Jekel, M., 2014. Pilot-Scale Investigation of Micropollutant Removal with Granular and Powdered Activated Carbon. Water Air Soil Pollut 226, 2260. https://doi.org/10.1007/s11270-014-2260-y

Melo, C.F., Dezotti, M., 2013. Evaluation of a horseradish peroxidase-catalyzed process for triclosan removal and antibacterial activity reduction. Journal of Chemical Technology & Biotechnology 88, 930–936. https://doi.org/10.1002/jctb.3924

Meng, F., Zhang, S., Oh, Y., Zhou, Z., Shin, H.-S., Chae, S.-R., 2017. Fouling in membrane bioreactors: An updated review. Water Research 114, 151–180. https://doi.org/10.1016/j.watres.2017.02.006

Meyer, W., Reich, M., Beier, S., Behrendt, J., Gulyas, H., Otterpohl, R., 2016. Measured and predicted environmental concentrations of carbamazepine, diclofenac, and metoprolol in small and medium rivers in northern Germany. Environ Monit Assess 188, 487. https://doi.org/10.1007/s10661-016-5481-2

Meyers, J.J., Liapis, A.I., 1999. Network modeling of the convective flow and diffusion of molecules adsorbing in monoliths and in porous particles packed in a chromatographic column. Journal of Chromatography A 852, 3–23. https://doi.org/10.1016/S0021-9673(99)00443-4

Miao, X.-S., Bishay, F., Chen, M., Metcalfe, C.D., 2004. Occurrence of Antimicrobials in the Final Effluents of Wastewater Treatment Plants in Canada. Environ. Sci. Technol. 38, 3533–3541. https://doi.org/10.1021/es030653q

Michael, I., Hapeshi, E., Michael, C., Varela, A.R., Kyriakou, S., Manaia, C.M., Fatta-Kassinos, D., 2012. Solar photo-Fenton process on the abatement of antibiotics at a pilot scale: Degradation kinetics, ecotoxicity and phytotoxicity assessment and removal of antibiotic resistant enterococci. Water Research 46, 5621–5634. https://doi.org/10.1016/j.watres.2012.07.049

Migneault, I., Dartiguenave, C., Bertrand, M.J., Waldron, K.C., 2004. Glutaraldehyde: behavior in aqueous solution, reaction with proteins, and application to enzyme crosslinking. BioTechniques 37, 790–802. https://doi.org/10.2144/04375RV01

Mohammadi, M., As'habi, M.A., Salehi, P., Yousefi, M., Nazari, M., Brask, J., 2018. Immobilization of laccase on epoxy-functionalized silica and its application in biodegradation of phenolic compounds. International Journal of Biological Macromolecules 109, 443–447. https://doi.org/10.1016/j.ijbiomac.2017.12.102

Monsan, P., 1978. Optimization of glutaraldehyde activation of a support for enzyme immobilization. Journal of Molecular Catalysis 3, 371–384. https://doi.org/10.1016/0304-5102(78)80026-1

Morozova, O.V., Shumakovich, G.P., Gorbacheva, M.A., Shleev, S.V., Yaropolov, A.I., 2007. "Blue" laccases. Biochemistry Moscow 72, 1136–1150. https://doi.org/10.1134/S0006297907100112

Murugesan, K., Chang, Y.Y., Kim, Y.M., Jeon, J.R., Kim, E.J., Chang, Y.S., 2010. Enhanced transformation of triclosan by laccase in the presence of redox mediators. Water Research 44, 298–308. https://doi.org/10.1016/j.watres.2009.09.058

Naghdi, M., Taheran, M., Brar, S.K., Kermanshahi-pour, A., Verma, M., Surampalli, R.Y., 2018a. Removal of pharmaceutical compounds in water and wastewater using fungal oxidoreductase enzymes. Environmental Pollution 234, 190–213. https://doi.org/10.1016/j.envpol.2017.11.060

Naghdi, M., Taheran, M., Brar, S.K., Kermanshahi-pour, A., Verma, M., Surampalli, R.Y., 2018b. Biotransformation of Carbamazepine by Laccase-Mediator System: Kinetics,

by-products and toxicity assessment. Process Biochemistry 67, 147–154. https://doi.org/10.1016/j.procbio.2018.02.009

Naghdi, M., Taheran, M., Brar, S.K., Kermanshahi-pour, A., Verma, M., Surampalli, R.Y., 2018c. Removal of pharmaceutical compounds in water and wastewater using fungal oxidoreductase enzymes. Environ. Pollut. 234, 190–213. https://doi.org/10.1016/j.envpol.2017.11.060

Nguyen, K.L., Wernert, V., Lopes, A.M., Sorbier, L., Denoyel, R., 2020. Effect of tortuosity on diffusion of polystyrenes through chromatographic columns filled with fully porous and porous –shell particles and monoliths. Microporous and Mesoporous Materials 293, 109776. https://doi.org/10.1016/j.micromeso.2019.109776

Nguyen, L.N., Hai, F.I., Dosseto, A., Richardson, C., Price, W.E., Nghiem, L.D., 2016a. Continuous adsorption and biotransformation of micropollutants by granular activated carbon-bound laccase in a packed-bed enzyme reactor. Bioresource Technology, Special Issue on Challenges in Environmental Science and Engineering (CESE-2015) 210, 108–116. https://doi.org/10.1016/j.biortech.2016.01.014

Nguyen, L.N., Hai, F.I., Dosseto, A., Richardson, C., Price, W.E., Nghiem, L.D., 2016b. Continuous adsorption and biotransformation of micropollutants by granular activated carbon-bound laccase in a packed-bed enzyme reactor. Bioresource Technology 210, 108–116. https://doi.org/10.1016/j.biortech.2016.01.014

Nguyen, L.N., Hai, F.I., Price, W.E., Leusch, F.D.L., Roddick, F., Ngo, H.H., Guo, W., Magram, S.F., Nghiem, L.D., 2014. The effects of mediator and granular activated carbon addition on degradation of trace organic contaminants by an enzymatic membrane reactor. Bioresource Technology 167, 169–177. https://doi.org/10.1016/j.biortech.2014.05.125

Nguyen, T.-T., Bui, X.-T., Luu, V.-P., Nguyen, P.-D., Guo, W., Ngo, H.-H., 2017. Removal of antibiotics in sponge membrane bioreactors treating hospital wastewater: Comparison between hollow fiber and flat sheet membrane systems. Bioresource Technology, Special issue on Challenges in Environmental Science and Engineering, CESE-2016 240, 42–49. https://doi.org/10.1016/j.biortech.2017.02.118

Nilsen, E., Smalling, K.L., Ahrens, L., Gros, M., Miglioranza, K.S.B., Picó, Y., Schoenfuss, H.L., 2019. Critical review: Grand challenges in assessing the adverse effects of contaminants of emerging concern on aquatic food webs. Environmental Toxicology and Chemistry 38, 46–60. https://doi.org/10.1002/etc.4290

Nimni, M.E., Cheung, D., Strates, B., Kodama, M., Sheikh, K., 1987. Chemically modified collagen: A natural biomaterial for tissue replacement. Journal of Biomedical Materials Research 21, 741–771. https://doi.org/10.1002/jbm.820210606

Ortner, A., Huber, D., Haske-Cornelius, O., Weber, H.K., Hofer, K., Bauer, W., Nyanhongo, G.S., Guebitz, G.M., 2015. Laccase mediated oxidation of industrial lignins: Is oxygen limiting? Process Biochemistry 50, 1277–1283. https://doi.org/10.1016/j.procbio.2015.05.003

Palace, V.P., Evans, R.E., Wautier, K.G., Mills, K.H., Blanchfield, P.J., Park, B.J., Baron, C.L., Kidd, K.A., 2009. Interspecies differences in biochemical, histopathological, and population responses in four wild fish species exposed to ethynylestradiol added to a whole lakeThis paper is part of the series “Forty Years of Aquatic Research at the Experimental Lakes Area”. Can. J. Fish. Aquat. Sci. 66, 1920–1935. https://doi.org/10.1139/F09-125

Park, J., Yamashita, N., Wu, G., Tanaka, H., 2017. Removal of pharmaceuticals and personal care products by ammonia oxidizing bacteria acclimated in a membrane bioreactor: Contributions of cometabolism and endogenous respiration. Science of The Total Environment 605–606, 18–25. https://doi.org/10.1016/j.scitotenv.2017.06.155

Patel, S.K.S., Kalia, V.C., Choi, J.H., Haw, J.R., Kim, I.W., Lee, J.K., 2014. Immobilization of Laccase on SiO2 Nanocarriers Omproves Its Stability and Reusability. Journal of Microbiology and Biotechnology 24, 639–647. https://doi.org/10.4014/jmb.1401.01025

Perini, J.A.L., Tonetti, A.L., Vidal, C., Montagner, C.C., Nogueira, R.F.P., 2018. Simultaneous degradation of ciprofloxacin, amoxicillin, sulfathiazole and sulfamethazine, and disinfection of hospital effluent after biological treatment via photo-Fenton process under ultraviolet germicidal irradiation. Applied Catalysis B: Environmental 224, 761–771. https://doi.org/10.1016/j.apcatb.2017.11.021

P. Haas, C., Müllner, T., Kohns, R., Enke, D., Tallarek, U., 2017a. High-performance monoliths in heterogeneous catalysis with single-phase liquid flow. Reaction Chemistry & Engineering 2, 498–511. https://doi.org/10.1039/C7RE00042A

P. Haas, C., Müllner, T., Kohns, R., Enke, D., Tallarek, U., 2017b. High-performance monoliths in heterogeneous catalysis with single-phase liquid flow. Reaction Chemistry & Engineering 2, 498–511. https://doi.org/10.1039/C7RE00042A

Phonsiri, V., Choi, S., Nguyen, C., Tsai, Y.-L., Coss, R., Kurwadkar, S., 2019. Monitoring occurrence and removal of selected pharmaceuticals in two different wastewater treatment plants. SN Appl. Sci. 1, 798. https://doi.org/10.1007/s42452-019-0774-z

Piao, M., Zou, D., Ren, X., Gao, S., Qin, C., Piao, Y., 2019. High efficiency biotransformation of bisphenol A in a fluidized bed reactor using stabilized laccase in porous silica. Enzyme and Microbial Technology 126, 1–8. https://doi.org/10.1016/j.enzmictec.2019.03.006

Pico, Y., Belenguer, V., Corcellas, C., Diaz-Cruz, M.S., Eljarrat, E., Farré, M., Gago-Ferrero, P., Huerta, B., Navarro-Ortega, A., Petrovic, M., Rodríguez-Mozaz, S., Sabater, L., Santín, G., Barcelo, D., 2019. Contaminants of emerging concern in freshwater fish from four Spanish Rivers. Science of The Total Environment 659, 1186–1198. https://doi.org/10.1016/j.scitotenv.2018.12.366

Prabhasankar, V.P., Joshua, D.I., Balakrishna, K., Siddiqui, I.F., Taniyasu, S., Yamashita, N., Kannan, K., Akiba, M., Praveenkumarreddy, Y., Guruge, K.S., 2016. Removal rates of antibiotics in four sewage treatment plants in South India. Environ Sci Pollut Res 23, 8679–8685. https://doi.org/10.1007/s11356-015-5968-3

Prasertkulsak, S., Chiemchaisri, C., Chiemchaisri, W., Itonaga, T., Yamamoto, K., 2016. Removals of pharmaceutical compounds from hospital wastewater in membrane bioreactor operated under short hydraulic retention time. Chemosphere 150, 624–631. https://doi.org/10.1016/j.chemosphere.2016.01.031

Prieto, A., Möder, M., Rodil, R., Adrian, L., Marco-Urrea, E., 2011. Degradation of the antibiotics norfloxacin and ciprofloxacin by a white-rot fungus and identification of degradation products. Bioresource Technology 102, 10987–10995. https://doi.org/10.1016/j.biortech.2011.08.055

Radjenović, J., Petrović, M., Barceló, D., 2009. Fate and distribution of pharmaceuticals in wastewater and sewage sludge of the conventional activated sludge (CAS) and

advanced membrane bioreactor (MBR) treatment. Water Research 43, 831–841. https://doi.org/10.1016/j.watres.2008.11.043

Rahmani, K., Faramarzi, M.A., Mahvi, A.H., Gholami, M., Esrafili, A., Forootanfar, H., Farzadkia, M., 2015. Elimination and detoxification of sulfathiazole and sulfamethoxazole assisted by laccase immobilized on porous silica beads. International Biodeterioration and Biodegradation 97, 107–114. https://doi.org/10.1016/j.ibiod.2014.10.018

Rajapaksha, A.U., Dilrukshi Premarathna, K.S., Gunarathne, V., Ahmed, A., Vithanage, M., 2019. 9 - Sorptive removal of pharmaceutical and personal care products from water and wastewater, in: Prasad, M.N.V., Vithanage, M., Kapley, A. (Eds.), Pharmaceuticals and Personal Care Products: Waste Management and Treatment Technology. Butterworth-Heinemann, pp. 213–238. https://doi.org/10.1016/B978-0-12-816189-0.00009-3

Ramírez-Cavazos, L.I., Junghanns, C., Ornelas-Soto, N., Cárdenas-Chávez, D.L., Hernández-Luna, C., Demarche, P., Enaud, E., García-Morales, R., Agathos, S.N., Parra, R., 2014a. Purification and characterization of two thermostable laccases from Pycnoporus sanguineus and potential role in degradation of endocrine disrupting chemicals. Journal of Molecular Catalysis B: Enzymatic 108, 32–42. https://doi.org/10.1016/j.molcatb.2014.06.006

Ramírez-Cavazos, L.I., Junghanns, C., Ornelas-Soto, N., Cárdenas-Chávez, D.L., Hernández-Luna, C., Demarche, P., Enaud, E., García-Morales, R., Agathos, S.N., Parra, R., 2014b. Purification and characterization of two thermostable laccases from Pycnoporus sanguineus and potential role in degradation of endocrine disrupting chemicals. Journal of Molecular Catalysis B: Enzymatic 108, 32–42. https://doi.org/10.1016/j.molcatb.2014.06.006

Riaz, L., Mahmood, T., Khalid, A., Rashid, A., Ahmed Siddique, M.B., Kamal, A., Coyne, M.S., 2018. Fluoroquinolones (FQs) in the environment: A review on their abundance, sorption and toxicity in soil. Chemosphere 191, 704–720. https://doi.org/10.1016/j.chemosphere.2017.10.092

Rivera-Utrilla, J., Sánchez-Polo, M., Ferro-García, M.Á., Prados-Joya, G., Ocampo-Pérez, R., 2013. Pharmaceuticals as emerging contaminants and their removal from water. A review. Chemosphere 93, 1268–1287. https://doi.org/10.1016/j.chemosphere.2013.07.059

Rizzo, L., Fiorentino, A., Grassi, M., Attanasio, D., Guida, M., 2015. Advanced treatment of urban wastewater by sand filtration and graphene adsorption for wastewater reuse: Effect on a mixture of pharmaceuticals and toxicity. Journal of Environmental Chemical Engineering 3, 122–128. https://doi.org/10.1016/j.jece.2014.11.011

Roberts, J., Kumar, A., Du, J., Hepplewhite, C., Ellis, D.J., Christy, A.G., Beavis, S.G., 2016. Pharmaceuticals and personal care products (PPCPs) in Australia's largest inland sewage treatment plant, and its contribution to a major Australian river during high and low flow. Science of The Total Environment 541, 1625–1637. https://doi.org/10.1016/j.scitotenv.2015.03.145

Rocha, L.S., Pereira, D., Sousa, É., Otero, M., Esteves, V.I., Calisto, V., 2020. Recent advances on the development and application of magnetic activated carbon and char for the removal of pharmaceutical compounds from waters: A review. Science of The Total Environment 718, 137272. https://doi.org/10.1016/j.scitotenv.2020.137272

Rodriguez, E., Campinas, M., Acero, J.L., Rosa, M.J., 2016. Investigating PPCP Removal from Wastewater by Powdered Activated Carbon/Ultrafiltration. Water Air Soil Pollut 227, 177. https://doi.org/10.1007/s11270-016-2870-7

Rodríguez-Delgado, M., Orona-Navar, C., García-Morales, R., Hernandez-Luna, C., Parra, R., Mahlknecht, J., Ornelas-Soto, N., 2016. Biotransformation kinetics of pharmaceutical and industrial micropollutants in groundwaters by a laccase cocktail from Pycnoporus sanguineus CS43 fungi. International Biodeterioration and Biodegradation 108, 34–41. https://doi.org/10.1016/j.ibiod.2015.12.003

Saaristo, M., Brodin, T., Balshine, S., Bertram, M.G., Brooks, B.W., Ehlman, S.M., McCallum, E.S., Sih, A., Sundin, J., Wong, B.B.M., Arnold, K.E., 2018. Direct and indirect effects of chemical contaminants on the behaviour, ecology and evolution of wildlife. Proceedings of the Royal Society B: Biological Sciences 285, 20181297. https://doi.org/10.1098/rspb.2018.1297

Sachse, A., Galarneau, A., Fajula, F., Di Renzo, F., Creux, P., Coq, B., 2011. Functional silica monoliths with hierarchical uniform porosity as continuous flow catalytic reactors. Microporous and Mesoporous Materials, High Surface Area Porous Materials 140, 58–68. https://doi.org/10.1016/j.micromeso.2010.10.044

Sadeghzadeh, S., Ghobadi Nejad, Z., Ghasemi, S., Khafaji, M., Borghei, S.M., 2020. Removal of bisphenol A in aqueous solution using magnetic cross-linked laccase aggregates from Trametes hirsuta. Bioresource Technology 306, 123169. https://doi.org/10.1016/j.biortech.2020.123169

Salai Mathi Selvi, M., Hariharan, G., Kannan, K., Heydari, M.H., 2018. Two reliable computational methods pertaining to steady state substrate concentration of an immobilized enzyme system. Alexandria Engineering Journal 57, 2377–2385. https://doi.org/10.1016/j.aej.2017.09.012

Sathishkumar, P., Chae, J.C., Unnithan, A.R., Palvannan, T., Kim, H.Y., Lee, K.J., Cho, M., Kamala-Kannan, S., Oh, B.T., 2012. Laccase-poly(lactic-co-glycolic acid) (PLGA) nanofiber: Highly stable, reusable, and efficacious for the transformation of diclofenac. Enzyme and Microbial Technology 51, 113–118. https://doi.org/10.1016/j.enzmictec.2012.05.001

Secundo, F., 2013. Conformational changes of enzymes upon immobilisation. Chemical Society Reviews 42, 6250–6261. https://doi.org/10.1039/C3CS35495D

Senthivelan, T., Kanagaraj, J., Panda, R.C., 2016. Recent trends in fungal laccase for various industrial applications: An eco-friendly approach - A review. Biotechnol Bioproc E 21, 19–38. https://doi.org/10.1007/s12257-015-0278-7

Sharma, B.M., Bečanová, J., Scheringer, M., Sharma, A., Bharat, G.K., Whitehead, P.G., Klánová, J., Nizzetto, L., 2019. Health and ecological risk assessment of emerging contaminants (pharmaceuticals, personal care products, and artificial sweeteners) in surface and groundwater (drinking water) in the Ganges River Basin, India. Science of The Total Environment 646, 1459–1467. https://doi.org/10.1016/j.scitotenv.2018.07.235

Sheldon, R.A., 2007. Enzyme immobilization: The quest for optimum performance. Advanced Synthesis and Catalysis 349, 1289–1307. https://doi.org/10.1002/adsc.200700082

Sheng, B., Cong, H., Zhang, S., Meng, F., 2018. Interactive effects between tetracycline and nitrosifying sludge microbiota in a nitritation membrane bioreactor. Chemical Engineering Journal 341, 556–564. https://doi.org/10.1016/j.cej.2018.02.013

Shi, B.-J., Wang, Y., Geng, Y.-K., Liu, R.-D., Pan, X.-R., Li, W.-W., Sheng, G.-P., 2018. Application of membrane bioreactor for sulfamethazine-contained wastewater treatment. Chemosphere 193, 840–846. https://doi.org/10.1016/j.chemosphere.2017.11.051

Shuster Ben-Yosef, V., Sendovski, M., Fishman, A., 2010. Directed evolution of tyrosinase for enhanced monophenolase/diphenolase activity ratio. Enzyme and Microbial Technology 47, 372–376. https://doi.org/10.1016/j.enzmictec.2010.08.008

Siemens, J., Huschek, G., Walshe, G., Siebe, C., Kasteel, R., Wulf, S., Clemens, J., Kaupenjohann, M., 2010. Transport of Pharmaceuticals in Columns of a Wastewater-Irrigated Mexican Clay Soil. Journal of Environmental Quality 39, 1201–1210. https://doi.org/10.2134/jeq2009.0105

Singh Arora, D., Kumar Sharma, R., 2010. Ligninolytic Fungal Laccases and Their Biotechnological Applications. Appl Biochem Biotechnol 160, 1760–1788. https://doi.org/10.1007/s12010-009-8676-y

Sipma, J., Osuna, B., Collado, N., Monclús, H., Ferrero, G., Comas, J., Rodriguez-Roda, I., 2010. Comparison of removal of pharmaceuticals in MBR and activated sludge systems. Desalination 250, 653–659. https://doi.org/10.1016/j.desal.2009.06.073

Sirtori, C., Zapata, A., Gernjak, W., Malato, S., Lopez, A., Agüera, A., 2011. Solar photo-Fenton degradation of nalidixic acid in waters and wastewaters of different composition. Analytical assessment by LC–TOF-MS. Water Research 45, 1736–1744. https://doi.org/10.1016/j.watres.2010.11.023

Snyder, S.A., Adham, S., Redding, A.M., Cannon, F.S., DeCarolis, J., Oppenheimer, J., Wert, E.C., Yoon, Y., 2007. Role of membranes and activated carbon in the removal of endocrine disruptors and pharmaceuticals. Desalination, Wastewater Reclamation and Reuse for Sustainability 202, 156–181. https://doi.org/10.1016/j.desal.2005.12.052

Solomon, E.I., Sundaram, U.M., Machonkin, T.E., 1996. Multicopper Oxidases and Oxygenases. Chem. Rev. 96, 2563–2606. https://doi.org/10.1021/cr950046o

Song, W., Guo, M., 2014. Residual Veterinary Pharmaceuticals in Animal Manures and Their Environmental Behaviors in Soils, in: He, Z., Zhang, H. (Eds.), Applied Manure and Nutrient Chemistry for Sustainable Agriculture and Environment. Springer Netherlands, Dordrecht, pp. 23–52. https://doi.org/10.1007/978-94-017-8807-6_2

Soriano, A.N., Adamos, K.G., Bonifacio, P.B., Adornado, A.P., Bungay, V.C., Vairavan, R., 2017. Determination of diffusion coefficients of various livestock antibiotics in water at infinite dilution. EPJ Web Conf. 162, 01083. https://doi.org/10.1051/epjconf/201716201083

Soto, A.M., Sonnenschein, C., 2010. Environmental causes of cancer: endocrine disruptors as carcinogens. Nat Rev Endocrinol 6, 363–370. https://doi.org/10.1038/nrendo.2010.87

Stadlmair, L.F., Letzel, T., Drewes, J.E., Graßmann, J., 2017. Mass spectrometry based in vitro assay investigations on the transformation of pharmaceutical compounds by oxidative enzymes. Chemosphere 174, 466–477. https://doi.org/10.1016/j.chemosphere.2017.01.140

Suda, T., Hata, T., Kawai, S., Okamura, H., Nishida, T., 2012. Treatment of tetracycline antibiotics by laccase in the presence of 1-hydroxybenzotriazole. Bioresource Technology 103, 498–501. https://doi.org/10.1016/j.biortech.2011.10.041

Szymańska, K., Pudło, W., Mrowiec-Białoń, J., Czardybon, A., Kocurek, J., Jarzębski, A.B., 2013. Immobilization of invertase on silica monoliths with hierarchical pore structure to obtain continuous flow enzymatic microreactors of high performance. Microporous and Mesoporous Materials 170, 75–82. https://doi.org/10.1016/j.micromeso.2012.11.037

Szymańska, U., Wiergowski, M., Sołtyszewski, I., Kuzemko, J., Wiergowska, G., Woźniak, M.K., 2019. Presence of antibiotics in the aquatic environment in Europe and their analytical monitoring: Recent trends and perspectives. Microchemical Journal 147, 729–740. https://doi.org/10.1016/j.microc.2019.04.003

Tadkaew, N., Sivakumar, M., Khan, S.J., McDonald, J.A., Nghiem, L.D., 2010. Effect of mixed liquor pH on the removal of trace organic contaminants in a membrane bioreactor. Bioresource Technology, Challenges in Environmental Science & Engineering, CESE – 2009: Waste Treatment: Challenges & Solutions 101, 1494–1500. https://doi.org/10.1016/j.biortech.2009.09.082

Taghizadeh, T., Talebian-Kiakalaieh, A., Jahandar, H., Amin, M., Tarighi, S., Faramarzi, M.A., 2020. Biodegradation of bisphenol A by the immobilized laccase on some synthesized and modified forms of zeolite Y. Journal of Hazardous Materials 386, 121950. https://doi.org/10.1016/j.jhazmat.2019.121950

Tahmasbi, H., Khoshayand, M.R., Bozorgi-Koushalshahi, M., Heidary, M., Ghazi-Khansari, M., Faramarzi, M.A., 2016. Biocatalytic conversion and detoxification of imipramine by the laccase-mediated system. International Biodeterioration & Biodegradation 108, 1–8. https://doi.org/10.1016/J.IBIOD.2015.11.029

Tallarek, U., Leinweber, F.C., Seidel-Morgenstern, A., 2002. Fluid Dynamics in Monolithic Adsorbents: Phenomenological Approach to Equivalent Particle Dimensions. Chemical Engineering & Technology 25, 1177–1181. https://doi.org/10.1002/1521-4125(20021210)25:12<1177::AID-CEAT1177>3.0.CO;2-V

Tambosi, J.L., de Sena, R.F., Favier, M., Gebhardt, W., José, H.J., Schröder, H.F., Moreira, R. de F.P.M., 2010. Removal of pharmaceutical compounds in membrane bioreactors (MBR) applying submerged membranes. Desalination 261, 148–156. https://doi.org/10.1016/j.desal.2010.05.014

Ternes, T.A., Stumpf, M., Mueller, J., Haberer, K., Wilken, R., Servos, M., 1999. Behavior and occurrence of estrogens in municipal sewage treatment plants - I. Investigations in Germany, Canada and Brazil. The Science of the Total Environment 225, 81–90.

Thiebault, T., Boussafir, M., Le Milbeau, C., 2017a. Occurrence and removal efficiency of pharmaceuticals in an urban wastewater treatment plant: Mass balance, fate and consumption assessment. Journal of Environmental Chemical Engineering 5, 2894–2902. https://doi.org/10.1016/j.jece.2017.05.039

Thiebault, T., Fougère, L., Destandau, E., Réty, M., Jacob, J., 2017b. Temporal dynamics of human-excreted pollutants in wastewater treatment plant influents: Toward a better knowledge of mass load fluctuations. Science of The Total Environment 596–597, 246–255. https://doi.org/10.1016/j.scitotenv.2017.04.130

Torres, E., Bustos-Jaimes, I., Le Borgne, S., 2003. Potential use of oxidative enzymes for the detoxification of organic pollutants. Applied Catalysis B: Environmental 46, 1–15. https://doi.org/10.1016/S0926-3373(03)00228-5

Tran, N.H., Urase, T., Kusakabe, O., 2010. Biodegradation Characteristics of Pharmaceutical Substances by Whole Fungal Culture Trametes versicolor and its Laccase. Journal of Water and Environment Technology 8, 125–140. https://doi.org/10.2965/jwet.2010.125

Trovó, A.G., Pupo Nogueira, R.F., Agüera, A., Fernandez-Alba, A.R., Malato, S., 2011. Degradation of the antibiotic amoxicillin by photo-Fenton process – Chemical and toxicological assessment. Water Research 45, 1394–1402. https://doi.org/10.1016/j.watres.2010.10.029

Tušek, A.J., Šalić, A., Zelić, B., 2017. Catechol Removal from Aqueous Media Using Laccase Immobilized in Different Macro- and Microreactor Systems. Appl Biochem Biotechnol 182, 1575–1590. https://doi.org/10.1007/s12010-017-2419-2

Tyler, C.R., Jobling, S., Sumpter, J.P., 1998. Endocrine Disruption in Wildlife: A Critical Review of the Evidence. Critical Reviews in Toxicology 28, 319–361. https://doi.org/10.1080/10408449891344236

Vasin, S.I., Filippov, A.N., 2009. Permeability of complex porous media. Colloid Journal 71, 31–45. https://doi.org/10.1134/S1061933X09010049

Verlicchi, P., Al Aukidy, M., Zambello, E., 2012. Occurrence of pharmaceutical compounds in urban wastewater: Removal, mass load and environmental risk after a secondary treatment—A review. Science of The Total Environment, Special Section - Arsenic in Latin America, An Unrevealed Continent: Occurence, Health Effects and Mitigation 429, 123–155. https://doi.org/10.1016/j.scitotenv.2012.04.028

Verliefde, A., Cornelissen, E., Amy, G., Van der Bruggen, B., van Dijk, H., 2007. Priority organic micropollutants in water sources in Flanders and the Netherlands and assessment of removal possibilities with nanofiltration. Environmental Pollution 146, 281–289. https://doi.org/10.1016/j.envpol.2006.01.051

Vystavna, Y., Huneau, F., Grynenko, V., Vergeles, Y., Celle-Jeanton, H., Tapie, N., Budzinski, H., Le Coustumer, P., 2012. Pharmaceuticals in Rivers of Two Regions with Contrasted Socio-Economic Conditions: Occurrence, Accumulation, and Comparison for Ukraine and France. Water Air Soil Pollut 223, 2111–2124. https://doi.org/10.1007/s11270-011-1008-1

Wang, J., Wang, S., 2016. Removal of pharmaceuticals and personal care products (PPCPs) from wastewater: A review. Journal of Environmental Management 182, 620–640. https://doi.org/10.1016/j.jenvman.2016.07.049

Wang, Y., Zhang, H., Zhang, J., Lu, C., Huang, Q., Wu, J., Liu, F., 2011. Degradation of tetracycline in aqueous media by ozonation in an internal loop-lift reactor. Journal of Hazardous Materials 192, 35–43. https://doi.org/10.1016/j.jhazmat.2011.04.086

Watkinson, A.J., Murby, E.J., Costanzo, S.D., 2007. Removal of antibiotics in conventional and advanced wastewater treatment: Implications for environmental discharge and wastewater recycling. Water Research 41, 4164–4176. https://doi.org/10.1016/j.watres.2007.04.005

Weissberg, H.L., 1963. Effective Diffusion Coefficient in Porous Media. Journal of Applied Physics 34, 2636–2639. https://doi.org/10.1063/1.1729783

Wen, Q., Yang, L., Zhao, Y., Huang, L., Chen, Z., 2018. Insight into effects of antibiotics on reactor performance and evolutions of antibiotic resistance genes and microbial community in a membrane reactor. Chemosphere 197, 420–429. https://doi.org/10.1016/j.chemosphere.2018.01.067

Wong, D.W.S., 2009. Structure and Action Mechanism of Ligninolytic Enzymes. Applied Biochemistry and Biotechnology 157, 174–209. https://doi.org/10.1007/s12010-008-8279-z

Xu, W., Zhang, G., Li, X., Zou, S., Li, P., Hu, Z., Li, J., 2007. Occurrence and elimination of antibiotics at four sewage treatment plants in the Pearl River Delta (PRD), South China. Water Research 41, 4526–4534. https://doi.org/10.1016/j.watres.2007.06.023

Yang, G.C.C., Tang, P.-L., 2016. Removal of phthalates and pharmaceuticals from municipal wastewater by graphene adsorption process. Water Sci Technol 73, 2268–2274. https://doi.org/10.2166/wst.2016.006

Yang, J., Lin, Y., Yang, X., Ng, T.B., Ye, X., Lin, J., 2017a. Degradation of tetracycline by immobilized laccase and the proposed transformation pathway. Journal of Hazardous Materials 322, 525–531. https://doi.org/10.1016/j.jhazmat.2016.10.019

Yang, J., Lin, Y., Yang, X., Ng, T.B., Ye, X., Lin, J., 2017b. Degradation of tetracycline by immobilized laccase and the proposed transformation pathway. Journal of Hazardous Materials 322, 525–531. https://doi.org/10.1016/j.jhazmat.2016.10.019

Yang, S., Hai, F.I., Nghiem, L.D., Price, W.E., Roddick, F., Moreira, M.T., Magram, S.F., 2013. Understanding the factors controlling the removal of trace organic contaminants by white-rot fungi and their lignin modifying enzymes: A critical review. Bioresource Technology 141, 97–108. https://doi.org/10.1016/j.biortech.2013.01.173

Yang, S.-F., Lin, C.-F., Yu-Chen Lin, A., Andy Hong, P.-K., 2011. Sorption and biodegradation of sulfonamide antibiotics by activated sludge: Experimental assessment using batch data obtained under aerobic conditions. Water Research 45, 3389–3397. https://doi.org/10.1016/j.watres.2011.03.052

Yang, W., Zhou, H., Cicek, N., 2014. Treatment of Organic Micropollutants in Water and Wastewater by UV-Based Processes: A Literature Review. Critical Reviews in Environmental Science and Technology 44, 1443–1476. https://doi.org/10.1080/10643389.2013.790745

Yao, W., Li, Y., Chen, N., 2013. Analytic solutions of the interstitial fluid flow models. Journal of Hydrodynamics, Ser. B 25, 683–694. https://doi.org/10.1016/S1001-6058(13)60413-8

Yousefi-Ahmadipour, A., Bozorgi-Koshalshahi, M., Mogharabi, M., Amini, M., Ghazi-Khansari, M., Faramarzi, M.A., 2016. Laccase-catalyzed treatment of ketoconazole, identification of biotransformed metabolites, determination of kinetic parameters, and evaluation of micro-toxicity. Journal of Molecular Catalysis B: Enzymatic 133, 77–84. https://doi.org/10.1016/J.MOLCATB.2016.07.015

Yuan, H., Chen, L., Cao, Z., Hong, F.F., 2020. Enhanced decolourization efficiency of textile dye Reactive Blue 19 in a horizontal rotating reactor using strips of BNC-immobilized laccase: Optimization of conditions and comparison of decolourization efficiency. Biochemical Engineering Journal 156, 107501. https://doi.org/10.1016/j.bej.2020.107501

Zdarta, J., Feliczak-Guzik, A., Siwińska-Ciesielczyk, K., Nowak, I., Jesionowski, T., 2020. Mesostructured cellular foam silica materials for laccase immobilization and tetracycline removal: A comprehensive study. Microporous and Mesoporous Materials 291, 109688. https://doi.org/10.1016/j.micromeso.2019.109688

Zdarta, J., Meyer, A.S., Jesionowski, T., Pinelo, M., 2018. Developments in support materials for immobilization of oxidoreductases: A comprehensive review. Advances in Colloid and Interface Science 258, 1–20. https://doi.org/10.1016/j.cis.2018.07.004

Zenker, A., Cicero, M.R., Prestinaci, F., Bottoni, P., Carere, M., 2014. Bioaccumulation and biomagnification potential of pharmaceuticals with a focus to the aquatic environment. Journal of Environmental Management 133, 378–387. https://doi.org/10.1016/j.jenvman.2013.12.017

Zhang, Y., Ge, J., Liu, Z., 2015. Enhanced Activity of Immobilized or Chemically Modified Enzymes. ACS Catal. 5, 4503–4513. https://doi.org/10.1021/acscatal.5b00996

Zhao, Y., Kuang, J., Zhang, S., Li, X., Wang, B., Huang, J., Deng, S., Wang, Y., Yu, G., 2017. Ozonation of indomethacin: Kinetics, mechanisms and toxicity. Journal of Hazardous Materials, Special Issue on Emerging Contaminants in engineered and natural environment 323, 460–470. https://doi.org/10.1016/j.jhazmat.2016.05.023

Zheng, F., Cui, B.K., Wu, X.J., Meng, G., Liu, H.X., Si, J., 2016. Immobilization of laccase onto chitosan beads to enhance its capability to degrade synthetic dyes. International Biodeterioration and Biodegradation 110, 69–78. https://doi.org/10.1016/j.ibiod.2016.03.004

Zou, Y., Ran, F., Huang, Q., Liu, X., Zhang, H., 2019. Facile Fabrication of a Novel and Reusable 3D Laccase Reactor for Efficient Removal of Pollutants from Wastewater. Catal Lett 149, 2706–2717. https://doi.org/10.1007/s10562-019-02732-8